universität wien

DISSERTATION

Molecular functions of endogenous and heterologous genetic RNA elements in the tick-borne encephalitis virus genome

angestrebter akademischer Grad

Doktor der Naturwissenschaften (Dr. rer. nat.)

Verfasser: Harald Rouha

Dissertationsgebiet Genetik und Mikrobiologie

Betreuer: Univ.-Prof. Dr. Timothy Skern

Univ.-Prof. DDr. Christian Mandl

Wien, im Juni 2010

Danksagung

Die vorliegende Arbeit entstand zwischen März 2007 und Mai 2010 am Department für Virologie der Medizinischen Universität Wien.

Mein Dank gilt vor allem Prof. Christian Mandl für die exzellente wissenschaftliche Betreuung dieser Dissertation, für seinen ansteckenden Optimismus und für all die wertvollen Diskussionen und Gespräche, auf die ich auch nach seinem Weggang vom Institut nicht verzichten musste. Ohne seinen transatlantischen Input wäre der Abschluss dieser Arbeit wohl kaum möglich gewesen. Weiters möchte ich mich bei Herrn Prof. Franz Heinz bedanken, der es mir ermöglicht hat, diese Dissertation am Department für Virologie durchzuführen und den ich stets und in allen Belangen um Rat fragen konnte. Herrn Prof. Tim Skern danke ich herzlich für die Übernahme der Betreuung nach dem Weggang von Herrn Prof. Mandl und Caroline Thurner für die interessante Zusammenarbeit mit der „Theoretischen Chemie" und für die Möglichkeit in einem ihrer Projekte gestaltend mitzuwirken. Ein großes Dankeschön möchte ich auch allen momentanen und ehemaligen Mitarbeitern des Departments/Instituts für Virologie aussprechen, allen voran den ehemaligen Mitgliedern der Mandl-Gruppe: Verena, Blaimi, Katrin, Sabrina, Gabriel, Klaus und Regina. Vielen Dank für die äußerst produktive und angenehme Atmosphäre am Institut, die erforderliche Einschulung und Unterstützung im Labor und die unterhaltsamen Stunden, in denen wir im „Steindl's" auf den Einsatz des Schnitzelklopfers gewartet haben. Danke auch an meine Freunde, die stets für nötige Abwechslung sorgten und die mich das Leben auch aus ganz anderen Perspektiven sehen lassen. Spezieller Dank gebührt natürlich meiner Freundin Steffi, die in all der Zeit die perfekte Partnerin zum Teilen aller Hoch- und Tiefpunkte war, sich unbeirrt von mir erklären ließ, was ich den ganzen Tag so tue und deren Unterstützung mir in jeder Hinsicht sicher war. Mein größter Dank gilt meinen Eltern, die mir meine Ausbildung ermöglicht haben, sowie meiner gesamten Familie, die in all den Jahren immer für mich da war und wohl nie die Hoffnung aufgeben wird, dass ich eines Tages „etwas finden werde"…

Content

SUMMARY

Flaviviruses are small enveloped viruses with a positive-stranded RNA genome that include important human pathogens such as Dengue virus, yellow fever virus and tick-borne encephalitis virus. The epidemiology of these viruses is largely determined by the ecological needs of the corresponding insect vectors, i.e. mosquitoes or ticks. The disease patterns they evoke range from mild febrile illness, to encephalitis and hemorrhagic fever.

The genome of all flaviviruses consists of a single RNA molecule that *per se* acts as an infectious messenger RNA and contains the coding sequence for the viral polyprotein. The single open reading frame is flanked by noncoding regions (NCRs) that reside on the terminal ends of the viral RNA strand and occupy important functions in RNA translation, replication and possibly also packaging. Compared to the protein-coding region, the noncoding regions are not well conserved between mosquito- and tick-borne flaviviruses.

The main objective of this thesis was the characterization of endogenous as well as heterologous sequence elements in the genome of tick-borne encephalitis virus (TBEV). The unique tick-borne encephalitis 3'-NCR is divided into a highly conserved core region, which comprises essential secondary structures that are involved in RNA replication, and a variable region of inconsistent length that completely lacks sequence conservation. The function of the variable region that is characterized by a poly-A stretch in some but not all TBEV strains is essentially unknown.

In our first approach we addressed the question whether the variable part of the 3'-NCR region has any effect on the efficiency of RNA replication or RNA translation. For this purpose we analyzed the impact of various manipulations of the 3'-NCR in a sensitive luciferase-based reporter replicon system. Our results revealed that truncation or complete removal of the poly-A stretch or even the deletion of the entire variable region does not cause a significant effect on any of these processes. Furthermore we observed that the replacement of the variable region with heterologous sequence elements was well tolerated during RNA replication and did not impair viral input RNA translation. These findings provided the basis for our second study in which we examined the capability of tick-borne encephalitis virus to encode functional microRNAs.

MicroRNAs are a class of small noncoding RNAs that have essential regulatory functions in eukaryotic gene expression by mediating the sequence-specific translational inhibition or degradation of mRNAs. Although DNA viruses have recently been shown to encode and exploit their own microRNAs in the complex interactions with their mammalian host cells, no such molecules have so far been identified from viruses with an RNA genome and a cytoplasmic replication cycle. Based on the current understanding that microRNA biogenesis is initiated in the nucleus and characterized by an RNA cleavage event, it is generally reasoned that this pathway

is not available and unusable for viruses that are confined to the cytoplasm and comprise an RNA genome. We addressed this issue experimentally and introduced a heterologous herpesvirus microRNA-precursor element into the TBEV 3'-NCR. In the subsequent characterization of this chimeric virus we were able to demonstrate for the first time that a functional microRNA can indeed be produced from such a virus without an impairment of viral RNA replication.

Additional studies of this thesis concentrated on the conserved RNA secondary structure elements in the 5'-NCR of TBEV. Recently the 5'-part of the TBEV cyclization sequence has been mapped to one of these motifs. To further determine the role of this and other hairpin elements we performed a mutational analysis in our luciferase-reporter system and screened for defects in viral RNA replication and translation. This approach also included the manipulation of the thermodynamic stability of these elements and revealed several new insights into the functional importance of the TBEV 5'-terminal stem-loop structures.

Taken together the results of this thesis extend the current knowledge on endogenous genetic RNA elements of TBEV, contribute to the inceptive understanding of the complex interplay of RNA viruses with the RNA silencing machinery, and also provide a rational basis for RNA virus vector design.

ZUSAMMENFASSUNG

Flaviviren sind kleine lipidumhüllte Viren mit einem positiv-strängigen RNA Genom, denen eine Reihe von humanpathogenen Krankheitserregern, wie das Dengue-Virus, das Gelbfieber-Virus und das FSME (Frühsommer-Meningoencephalitis)-Virus angehören. Die Epidemiologie dieser Viren wird weitestgehend durch die ökologischen Anforderungen ihrer Insektenvektoren (Stechmücken oder Zecken) bestimmt und die Krankheitsbilder, die sie hervorrufen, reichen von milden, fieberhaften Symptomen über Hirnhautentzündung bis hin zu hämorrhagischem Fieber.

Das Genom aller Flaviviren besteht aus einem einzigen RNA-Molekül, das die kodierende Sequenz für das virale Polyprotein enthält und das selbst als infektiöse mRNA fungiert. Der einzige offene Leserahmen auf diesem RNA-Molekül ist an den beiden Enden von nicht-kodierenden Regionen flankiert, die eine entscheidende Rolle in der Translation, der Replikation und möglicherweise auch in der Verpackung der Virus-RNA spielen. Verglichen mit den kodierenden Sequenzbereichen des Genoms, sind diese nicht-kodierenden Regionen zwischen den beiden Hauptgruppen, den Insekten- und den Zecken-übertragenen Flaviviren, allerdings nur sehr schwach konserviert.

Das Hauptziel der vorliegenden Arbeit war die Charakterisierung von endogenen wie auch von heterologen Sequenzelementen im FSME-Virus Genom. Die innerhalb der Flaviviren einzigartige, nicht-kodierende Region am 3'-Ende der viralen RNA (3'-NCR) wird in eine hoch konservierte „Kernregion" und eine hinsichtlich ihrer Sequenz flexible „variable Region" unterteilt. Die näher am 3'-Ende liegende „Kernregion" enthält hoch konservierte RNA-Sekundärstrukturen, die unter anderem essentiell für die Virusreplikation sind. Die weiter innen angeordnete „variable" Region differiert stark hinsichtlich ihrer Länge und ist auch zwischen einzelnen Stämmen innerhalb der FSME-Virus Familie nicht konserviert. Die Funktion der variablen Region, die in manchen FSME-Virus Stämmen durch eine Poly-A Sequenz gekennzeichnet ist, ist im Wesentlichen unbekannt.

Im ersten Teil dieser Arbeit gingen wir der Frage nach, ob die variable Region in der 3'-nicht-kodierenden Sequenz des FSME-Virus einen Einfluss auf die Replikation und/oder Translation der viralen RNA ausübt. Dazu führten wir Mutationen in diesen Sequenzbereich ein und analysierten in einem sensitiven Luziferase-Reporter-Replikon System potentielle Effekte auf Translation und Replikation. Unsere Ergebnisse zeigten, dass eine Verkürzung oder Entfernung der Poly-A Sequenz, aber auch eine Deletion der gesamten variablen Region, keinen signifikanten Effekt auf einen dieser beiden Prozesse ausübt. Darüber hinaus wurde klar, dass die variable Region ohne Beeinträchtigung der Translation oder Replikation durch heterologe Sequenzelemente ersetzt werden kann. Letztere Erkenntnis lieferte den Grundstein für unser

zweites Projekt, in dem wir untersuchten, ob das FSME-Virus in der Lage ist, funktionelle microRNAs zu kodieren.

MicroRNAs sind eine Klasse von kleinen, nicht-kodierenden RNAs, die essentielle regulatorische Funktionen in der eukaryotischen Genexpression innehaben. Sie vermitteln dabei die sequenz-spezifische, post-translationale Inhibierung oder den Abbau von mRNAs. Obwohl kürzlich gezeigt werden konnte, dass DNA-Viren eigene microRNAs kodieren und diese in der Wirtszelle auch zu ihren Gunsten einsetzen können, gibt es keine Berichte über microRNAs von Viren mit einem RNA-Genom und einem zytoplasmatischen Lebenszyklus. Dem momentanen Wissensstand zufolge beginnt die Biogenese von microRNAs im Zellkern und zeichnet sich dort unter anderem durch einen Schnitt im RNA-Molekül aus, der den microRNA Vorläufer für die weitere Prozessierung freisetzt. Es wird daher allgemein angenommen, dass dieser Biogenese-Weg für Viren mit einem RNA-Genom und einem zytoplasmatischen Lebenszyklus weder zugänglich noch nutzbar ist. Unser Ziel war es, diese Annahme hinsichtlich ihrer Gültigkeit in einem Modellsystem zu überprüfen. Wir klonierten dazu einen heterologen Herpesvirus microRNA-Vorläufer in die nicht-kodierende 3'-Region des FSME-Virus. In der nachfolgenden Charakterisierung dieser chimären Mutante gelang uns der erstmalige Nachweis, dass eine funktionelle microRNA auch von einem zytoplasmatisch replizierenden Virus mit einem RNA-Genom generiert werden kann, ohne dass das notwendigerweise mit einer signifikanten Beeinträchtigung der RNA Replikation einhergehen muss.

Im dritten Teil der vorliegenden Arbeit befassten wir uns mit konservierten RNA-Sekundärstrukturen am 5'-Ende des viralen RNA Moleküls. Kürzlich konnte der 5'-Teil der FSME-Virus Zyklisierungssequenz einer Haarnadelstruktur in diesem Genombereich zugeordnet werden. Um die Rolle dieses und anderer Sequenzelemente hinsichtlich ihrer Funktion zu untersuchen, führten wir in unserem Luziferase-Reportersystem eine Mutationsanaylse durch, die auch eine gezielte Veränderung der thermodynamischen Stabilität beinhaltete und so neue Einblicke in die Wirkungsweisen dieser Elemente in der viralen Replikation und Translation liefern konnte.

Zusammenfassend lässt sich sagen, dass die Ergebnisse dieser Arbeit den derzeitigen Wissensstand über die Funktion endogener RNA-Elemente im Genom des FSME-Virus erweitern, dass sie wesentlich zu einem besseren Verständnis der komplexen Interaktion von RNA-Viren mit der RNA-Interferenz-Maschinerie der Wirtszelle beitragen, und dass sie darüber hinaus eine wertvolle Grundlage für das Design von RNA-Virus Vektoren liefern.

1 GENERAL INTRODUCTION

1.1 Flaviviridae

1.1.1 Classification and taxonomy

The family *Flaviviridae* comprises one of the three superfamilies of positive-stranded RNA viruses and is subdivided into three genera: the genus *Flavivirus*, the genus *Pestivirus* and the genus *Hepacivirus*. All three genera share common structural features, such as lipid-enveloped virions with two glycoproteins on its surface (E, envelope and M, membrane) and a positive-stranded RNA genome that forms a nucleocapsid by complexing with multiple units of the capsid protein C (1).

The genus *Pestivirus* contains several important animal pathogens that primarily infect goat, sheep and cattle, and is therefore of significant interest for livestock industry. The genus *Hepacivirus* contains the human hepatitis C virus (HCV) that is one of the major reasons for chronic liver disease and hepatocellular carcinomas in humans (1).

The largest genus *Flavivirus* consists of more than 70 viruses that are mainly transmitted to vertebrates by infected arthropods such as mosquitoes or ticks. Flaviviruses can be further subdivided into antigenic complexes, clades and clusters (Fig. 1),(1-3). They cause a large spectrum of diseases in humans ranging from asymptomatic infections to febrile illness, fatal encephalitis and hemorrhagic fever (1,3).

The next section provides an overview about the epidemiology and disease of the most important human flaviviruses West Nile virus (WNV), Japanese encephalitis virus (JEV), yellow fever virus (YFV) and Dengue virus (DENV), all of them mosquito-borne flaviviruses, and the tick-transmitted tick-borne encephalitis virus (TBEV).

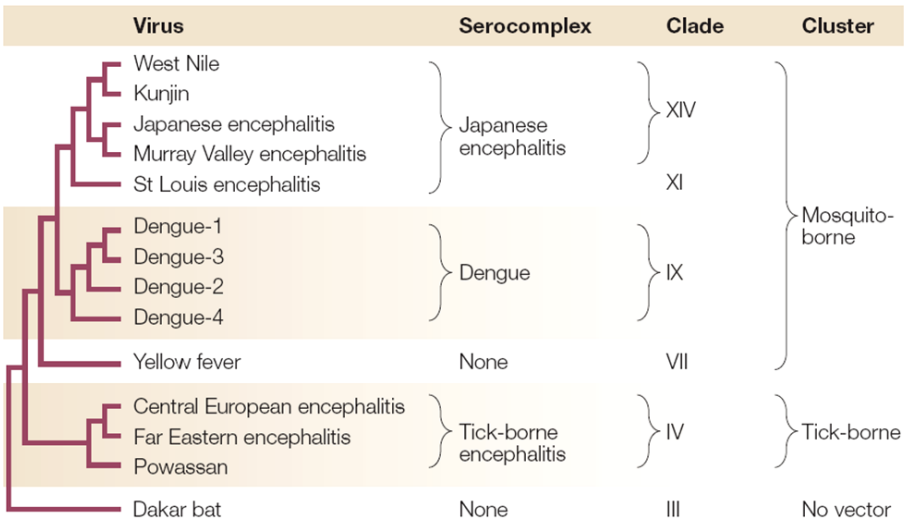

Figure 1. Flavivirus classification. The genus *Flavivirus* is subdivided into different serocomplexes, clades and clusters, according to antigenic properties, molecular phylogeny and the mode of transmission. Adapted from Mukhopadhyay *et al.*, Nature Reviews Microbiology, 2006.

1.1.2 Epidemiology and disease

1.1.2.1 West Nile virus

Until recently West Nile virus was not considered as an emerging viral pathogen. Infections were mainly restricted to rural areas in Africa and Asia and the number of severe neurological illnesses remained relatively low (4). This changed when a more virulent strain of the virus was introduced into the US in 1999. Since then its geographic distribution has expanded remarkably (5),(Fig. 2). Soon WNV has become the leading cause for arboviral encephalitis in the United States (6). The virus circulates between various bird species that represent the natural reservoir of the virus and the preferred vector, mosquitoes of the genus *Culex*. Humans and other mammals are incidental hosts that do – except from horses – not produce a high enough viremia to actively contribute to the transmission cycle (4). Approximately 80% of all WNV infections remain asymptomatic, 20% of infected humans generate “West Nile fever”, a self limited, febrile illness. In approximately one out of 150 patients, infection results in severe neurological disease (West Nile neuroinvasive disease), including encephalitis, meningitis and acute flaccid paralysis (4). It should be mentioned,

however, that case numbers in the US between 2004 and 2007 remained stable and that WNV infections might have reached an endemic level that more likely tends to a decline in the number of cases rather than to an increase (6). Although several human vaccines are currently under development, the only licensed ones are restricted to use in horses (7).

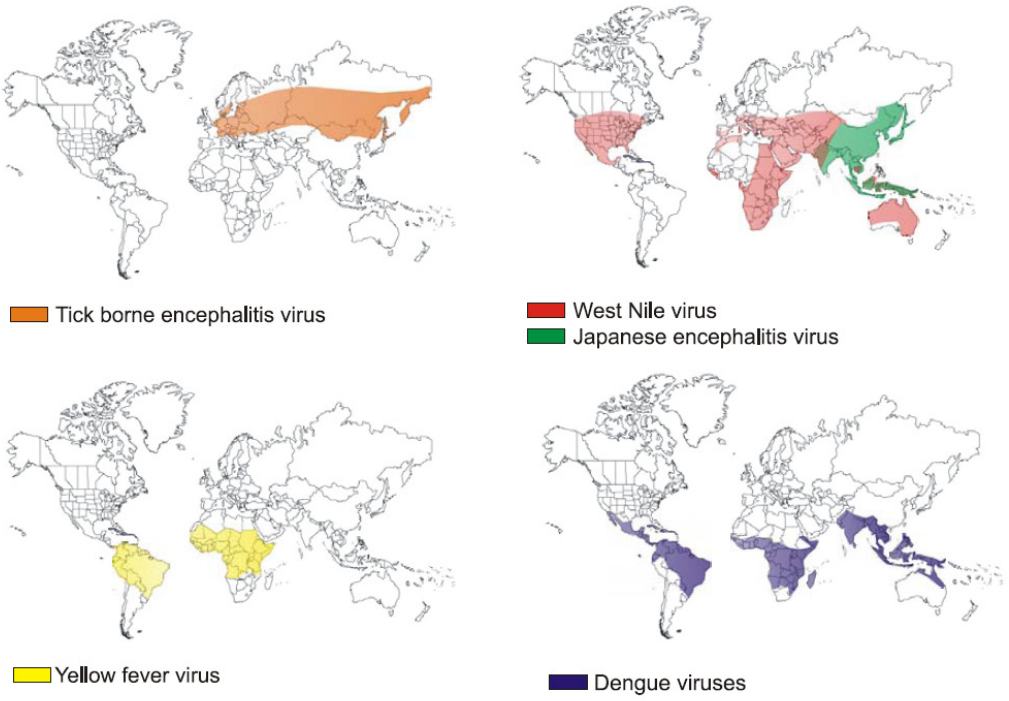

Figure 2. Endemic regions of the most important human flaviviruses. Adapted from Klaus Orlinger, "Construction and Application of Bicistronic Flaviviruses", (Ph.D. thesis, University of Vienna, 2007).

1.1.2.2 Dengue virus

Dengue virus represents a major health problem in tropical and subtropical regions, with a growing global incidence. Approximately two fifths of the world population are currently at risk of infection and it is estimated that there are more than 50 million cases per year (8). Dengue viruses can be subdivided into 4 serotypes (DENV 1-4) and all of them are transmitted to humans through a bite of infected Aedes mosquitoes (9). The outcome ranges from an asymptomatic infection or a febrile illness (dengue fever) to severe Dengue, a clinical syndrome that is characterized by increased vascular permeability and plasma leakage from blood vessels into tissues (Dengue hemorrhagic fever, DHF). This might in the

worst case cause shock (Dengue shock syndrome, DSS),(10). Although Dengue virus is the leading cause of serious illness and death among children in some Asian countries, there is currently no vaccine available. One of the reasons for this is that while infection with any of the 4 serotypes induces a life-long homotypic immunity, antibodies produced during this primary infection may cause a more severe form of the disease (with a higher risk of obtaining DHF or DSS) among secondary heterotypic dengue infection. The mechanism underlying this phenomenon is most likely antibody-dependent enhancement (ADE), a process in which pre-existing subneutralizing antibodies form complexes with the virus, which in turn leads to increased uptake of the virus by Fc-receptor bearing cells (11,12). For this reason, the major challenge in the development of a safe and successful Dengue virus vaccine is, to find a formulation that provides equal protection against all four serotypes. Although the development of such a vaccine is problematic, several multivalent candidate vaccines, including live attenuated viruses and chimeric vaccines, have already reached the phase of clinical testing (13).

1.1.2.3 Japanese encephalitis virus

Japanese encephalitis virus is mainly endemic in Eastern, South-Eastern and Southern Asia but it has also caused an epidemic in Australia (14). Like WNV that belongs to the same serocomplex of flaviviruses, it is transmitted by Culex mosquitoes that feed on humans, pigs, birds and even amphibian and reptiles (10,15). Although humans are only incidental hosts and most infections remain subclinical, JEV infection is with more than 50,000 reported cases annually, the major cause of viral encephalitis in Asia. In a severe form the disease can progress to paralysis, seizures, coma and death (16). Several inactivated and live attenuated vaccines are in use in Asia but not licensed in Europe or the United States. JE-VAX® (Sanofi-Pasteur), an inactivated mouse-brain-derived inactived JE vaccine with US-approval, is not manufactured any more. A new cell-culture based inactived JE vaccine (IXIARO®), developed by the Austrian biotech company Intercell, successfully

launched the market in 2009. This vaccine, however, is not yet licensed for the use in children (17).

1.1.2.4 Yellow fever virus

The mosquito-borne yellow fever virus is endemic in sub-saharan Africa and in parts of Southern America (18). Although YFV is transmitted by the same mosquito-species as Dengue virus (*Aedes aegypti*) it is remarkably less widespread and has never appeared in Asia (10). It is estimated that around 200,000 cases occur annually (19). Clinical symptoms of YFV infection range from influenza like patterns including headache, backache, muscle pain and fever to severe hepatitis (that causes the yellow jaundice), hemorrhagic fever, and multisystem-organ failure (20). A YFV strain 17D derived attenuated live virus vaccine is efficiently used since decades (20).

1.1.2.5 Tick-borne encephalitis virus

Tick-borne encephalitis virus is endemic in many European countries as well as in the Far-East and in Asia (Fig. 2). Based on moderate differences in their nucleotide sequences and “signatures” on protein level, TBE viruses are grouped into three closely related subtypes: a European subtype (including strain Neudoerfl, the prototype strain used throughout the studies presented in manuscripts 1-3), a Far-Eastern subtype and a Siberian subtype (21). Small rodents are the main host of TBEV, and ticks that can be chronically infected act as transmission vectors. Humans, as well as larger animals such as goat, sheep and cow are incidental hosts that do only play a minor role in the natural TBEV transmission cycle (22). The Central European subtype is transmitted by *Ixodes ricinus*, whereas the main vector for tick-borne encephalitis in Eastern countries is *Ixodes persulcatis* (23). Tick-bites, however, are not the only way of getting infected with the virus. Outbreaks of tick-borne encephalitis have also been reported after consumption of unpasteurized milk from viremic livestock (22,24). Interestingly, although TBEV can be found in a very large geographical area, the sole presence of the corresponding tick-vector does not necessarily imply a coincidence with the virus. *Ixodes ricinus* for instance is widely distributed throughout entire

Austria, the virus itself, however, accumulates only at restricted geographic hotspots. The micro-ecological specifications that underlie these patchy geographical clustering of suitable virus biotypes are largely unknown (25).

In about 70% of all cases, infection with TBEV remains asymptomatic. In the remaining 30% a biphasic febrile illness may follow that can include fever, malaise, anorexia, muscle aches, headache, nausea, and/or vomiting. This initial phase lasts about 2-4 days and corresponds to the viremic phase of virus infection. In 20 to 30% of patients, a second phase may occur that involves the central nervous system. This phase is accompanied by symptoms of encephalitis and meningitis and can result in persisting spinal nerve paralysis. The mortality rate of patients whose central nervous system is affected is approximately 1-2% for the European subtype (26,27). Infection with TBEV can effectively be prevented by vaccination. Austria, with a current vaccination rate of approximately 90% is a good example for the effectiveness of this vaccine: In the pre-vaccination era, 600-700 TBEV infections were reported per year which has dropped now to 60-70 annual cases (26,28). Apart from Russian vaccines (based on the Far Eastern subtype), two inactivated whole virus vaccines are available in Europe that are based on the European subtype: FSME-IMMUN^{TM}, manufactured by Baxter (Austria), and Encepur^{TM}, produced from Novartis (Germany),(28).

1.1.3 Molecular organization of flaviviruses

1.1.3.1 Virion structure

Flavivirus virions are relatively small (~50 nm) particles that are composed of a dense core that contains the nucleopcapsid and which is surrounded by a lipid envelope. The surface of the mature virion contains two viral structural proteins, the envelope protein (E) and the membrane protein (M). Glycoprotein E mediates binding and fusion of the virus and is the major antigenic determinant. The M protein is produced during the maturation process of the virus by Furin cleavage of the precursor-M (prM) protein. This results in a structural rearrangement of the 60 heterotrimeric prM-E glycoproteinspikes into 90 antiparallel

homodimers which can be found on the smooth surface of the mature particle (Fig. 3), (1,29). The third structural protein of the virus, the capsid protein C, is complexed with the viral RNA and forms the nucleocapsid core that does not appear to have a symmetric structure (1).

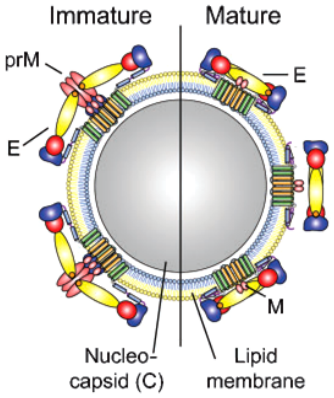

Figure 3. Structure of the immature (left) and mature (right) flavivirus particle. Adapted from Stiasny and Heinz, Journal of General Virology, 2006.

1.1.3.2 Genome structure

The genome of flaviviruses is composed of a single positive-stranded RNA molecule of about 11 kb length that contains only one open reading frame (Fig. 4). It is infectious when introduced into a host cell and can be directly translated into an endoplasmatic reticulum (ER) - anchored polyprotein that is cleaved into the 10 viral proteins (three structural proteins, C, prM and E that composite the viral particle and seven non-structural proteins, NS1, NS2A, NS2B, NS3, NS4A, NS4B and NS5 that are involved in viral replication). The RNA is capped with a 5'-type-I cap but unlike cellular messenger RNAs the 3'-end does not

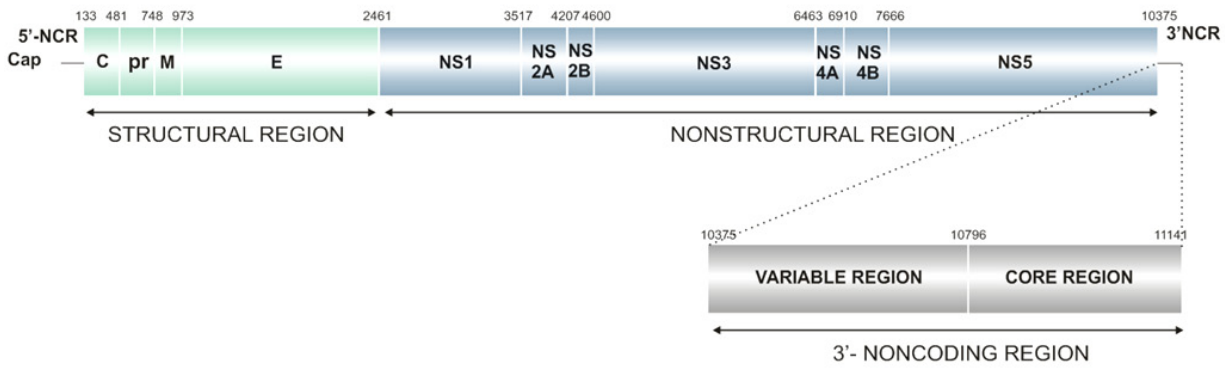

Figure 4. Flavivirus genome structure.

contain a poly-A tail (1,30). The highly structured 5'- and 3'-noncoding regions of the genome contain regulatory elements that are involved in a variety of important viral processes such as RNA translation and replication and are treated separately in chapter 1.1.5.

1.1.4 The flavivirus life cycle

After cellular attachment the flavivirus particle is internalized by receptor-mediated endocytosis (Fig. 5). The knowledge on flavivirus receptors is still fragmentary but most likely flaviviruses are able to use multiple receptors in different cell types and hosts (1). Several studies have indicated an involvement of cellular heparansulfate (HS), a highly sulfated glycosaminoglycan, on viral attachment and entry (31,32). However, the presence of HS on the cellular surface is not mandatory for virus uptake.

In the endosome the viral particle is exposed to acidic pH that triggers the trimerization of the E protein and insertion of the E protein fusion peptide into the endosomal membrane (29,33). This results in fusion of the two lipid membranes and subsequent release of the viral nucleocapsid into the cytoplasm. Once inside the cytoplasm, the viral RNA and the capsid proteins dissociate from each other and the viral RNA is readily translated by the host cell translational machinery (3). This occurs at the membrane of the endoplasmatic reticulum, where the polyprotein integrates into the ER membrane and is co- and post-translationally cleaved by the viral NS2B/3 serine protease (cleavages between NS2A/2B, NS2B/3, NS3/4A, NS4A/2K and NS4B/5 junctions) and the host signal peptidase (C/prM, prM/E, E/NS1 and 2K/NS4B),(1). Initiation of translation occurs by ribosome scanning through the genome 5' end but the strategies for proper selection of the start codon may not be uniform for all flaviviruses (see 1.1.5.3).

Following translation, a replicase complex is assembled for viral RNA amplification. First, a minus-strand copy of the genomic positive-strand is synthesized. This is mediated by cyclization of the viral genome and does not require a pre-existing RNA primer. The minus-strand then serves as a template for additional plus-strands in an asymmetric process, that

gives rise to around 10-fold more positive- than negative-strands (1).The process of RNA replication takes place in double-layered vesicle packets in close association with the perinuclear membrane (1,34). The most important viral proteins involved in RNA synthesis are the viral RNA-dependent RNA polymerase NS5 (which also functions as a capping enzyme) and the NS3 protein that acts in unwinding the double-stranded RNA intermediate structure (35).

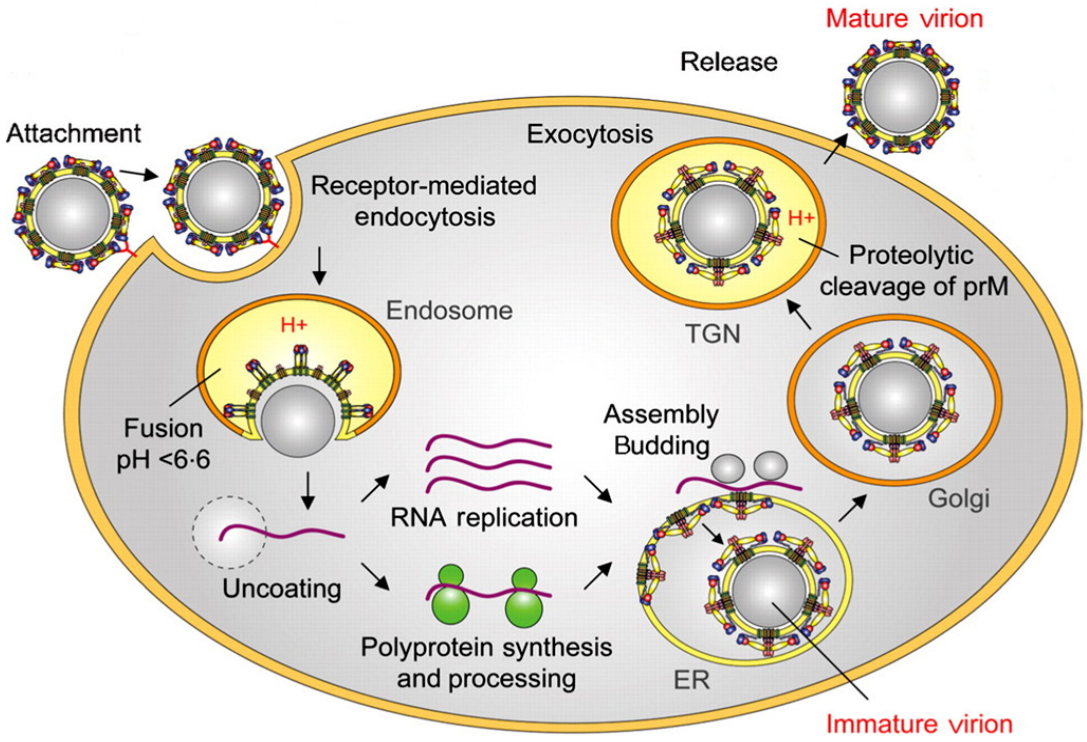

Figure 5. The flavivirus life cycle. See text for details. Modified from Stiasny and Heinz, Journal of General Virology, 2006.

The first step in virion assembly is the formation of a nucleocapsid at the cytoplasmic site of the ER. The capsid then buds into the ER lumen, where the viral surface proteins prM and E are residing as a consequence of polyprotein processing and thus are available for the formation of the ER-membrane derived envelope that surrounds the nucleocapsid of a newly formed virus particle. The immature prM containing virion is then transported through the host cell secretory pathway. PrM cleavage by Furin in the late trans-Golgi network (TGN) causes the already mentioned structural rearrangement of the E protein and generates the

mature, infectious virus particle that is ultimately released from the cell by fusion of the Golgi vesicle with the host cell plasma membrane (29,36,37).

1.1.5 Conserved RNA motifs involved in RNA replication and translation

The genome of flaviviruses contains RNA secondary structure elements that contribute to the overall RNA stability but also mediate essential inter- and intramolecular interactions for initiation of RNA replication and translation or for the interaction of the viral RNA with cellular proteins that facilitate or regulate such processes (38,39). The majority of those cis-acting RNA elements are located within or in close proximity to the noncoding regions at the terminal ends of the viral genome.

This section treats elements that are involved in translation and replication of the viral RNA and points out significant differences between tick-borne and mosquito-borne flaviviruses.

1.1.5.1 The 5'-NCR

The flavivirus 5'-NCR is relatively short (approximately 100 nt in length) and generally not very well conserved between different members of the genus. Mosquito-borne flaviviruses tend to have even shorter 5'-NCRs than tick-borne viruses (132 nt for TBEV strain Neudoerfl, 96 nt for WNV strain NY99).

As already mentioned, translation initiation of flavivirus RNA occurs in a cap-dependent mechanism (40), comparable to the mechanism for cellular mRNAs. In contrast to some other positive-stranded RNA viruses that lack a 5'-cap (e.g. polioviruses), there is therefore no need for a longer, more complex RNA secondary structure that could act as an internal ribosomal entry site (IRES),(41). The most conserved linear sequence feature that is present in all flavivirus genomes (except Cell fusing agent, CFA) is the 5'-terminal dinucleotide 5'-AG which exhibits perfect complementarity to the equally conserved 3'-terminal end of the genome (CU-3') and is engaged in long range interaction between the

terminal ends of the viral RNA molecule (30,41,42). In addition several conserved secondary structures are predicted in the genomes of tick-borne as well as mosquito-borne flaviviruses (Fig. 6). A common element is a large Y-shaped structure (43) at the 5' terminal end of the genome (termed 5'-SL1 for tick-borne flaviviruses and SLA for mosquito-borne viruses) that is of significant importance for viral RNA replication (44) and RNA capping (45), and that has been proposed to act as promoter for negative-strand RNA synthesis (46,47).

Downstream of the 5'-SL1 (or SLA, respectively), additional conserved stem-loop elements have been described. For mosquito-borne flaviviruses these are a smaller hairpin (SLB) that is located at or close to the translational start codon and a conserved small hairpin in the capsid coding region (cHP). In tick-borne encephalitis virus, three additional hairpins have been predicted: the 5'-SL2, the 5'-SL3 and the 5'-SL4 (Fig. 6A). The role of these hairpins in viral input RNA translation and replication was subject to analysis in manuscript 3 of this thesis.

1.1.5.2 Long-range interactions and cyclization sequences

One function of the conserved viral 5'-end is the mediation of long-range interactions with the 3'-end of the viral genome. This has been shown to be essential for viral replication (48) and supports the idea that the promoter for minus-strand synthesis is located at the 5'-end of the positive-strand. As minus-strand RNA synthesis starts at the 3'-end of the positive-strand, the 5'- and the 3'-end of the genome have to be brought into close proximity. This is accomplished by sequence complementarity between the genomic ends of the viral RNA molecule that enable a structural rearrangement and a switch from a linear into a circular conformation (a panhandle-like structure).

Although genome cyclization is thought to be mandatory for all flaviviruses, differences exist in the genomic regions that participate in this process. In the case of tick-borne encephalitis virus, a 5'-CS-A element located within the 5'-SL2 binds to a corresponding 3'-CS-A element in the terminal stem-loop 3'-SL1 (see green line in Fig. 6A),(48,49). A second long-range interaction that has been predicted between the 5'-

SL4 and the region between the terminal stem-loops 3'-SL5 and 3'-SL4 (50) has shown to be dispensable for viral RNA replication (49). In contrast, two pairs of long-range interactions have been proposed to be important for the replication of mosquito-borne flaviviruses. The 5'-3'-UAR (upstream AUG region) interaction (51) mediated by complementary parts of SLB and 3'-SL, respectively (Fig 6B, red line) and the complementarity between the 5'-3'-CS elements, located within the coding sequence of the capsid protein in the 5'-end and in the 3'-NCR of the viral 3'-end (Fig. 6B, blue line),(50,52,53).

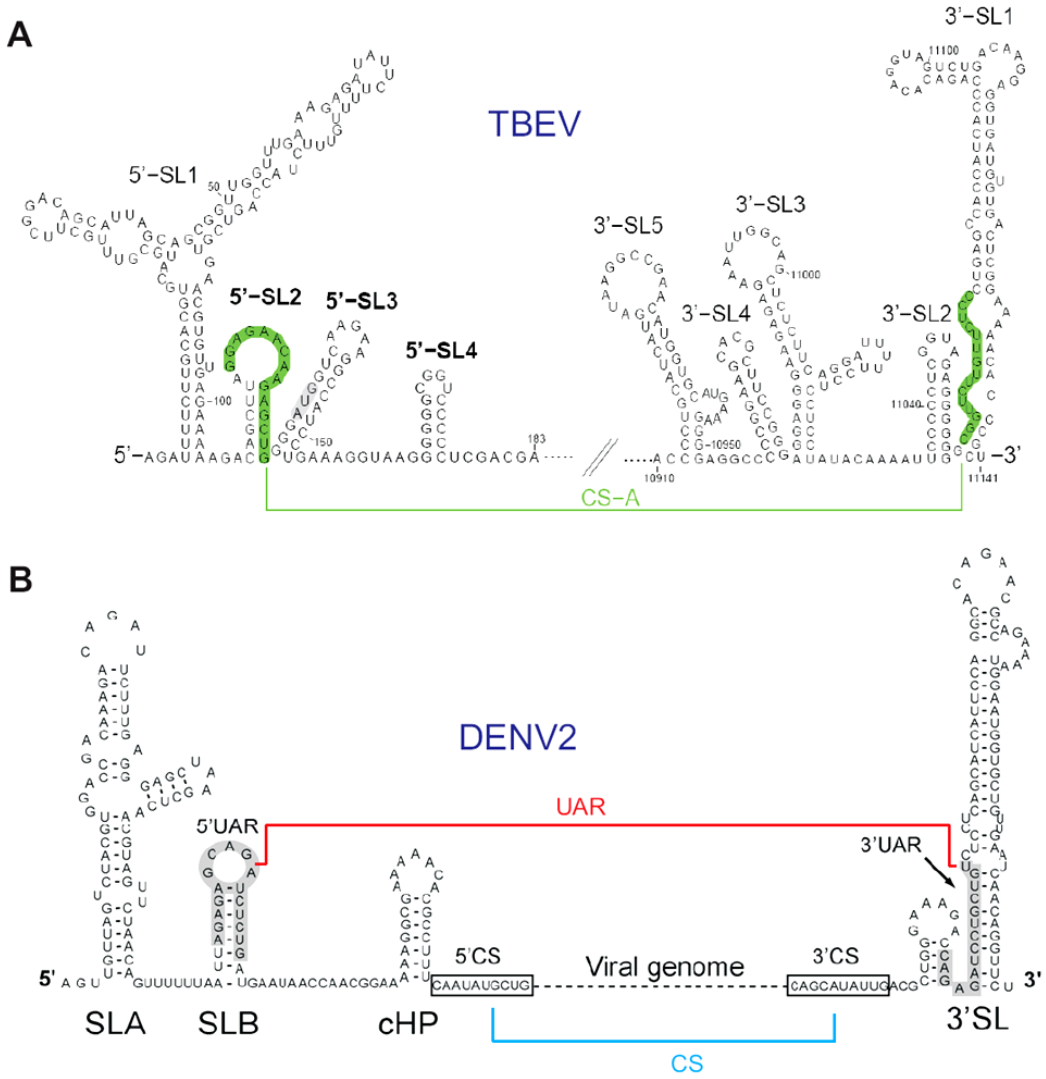

Figure 6. Conserved secondary structures in the 5'- and 3'-noncoding regions of tick-borne (e.g. TBEV) and mosquito-borne (e.g. DENV) flaviviruses. Long-range interactions are indicated by coloured lines. Panel B modified from Villordo and Gamarnik, Virus Research, 2009.

1.1.5.3 The role of conserved hairpin elements in flavivirus translation initiation

In addition to their prominent role in viral RNA replication some of the conserved stem-loop elements at the 5'-end of the viral RNA molecule might also function in translation initiation. Cap-dependent translation requires the eukaryotic translation initiation factor 4E, a component of the cap-binding complex eIF4F. Nevertheless a novel non-canonical translation initiation mechanism that does not require the cap-binding protein 4E, has been recently described for Dengue virus (54). It was shown that the conserved, thermodynamically stable hairpin structure element cHP in the capsid coding region (Fig. 6B) is able to direct translational start site selection when cap-dependent translation is inhibited (54,55). The proposed mechanism is that the translation complex stalls due to the unwinding of the secondary structure of the cHP and thereby interacts with the first AUG codon (55). As the start codon of Dengue virus is in a poor Kozak inititation context (meaning that the efficiency of the codon is low due to the sequence composition of the immediate upstream and downstream region (56)), it is likely that the cHP directs start codon selection even in the presence of 4E. This is in good agreement with a previous report in which it was shown that the insertion of a stable secondary structure element downstream of an AUG codon in a poor Kozak initiation context can enhance the selection of this codon for translation initiation (55,57).

The situation for tick-borne encephalitis virus is largely unknown. Although the translational start codon is embedded in a strong Kozak initiation context, a thermodynamically stable, conserved hairpin structure element is predicted to be maintained in the N-terminal end of the capsid coding region (5'-SL4). Whether the TBEV 5'-SL4 has a similar function in viral RNA translation as the cHP element in mosquito-borne flaviviruses was subject to analysis in manuscript 3.

1.1.5.4 The 3'-noncoding region of tick-borne encephalitis virus

Although the 3'-NCRs of mosquito- and tick-borne flaviviruses are functionally related, the structural organization of the tick-borne encephalitis virus 3'-NCR is substantially different

from the one of mosquito-borne flaviviruses. Similarities are mainly confined to the presence of a characteristic 3'-terminal stem-loop structure (3'-SL1 for tick-borne viruses and 3'-SL for mosquito-borne flaviviruses) that mediates the interaction with the viral NS3 and NS5 proteins and contributes to genome cyclization, replication and translation (1). Another common feature has been discovered only recently: All flaviviruses produce a highly structured, subgenomic RNA that is derived from the 3'-NCR and apparently required for viral pathogenicity (58).

The tick-borne encephalitis virus 3'-NCR is subdivided into a highly conserved, 325 nt long core region at the 3'-terminal end of the virus and a non conserved variable region upstream of the core region, ranging from 450 to 800 nts in length in natural isolates (41,59). Interestingly, the variable region of some isolates has been shown to contain an internal poly-A stretch of inconsistent length (60) (49 nts for strain Neudoerfl) that is sometimes spontaneously deleted or further elongated during viral passaging (61). The core region comprises the essential sequence elements that are involved in genome cyclization and RNA replication (49,59,61,62) and appears to be sufficient for a viable TBE virus (41). TBEV strain RK1424 for instance does virtually not contain a variable region (41). Furthermore it has been demonstrated that removal of the variable region does not abolish viral infectivity of TBEV strain Neudoerfl (61) and that the variable region can be replaced by heterologous genetic information (63-66).

In manuscript 1 we performed a functional analysis of the variable region of the TBEV 3'-NCR by sensitive measurement of primary translation and RNA replication in a luciferase-based replicon assay and further replaced this region with heterologous expression cassettes. In manuscript 2 we extended the variable region with the microRNA-precursor element of a herpesvirus.

1.2 Small silencing RNAs

In 1993, the first small silencing RNA, the lin-4 microRNA, was discovered in the nematode worm *Caenorhabditis elegans (67,68).* Since then, thousands of tiny non-protein-coding (nc) RNAs have been found and shown to be involved in almost all physiological processes in eukaryotic cells by mediating post-transcriptional silencing of gene expression. All of these tiny regulatory RNAs share common themes in their biology, such as their limited size (~20-30 nucleotides) and their association with Argonaute (Ago-) family proteins, catalytic components of the RNA-induced silencing complex (RISC). This section aims to provide an overview about different classes of small silencing RNAs, summarizes briefly our current knowledge on RNA interference (RNAi) and its role in antiviral defense, and focuses in more detail on microRNAs and their role in animal virus infection.

1.2.1 Classes of small silencing RNAs

Based on the mechanism of their biogenesis and the class of Ago proteins they are associated with, small silencing can be grouped into three different classes: microRNAs (miRNAs), small interfering RNAs (siRNAs) and Piwi-interacting RNAs (piRNAs),(69,70). However, as it is becoming clear since recently that numerous small RNAs are products of non-canonical pathways, the boundaries between these different classes of small RNAs in animals are ambiguous (69).

MicroRNAs are the best characterized small silencing RNAs and their biogenesis and biological roles are described in more detail in section 1.2.3. SiRNAs are the effector molecules of RNA interference, which is discussed in more detail below. PiRNAs were recently discovered in germ cells of Drosophila and have been proposed to be important regulators of cellular development (71). Piwi-proteins are a subclass of Argonaute proteins and have been shown to be essential in germ line stem cells. Compared to microRNAs and siRNAs, piRNAs are longer in size (24-29 nt). Most of them are derived from intergenic

repetitive elements on chromosomes, including retrotransposons (69). The biogenesis of piRNAs is not well elucidated. It has been shown, however, that in contrast to siRNAs and miRNAs their production is not necessarily dependent on Dicer (72). The most important biological function of piRNAs is the silencing of "selfish" retrotransposons in germ cells, an essential process that has been linked to spermatogenesis (73).

1.2.2 RNA interference (RNAi)

1.2.2.1 History and mechanism of RNAi

RNA interference is an evolutionary conserved, highly efficient pathway in which short double-stranded (ds) RNA molecules specifically trigger the inhibition of gene expression (74,75). RNAi is one of the most powerful technologies in modern biology and it remarkably facilitates the study of gene function as it allows the specific depletion of protein-coding mRNAs. First hints of the existence for an RNA interference pathway came from experiments in plants, when Napoli *et al*. tried to increase the purple colour of petunias in 1990. Unexpectedly, the introduction of additional gene copies encoding the coloration key enzyme chalcone synthase (CHS), did not result in darker pigmentation but instead yielded partially or fully white flowers (76). Related observations were also made in the fungus *Neurospora crassa*, where the introduction of the par-1 RNA resulted in the silencing of the par-1 gene expression (77). A few years later virologists found that plants carrying virus-derived non protein-coding transgenes, were protected from infection of viruses containing similar nucleotide sequences (78). Furthermore it was shown in a reverse experiment that the expression of plant genes can be suppressed by infection with a virus, containing parts of the plant gene nucleotide sequence (79).

At this time the introduction of antisense RNAs for gene silencing has already become a popular method to study gene function but it took three more years until the mechanistic trigger behind this phenomenon was ultimately elucidated. Finally, in 1998, Craig Mello and Andrew Fire found that dsRNA was substantially more effective at producing

interference that was either strand individually (80). Thereby they demonstrated that the trigger for the antisense-RNA effects was double-stranded RNA.

Initially RNAi was prevented from being applied in mammalian cells, since the used dsRNA were longer than 30 nts and thus potent inducers of the interferon system, present in higher organisms (74). Just a few years later in 2001, however, the lab of Thomas Tuschl reported that RNAi can also efficiently be triggered in mammalians cells by introducing only ~21 nt long RNA duplexes, that evade a stimulation of the innate immune reponse. These short dsRNAs were called small interfering RNAs (siRNAs),(81-83) and are still one of the most attractive means in the induction of post-transcriptional gene silencing. For their landmark discovery of RNAi that opened a new chapter in life-science research, Mello and Fire were awarded with the Nobel Prize in 2006.

1.2.2.2 RNAi – an intrinsic antiviral defense mechanism in mammals?

There is strong evidence for a natural, antiviral role of RNAi in plants and invertebrates (84-86). In these organisms, viral double-stranded RNA that is produced as an essential replication intermediate from all RNA viruses (except from retroviruses) is recognized by RNAse III enzymes of the Dicer family and processed into small interfering RNAs (87). Single strands of these siRNAs are then incorporated into the RNA induced silencing complex, where they guide the degradation of complementary viral mRNA sequences (88). The importance of RNA interference as defence mechanism in these organisms has been further supported by the discovery of a variety of counter-defence strategies that have been evolved from viruses to avert or diminish the effect of this pathway on viral pathogenesis.

The expression of effective silencing suppressors from insect and plant viruses was first shown for Flock-house virus (FHV), a member of the genus *Alpha-nodavirus.* The FHV B2-protein is essential for viral infection of insect cells (89) and has a dual role: it inhibits Dicer cleavage by binding to the dsRNA and also prevents the incorporation of already

cleaved viral RNAs into RISC (90-92). Thereby it enables FHV to accumulate effectively in infected insect cells (89).

So while it is well established that RNAi has an instrumental role in natural viral defense in plants and invertebrates, the contribution of RNAi to natural innate defense in mammals is less clear. The invasion of RNA viruses in vertebrates is handled differently: Three types of pattern recognition receptors (PRRs) sense double-stranded viral RNA: Toll-like receptors (TLRs), RIG-I like receptors (RLRs) and nucleotide oligomerization domain-like receptors (NLRs),(93). The primary reaction to viral dsRNA is the activation of cytokine expression and the induction of a type-I interferon response. As a consequence, the binding of type-I IFNs to the corresponding receptors (IFNARs) leads to the expression of more than 300 IFN-stimulated genes (ISGs), which cause a so-called antiviral state and – in an amplification loop - a further increase in pattern-recognition receptors that detect virus infection and protect from viral spread (94,95).

Without any doubt, IFNs constitute a key component of the first line of defense against viral infection in mammals. This is further underlined by the fact that defects in interferon signaling lead to increased susceptibility to virus infection, that interferon therapy can successfully be used for the treatment of viral infection and, finally, that many mammalian viruses have evolved potent suppressors of the IFN pathway (93,94,96-98). The general understanding is therefore that the potent dsRNA-activated antiviral interferon system has replaced an antiviral function of the RNAi response and that RNAi interference is not involved in the intrinsic antiviral immunity in mammalian cells (99-101). The finding that induced RNAi by siRNAs or short hairpin RNAs (shRNAs) is able to trigger sequence specific inhibition of viral replication also in mammals (102), can be explained by the fact, that the molecules used in triggered RNAi (short dsRNA duplexes or short hairpin RNAs) mimic microRNA duplex intermediates of the natural microRNA biogenesis pathway, which is conserved all the way from plants, to invertebrates and mammals (99).

Nevertheless this black and white picture is becoming increasingly disputed. It has been shown for example that many IFN antagonists that are encoded by mammalian viruses

(e.g. vaccinia virus E3L, influenza A virus NS1 and Ebola virus VP35) also represent effective RNA-silencing suppressors (RSS) and a very recent study found virus-derived small RNAs in the size of siRNAs in mammalian cells infected with various RNA viruses (103). Whether these molecules are the product of an active RNAi response, however, remains to be clarified and thus the question whether siRNAs contribute to antiviral immunity in mammalian cells cannot be answered yet.

1.2.3 MicroRNAs

1.2.3.1 Biogenesis of microRNAs

Until very recently it was thought that microRNA generation is a universal process for all mature mammalian miRNAs. However, in addition to the canonical microRNA processing pathway (Fig. 7), pathways have been discovered that do not follow the classical cascade to generate functional microRNAs in animals. The major, canonical (linear) and the best characterized, non-canonical pathway, the so-called mirtron pathway, are described below.

1.2.3.1.1 The canonical (linear) pathway of microRNA processing

Typically microRNA biogenesis starts with the synthesis of a primary microRNA transcript in the nucleus by RNA polymerase II or III (104-107). Many microRNA genes are located in introns of mRNAs but some have also been shown to be derived from protein coding regions (108). Mostly, these transcripts are capped and polyadenylated and consist of an imperfectly paired stem of approximately 33 bp, with a terminal loop and single-stranded flanking segments (109-111). Two sequential cleavage steps are then exerted that trim this transcript into the mature microRNA. First, Drosha, a RNAse III enzyme located in the nucleus, recognizes the local hairpin structure and cleaves at the base of the stem-loop. This releases a small hairpin that is called precursor-miRNA (pre-miRNA),(105,112). The catalyzation of this cleavage event also requires the activity of a co-factor, the DiGeorge

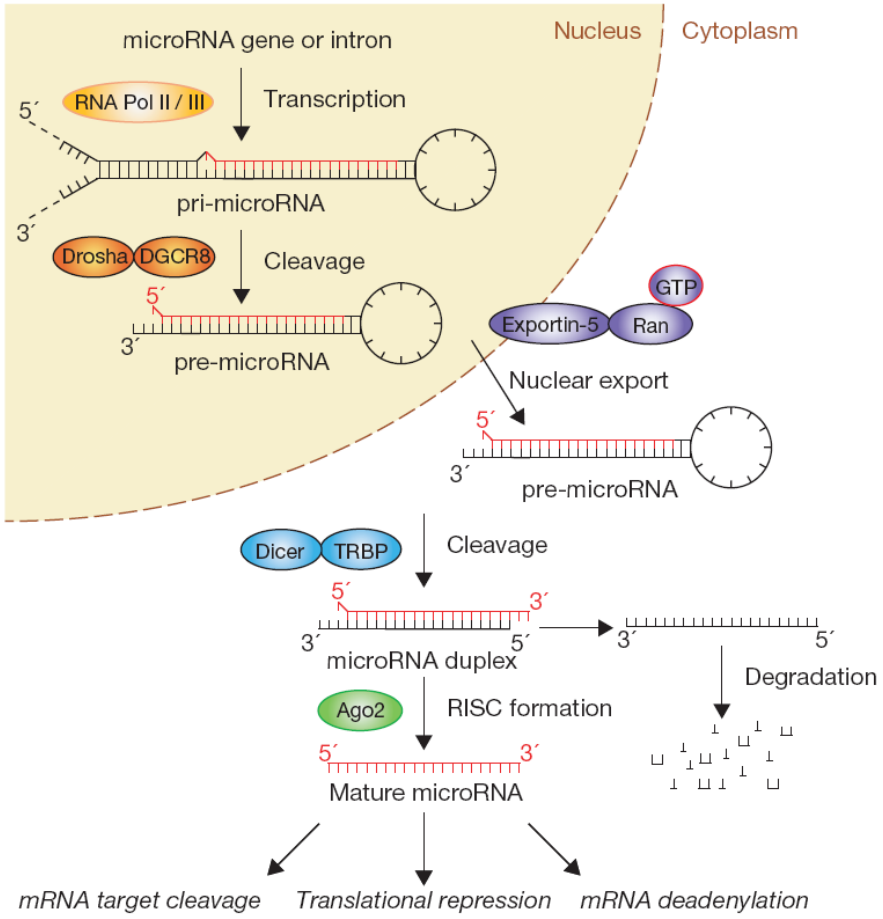

Figure 7. The canonical microRNA processing pathway. A primary microRNA is transcribed in the nucleus and cleaved by Drosha/DGCR8 into a precursor-miRNA that is transported to the cytoplasm by Exportin-5. In the cytoplasm, Dicer exerts a second cleavage step that finally gives rise to a mature microRNA that is loaded into the RNA-induced silencing complex (RISC) to guide mRNA target cleavage, translational repression or mRNA deadenylation. Adapted from Winter *et al.*, Nature Cell Biology, 2009.

syndrome critical region gene 8 (DGCR8),(113). Together Drosha and DGCR8 form the so-called microprocessor complex (114-116). The nuclear export protein Exportin-5 then mediates the transport of the pre-miRNA to the cytoplasm (117), where a second cleavage step is performed by the RNAse III enzyme Dicer and its partner protein TRBP (Dicer and TAR RNA binding protein),(118-120). The enzymatic activity of Dicer and TRBP removes the terminal loop from the pre-miR-stem and gives rise to a microRNA duplex intermediate of approximately 22 bp length that correlates to the two sides of the stem (109). These two sides correspond to the guide- and the passenger-strand of an siRNA duplex and similar criteria influence the choice of the guide miRNA-strand versus the passenger miRNA-strand

(121,122). The mature microRNA can therefore theoretically arise from either arm of the precursor-microRNA hairpin. In many cases, however, the ratio of microRNAs originated from the 5'- and the 3'-arm respectively, is asymmetric, favoring the incorporation of only one strand into RISC (70).

1.2.3.1.2 The mirtron pathway

Microprocessor mediated cleavage is not the only way to generate mammalian precursor-miRNAs. Recently it has been reported that pre-miR can also be generated by the nuclear splicing machinery, independent of Drosha cleavage (123-125), (Fig. 8). Such precursor-miRNA-like introns (mirtrons) are produced by splicing messenger RNA precursors. The spliced introns first accumulate as lariat products and subsequent debranching of these structures yields authentic microRNA precursors that can be fed into the standard microRNA biogenesis pathway (70).

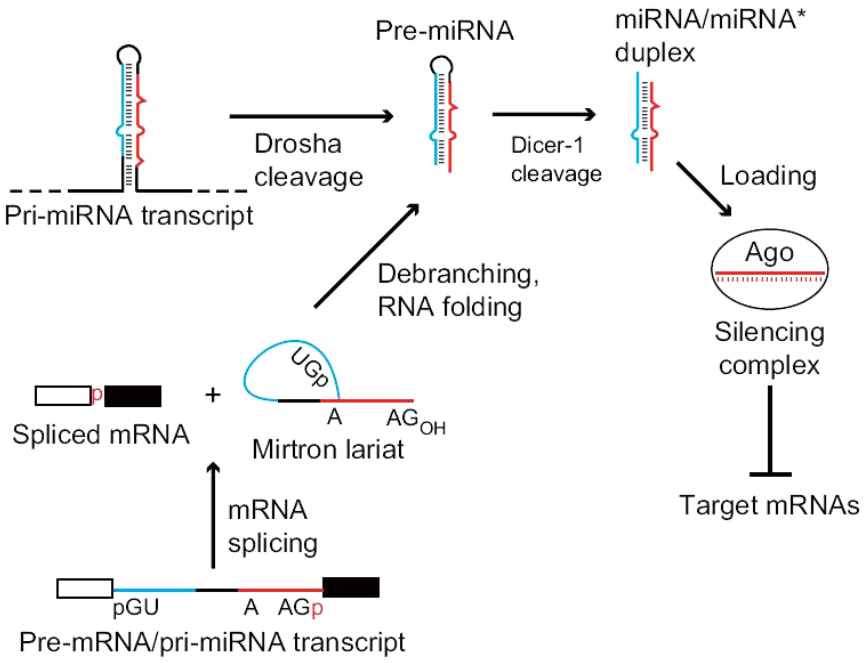

Figure 8. The mirtron pathway. In the mirtron pathway Drosha cleavage is bypassed. MicroRNA precursors are released from mRNAs after splicing. This requires the splicing machinery and a lariat debranching enzyme that forms the hairpin, resembling a precursor miRNA. Further processing is then following the classical microRNA biogenesis pathway. Adapted from Ruby *et al.*, Nature, 2007.

1.2.3.2 Biological roles of microRNAs

MicroRNAs have been implicated in almost all biological processes examined so far and it soon became clear that they have an essential role in the biology of animals and plants. More than 850 microRNAs have so far been identified alone in humans and it is predicted that at least 30% of all human mRNAs are regulated by microRNAs (126,127). Undisputedly they play a central role in cell metabolism, differentiation and apoptosis. Loss of Dicer or miRNA-associated Argonaute proteins is almost always lethal in animals as it causes severe developmental defects. Mice lacking Dicer, for instance, die as early embryos, most likely due to a defect in stem cell development (70). In addition, dysregulation of microRNA expression can also contribute to disease development. Several examples of important oncogenic and tumor suppressor miRNAs have been reported and several studies revealed that miRNA signatures in different cell types and tissues have a high diagnostic value and may become valuable tools in the clinical therapy of cancer (127). Further implications of miRNAs in disease development have been reported in Alzheimer's disease, Parkinson's disease and heart diseases (127-130). The effects of microRNAs are therefore extremely wide-spread. They represent an essential class of gene regulators with a huge impact but our knowledge of their precise, multiple functions in eukaryotic cell systems is still in its infancy. Clearly, one of the main challenges on the way to a more accurate understanding of their biological roles in health and disease is a more precise approach for microRNA target prediction. Currently the number of newly discovered microRNAs is exploding, whereas the number of those, with known targets and functions remains relatively low.

1.2.3.3 MicroRNAs in virus-host interactions

Considering the small size of microRNAs and their lack of immunogenicity, it is not surprising that these molecules have also been exploited by mammalian viruses as effective regulators of gene expression. Potential mechanisms of such virus-host microRNA interactions include (I) the targeting of viral transcripts by virally encoded miRNAs, (II) viral

microRNAs that target host cell transcripts and (III) cellular microRNAs that directly or indirectly promote or potentially also limit virus replication (131),(Fig. 9).

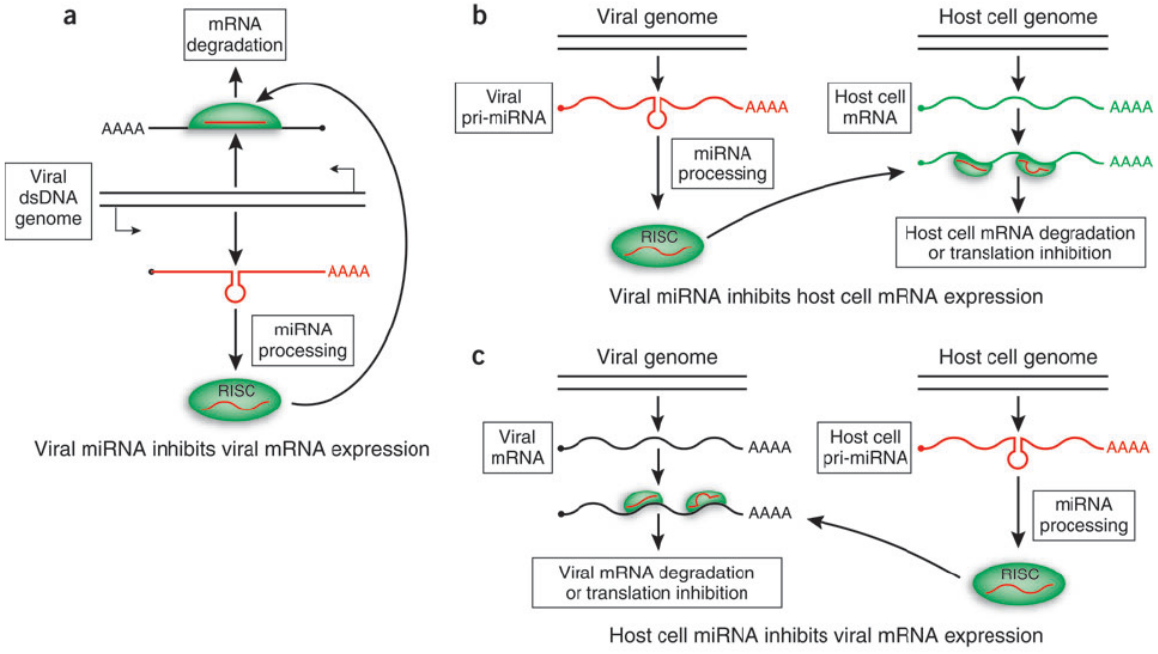

Figure 9. MicroRNAs in virus-host interactions. (a) Viral microRNAs may inhibit viral mRNA expression (e.g. EBV-miR-BART2), (b) viral microRNAs may inhibit the expression of genes in the host cell (e.g. KSHV-miR-K12-11) or (c) host cell microRNAs may interfere with viral gene expression (this interference may also have positive effects on viral replication - see section 1.2.3.4). Adapted from Cullen, Nature Reviews Genetics, 2006.

The first virus-encoded microRNAs were discovered in 2004, in human B cells infected with Epstein-Barr virus (132). Up to now all herpesviruses examined so far have been shown to encode microRNAs (101). In addition, virus-derived microRNAs have been found in cells infected with the human adenovirus, Heliothis virescens ascovirus (HvAc) and several polyomaviruses (101). Currently known microRNAs are summarized in Table 1. Notably, this list does not contain human immunodeficiency virus 1 (HIV-1) derived microRNAs that have been proposed by several groups (133-135). The existence of these microRNAs could not be confirmed by other groups and is therefore heavily disputed (101,136,137). At miR-Base, HIV-1 derived miRNAs are currently listed with subject to be “at risk of deletion” (126). So, up to now all viral microRNAs that have been discovered so far

are derived from dsDNA viruses or – if HIV is to included into the list of miRNA encoding viruses, from viruses that involve a nuclear dsDNA stage in their replication cycle. All approaches to identify viral microRNAs derived from RNA viruses came so far up empty-

Virus Family	Subfamily/Genus	Name	Host	Number of pre-miRNAs	References
Herpesvirus	α/Simplexvirus	HSV-1	Human	6	Cui et al. 2006; Umbach et al. 2008
		HSV-2	Human	3	Tang et al. 2008, 2009
	α/Mardivirus	MDV-1	Avian	14	Burnside et al. 2006; Yao et al. 2008
		MDV-2	Avian	17	Yao et al. 2007
	β/Cytomegalovirus	hCMV	Human	11	Grey et al. 2005; Pfeffer et al. 2005
		mCMV	Murine	18	Buck et al. 2007; Dölken et al. 2007
	γ_1/Lymphocryptovirus	EBV	Human	25	Pfeffer et al. 2004; Cai et al. 2006; Grundhoff et al. 2006; Zhu et al. 2009
		rLCV	Simian	16	Cai et al. 2006
	γ_2/Rhadinovirus	KSHV	Human	12	Cai et al. 2005; Pfeffer et al. 2005; Samols et al. 2005; Grundhoff et al. 2006
		RRV	Simian	7	Schäfer et al. 2007
		MHV68	Murine	9	Pfeffer et al. 2005
Polyomavirus		SV40	Simian	1	Sullivan et al. 2005
		SA12	Simian	1	Cantalupo et al. 2005
		MCV	Simian	1	Seo et al. 2009
		BKV	Human	1	Seo et al. 2008
		JCV	Human	1	Seo et al. 2008
		mPy	Murine	1	Sullivan et al. 2009
Adenovirus		hAV	Human	1	Aparicio et al. 2006; Sano et al. 2006
Ascovirus		HvAV	Lepidopteran	1	Hussain et al. 2008

Table 1. Summary of currently known viral microRNAs. Adapted from Umbach and Cullen, Genes and Development, 2009.

handed. The most comprehensive small-RNA cloning study that identified numerous new microRNAs of the herpesvirus-family did not lead to the identification of any microRNAs in cells infected with HCV, YFV and HIV-1 (137).

It is therefore generally assumed that viruses with an RNA genome and/or a cytoplasmic replication cycle are not able to encode microRNAs and that they lack this class of regulatory molecules. This conclusion is also supported by two theoretical barriers that arise from the life cycle of such viruses and the microRNA biogenesis pathway. First of all, microRNA biogenesis is initiated in the nucleus (with the excision of a precursor-miRNA hairpin from a primary miRNA transcript by Drosha). So even if such a virus that replicates in the cytoplasm of an infected cell encoded a microRNA hairpin, the separation from the microprocessor complex in the nucleus may not allow the processing of this hairpin (138). Secondly, even if there is a way to liberate the genomically encoded miRNA hairpin, the excision is expected to

result in cleavage and degradation of the viral genome (131), which is as a consequence expected to impair viral RNA replication. Interestingly, however, the lack of experimental identification of RNA virus microRNAs is not directly reflected by the outcome of computational microRNA hairpin predictions. The viral microRNA database (Vir-mir db) for instance that provided the first large scale microRNA prediction in viral genomes, revealed a high number of candidate hairpins also in RNA virus genomes (139).

In manuscript 2 we addressed the question whether there is a fundamental incapability of RNA viruses to produce functional microRNAs. We used a model system, in which we inserted a known microRNA precursor into the genome of a cytoplasmic RNA virus and we were able to show for the first time that there is no fundamental barrier for RNA viruses to generate these molecules.

1.2.3.4 MicroRNA-122 and hepatitis C virus – exceptions prove the rule

MicroRNA binding to an mRNA does not necessarily lead to mRNA degradation or translational inhibition. One striking example for a positive effect, exerted by a cellular microRNA on viral gene expression, is the interaction of the human microRNA-122 with the RNA genome of hepatitis C virus. MiR-122 is a highly liver-specific microRNA and it accounts for approximately 70% of the microRNA repertoire in liver cells, where it regulates fatty acid and cholesterol biosynthesis (140-142). The importance of miR-122 for HCV was demonstrated by Jopling *et al*., who reported that the inhibition of miR-122 impairs RNA replication of the virus (142). Furthermore it was shown that the binding site of miR-122 is highly conserved in all 6 HCV genotypes, which is a strong indication of the relevant role of this microRNA *in vivo* and, as microRNA-122 is exclusively expressed in the liver, also compelling evidence for the contribution of microRNA-122 to the tissue tropism of HCV (131,142). Two adjacent binding sites for this microRNA have been identified in the 5'-UTR of HCV. However, the exact mechanism how this small RNA facilitates virus replication and/or translation has yet to be elucidated (101,142,143).

1.2.3.5 Epstein-Barr virus microRNA-BART2

One of the best characterized viral microRNAs is microRNA-BART2, expressed from Epstein-Barr virus (EBV). It was identified together with several other microRNAs derived from the same virus by cloning the small RNAs from a Burkitt's lymphoma cell line latently infected with EBV (132). In total, EBV encodes at least 23 microRNAs. The B95.8 strain (Fig. 10) has a deletion of 12 kb and encodes only 8 microRNA genes (144).

MiR-BART2 is encoded in the BART (Bam HI-A region rightward transcript) region of the EBV virus genome on the complementary strand of the gene encoding the viral DNA polymerase protein BALF5 (Fig. 10). The mRNA of BALF5 has been shown to be the target of microRNA-BART2 and binding of miR-BART2 leads to cleavage of the transcript (144). The functional significance of this inhibition remains to be demonstrated. It is assumed, however, that the reduction of viral replication levels promotes latency and prevents EBV from switching to the lytic stage of its life cycle. This is also supported by the finding that microRNAs encoded in the EBV-BART cluster are expressed at very low levels in freshly infected B-cells, but at significantly higher levels in infected cells that undergo type II latency (131,145).

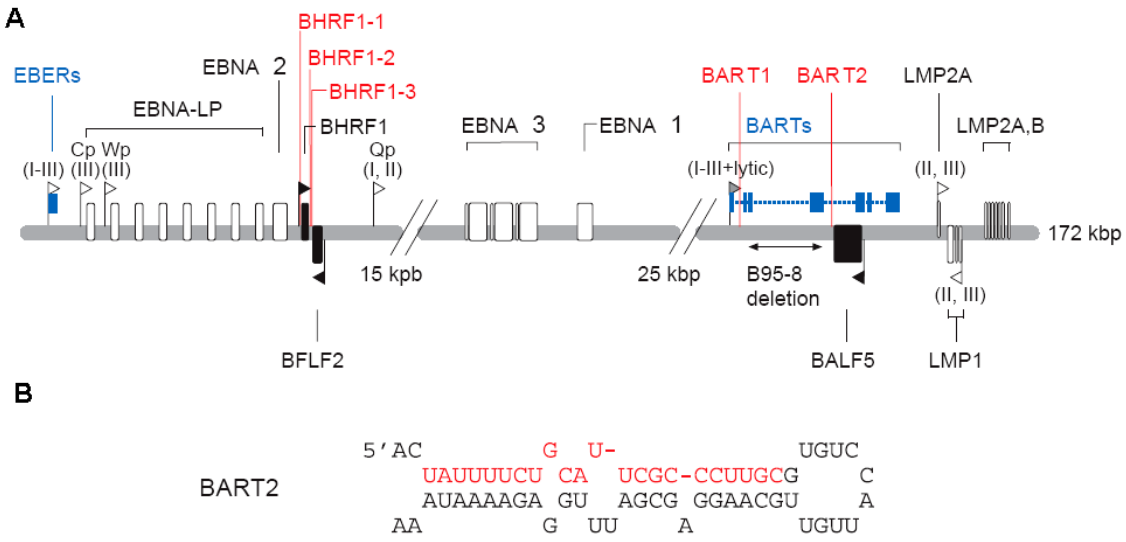

Figure 10. Genomic position and predicted secondary structure of EBV miR-BART2. A) miR-BART2 is encoded antisense to the BALF5 DNA Polymerase gene. B) The mature microRNA BART2 (marked in red) corresponds to the 5'-arm of the precursor-microRNA hairpin (red). Modified from Pfeffer *et al.*, Science, 2004.

2 AIMS

The aim of this thesis is the characterization of endogenous as well as heterologous RNA sequence elements in the terminal regions of the tick-borne encephalitis virus. This overall goal can be subdivided into three individual projects that address different but interrelated questions:

(I) Unraveling the role of the tick-borne encephalitis virus 3‘-noncoding region in viral translation and replication.

The 3‘-NCR region of tick-borne encephalitis virus is composed of a variable and a core region. In some strains the variable region also contains an internal poly-A stretch. Although the core region has been subject to several studies that amongst others led to the identification of the genome cyclization sequences which are involved in viral RNA replication, less is known about the role of the variable region. Using a sensitive luciferase-based replicon system, mutations and alterations should be engineered in the variable region and tested for their effect on viral input RNA translation and/or RNA replication. This should also include the complete removal of the poly-A tract and the substitution of the variable region with heterologous protein binding elements.

(II) Assessment of the capability of tick-borne encephalitis virus to encode functional microRNAs.

Although it has been shown for several DNA viruses that they encode microRNAs for post-transcriptional regulation of host or viral gene expression, no RNA virus microRNAs have so far been identified. Viruses that replicate in the cytoplasm of a host cell and whose genome is composed of a single RNA molecule are believed to be incompatible with microRNA biogenesis. Reasons for this assumption are that microRNA biogenesis is initiated in the nucleus and characterized by an RNA

cleavage step for the liberation of the microRNA hairpin, which in turn is expected to result in an impairment of RNA replication.

To experimentally address the question whether the lack of identified RNA virus microRNAs necessarily means that these viruses are unable to encode and to generate these regulatory molecules, a heterologous DNA virus microRNA-precursor should be selected and inserted into the genome of TBEV, followed by the characterization of this virus and a screen for generated microRNAs. In addition a dual luciferase reporter assay should be developed to simultaneously monitor viral RNA replication levels and microRNA activity in a replicon system. Thereby the results of this project should contribute to the conceptive understanding of microRNA biogenesis in the context of RNA virus genomes and reach far beyond the used model virus tick-borne-encephalitis virus.

(III) Mutational analysis of the conserved RNA stem-loop sequence elements 5‘-SL2, 5‘-SL3 and 5‘-SL4 in the tick-borne encephalitis 5‘-noncoding region.

The 5‘-terminal region of flaviviruses contains conserved RNA stem-loop motifs that are crucial for RNA replication and translation. It has been shown for instance that the 5‘-SL2 contains the 5‘-part of the genome cyclization sequence. As the essential switch of the genomic RNA from the linear to a circular form is feasible only, if the hairpin retains the possibility to break up, it is very likely that the thermodynamic stability of this structure is of substantial importance in this process.

To clarify which of those hairpins are involved in viral RNA translation and/or replication and to analyze the importance of their thermodynamic stability, stabilizing, destabilizing and hairpin obviating mutations should be introduced and tested for their effect on RNA replication and translation in the luciferase replicon system developed in (I).

3 MANUSCRIPT 1

Analysis of the Effects of Alterations in the Tick-Borne Encephalitis Virus 3'-Noncoding Region on Translation and RNA Replication using Reporter Replicons

Verena M. Hoenninger[a], Harald Rouha[a], Klaus K. Orlinger[a,b], Lisa Miorin [c], Alessandro Marcello[c], Regina M. Kofler[a,d] and Christian W. Mandl[a,e,†]

published in "Virology"

[a]Department of Virology, Medical University of Vienna, Vienna, Austria.
[b]Present address: Baxter AG, Biomedical Research Center, Vienna, Austria.
[c]Laboratory of Molecular Virology, International Centre for Genetic Engineering and Biotechnology (ICGEB), Trieste, Italy.
[d]Present address: Lambda GmbH, Freistadt, Austria.
[e]Present address: Novartis Vaccines and Diagnostics, Inc., Cambridge, MA, USA.
[†]Corresponding author.

Virology 377 (2008) 419–430

Contents lists available at ScienceDirect

Virology

journal homepage: www.elsevier.com/locate/yviro

Analysis of the effects of alterations in the tick-borne encephalitis virus 3′-noncoding region on translation and RNA replication using reporter replicons

Verena M. Hoenninger [a], Harald Rouha [a], Klaus K. Orlinger [a,1], Lisa Miorin [b], Alessandro Marcello [b], Regina M. Kofler [a], Christian W. Mandl [a,*,2]

[a] Clinical Institute of Virology, Medical University of Vienna, Austria
[b] Laboratory of Molecular Virology, International Centre for Genetic Engineering and Biotechnology (ICGEB), Trieste, Italy

ARTICLE INFO

Article history:
Received 11 March 2008
Returned to author for revision
19 April 2008
Accepted 25 April 2008
Available online 3 June 2008

Keywords:
Flavivirus
TBEV
RNA replication and translation
Replicon
Noncoding region

ABSTRACT

The 3′-noncoding region (3′-NCR) of the flavivirus genome includes a variable region that tolerates the insertion of heterologous genetic information. Natural isolates of tick-borne encephalitis virus (TBEV) have particularly long variable regions, which, for some strains, include an internal poly(A) tract. We constructed luciferase reporter replicons of TBEV to analyze the impact of various manipulations of the 3′-NCR on viral RNA translation and replication. The choice of the reporter gene, its position and processing within the viral polyprotein, and the choice of standards were found to be important for obtaining a sensitive and reliable test system. We observed that truncation or complete removal of the internal poly(A) tract, or even the entire variable region, had no significant impact on translation and replication of the RNA in mammalian cell culture. Substitution of the variable region with foreign genetic elements impaired RNA replication to various degrees but generally had no influence on viral translation. Expression cassettes driven by an IRES element inhibited RNA replication more strongly than did repetitive protein-binding elements derived from a bacteriophage, even when the ligand that binds these elements was co-expressed in the cells. Previously identified mutations in the IRES partially relieved this inhibition when introduced into the reporter replicon but provided no evidence for intramolecular competition for translation factors. Impairment of replication appeared to depend more on the type of foreign insert than on its length. These results provide a rational basis for the construction of TBEV-based vectors or vaccines as well as molecular tools for studying flavivirus replication.

Introduction

Flaviviruses (members of the genus *Flavivirus*, family *Flaviviridae*) are small enveloped viruses with a positive-stranded RNA genome (Lindenbach et al., 2007). Most flaviviruses are transmitted by arthropods to vertebrates and replicate in both hosts. The genus can be further divided into two major groups based on the arthropod vector in which the virus can replicate: the mosquito-borne flaviviruses, which include the dengue viruses, yellow fever virus, West Nile virus, and Japanese encephalitis virus, and the tick-borne flaviviruses, of which tick-borne encephalitis virus (TBEV) is the most important human-pathogen (Gubler et al., 2007). Although the overall genome structure, replication strategy, and individual protein functions are conserved between the mosquito- and tick-borne flaviviruses, there are nevertheless important differences that determine their vector specificity and pathogenic potential.

All flaviviruses have a genome consisting of a single positive-sense RNA molecule that is approximately 11 kb long, has a 5′ methylguanylate cap, and lacks a poly(A) tail (Lindenbach et al., 2007; Wengler, 1981; Wengler and Gross, 1978). This genomic RNA is infectious when introduced into cells by transfection and can be used immediately as an mRNA for translation of a single open reading frame that encodes a polyprotein precursor of the three structural (C, prM, and E) and seven nonstructural (NS1, NS2A, NS2B, NS3, NS4A, NS4B, and NS5) proteins. The individual viral proteins are made from the precursor by co- and posttranslational processing by the viral NS2B/3 protease and host-cell proteases (Lindenbach et al., 2007). The genomic RNA is also used as a template for minus-strand RNA synthesis and genome replication (Chu and Westaway, 1985). It can also be packaged into infectious virions after sufficient amounts of the necessary structural components have been synthesized. Genomes from which some or all of the structural genes have been deleted are still able to replicate in the cell, and these artificial replicons have a number of potentially useful applications, both as tools for basic research and for development of gene-delivery systems and vaccines (Gehrke et al., 2005; Khromykh, 2000; Shi et al., 2002; Yoshii et al., 2005). One way in which mosquito- and tick-borne flaviviruses differ is in the sequences and positions of specific functional RNA elements located near the 5′ and 3′ ends of the RNA genome

* Corresponding author. Clinical Institute of Virology, Medical University of Vienna, Kinderspitalgasse 15, A-1095 Vienna, Austria. Fax: +43 1 40490 9795.
E-mail address: christian.mandl@meduniwien.ac.at (C.W. Mandl).
URL: http://www.viroman.at (C.W. Mandl).
[1] Current address: Baxter AG, Biomedical Research Center, Vienna, Austria.
[2] Current address: Novartis Vaccines and Diagnostics, Inc., Cambridge, MA, USA.

0042-6822/$ – see front matter © 2008 Elsevier Inc. All rights reserved.
doi:10.1016/j.virol.2008.04.035

(Kofler et al., 2006; Mandl et al., 1993). These regions are involved in RNA replication, translation, and possibly also genome packaging (Markoff, 2003). Although the specific functions of some elements have been identified, it is often difficult to distinguish between these functions because they are interdependent, and most assay systems measuring the effects of specific mutations on virus growth, viral protein expression, or synthesis of viral RNA are actually measuring a combination of effects.

Using various artificial experimental systems including replicons and reporter constructs, it has already been possible to define the roles of particular conserved RNA elements in the 5′- and 3′-terminal regions of mosquito-borne flaviviruses (Alvarez et al., 2005; Chiu et al., 2005; Deas et al., 2005; Edgil et al., 2003; Filomatori et al., 2006; Holden and Harris, 2004; Holden et al., 2006; Lo et al., 2003; Tilgner et al., 2005; Tilgner and Shi, 2004). However, some of the analogous elements in tick-borne flaviviruses have different sequences and secondary structures from those of the mosquito-borne viruses, and sometimes they are located at a different position in the genome (Mandl et al., 1993; Markoff, 2003). For example, it was shown recently that the RNA cyclization elements that are used in the TBEV replication mechanism are not only different in sequence from those in mosquito-borne flaviviruses, but they are also closer to the ends of the RNA molecule and do not overlap with the coding region (Kofler et al., 2006). Additional experimental systems are therefore needed to functionally map the noncoding regions of tick-borne flaviviruses and to compare them to those of the mosquito-borne flaviviruses.

The 3′-NCR (3′-noncoding region) of TBEV is extremely variable in length, ranging from about 450 to 800 nucleotides (nts) in natural isolates (Wallner et al., 1995). It is further subdivided into a highly conserved "core" region of about 340 nucleotides at the extreme 3′ end and a "variable" region between the core and the end of the coding region. The core consists primarily of conserved RNA secondary structures that are essential for viral replication (Hahn et al., 1987; Mandl et al., 1993, 1998; Pletnev, 2001; Rauscher et al., 1997; Wallner et al., 1995). The variable region lacks sequence conservation and can be of different lengths. In some, but not all, TBEV isolates, it contains an internal poly(A) tract that can range in size from just a few to 200 or more consecutive adenine residues (Mandl et al., 1998, 1991). While it has been shown that the components of the variable region are not essential for virus growth, it still remains to be established whether they might have an effect on the efficiency of RNA replication or translation under some conditions.

TBEV and replicons derived from it have been shown in earlier studies to have potential as a basis for constructing replicating RNA vectors for use in basic research as well as vaccine development, and these vectors have advantages over DNA-based systems in terms of efficiency and safety (Khromykh, 2000; Khromykh and Westaway, 1997). Bicistronic expression systems have been successfully constructed by replacing the variable region with expression cassettes containing an internal ribosome entry site (IRES), but, for reasons that are not yet completely clear, these replicate inefficiently compared to the parental replicon (Jones et al., 2005; Khromykh and Westaway, 1997; Orlinger et al., 2006; Scholle et al., 2004; Shi et al., 2002).

In this study, we have established a luciferase reporter replicon system for TBEV that allows effects of alterations in the genome on translation and RNA replication to be analyzed separately. Using appropriate standards for normalization, we have now been able to do quantitative comparisons between different constructs and thus assess the effects of different changes in the 3′-NCR. We have used this system to do a systematic deletion analysis of the variable region and found that this region does not significantly affect translation or RNA replication efficiency. We have also tested the effects of inserting different expression cassettes and RNA elements that bind specific proteins and found that these also do not affect translation, although they have a negative effect on RNA replication. The results of this study underscore the great practical potential for using the variable region of the TBEV 3′-NCR as a site for insertion of various genes and RNA elements for the purpose of establishing replicating systems for foreign gene delivery, studies of RNA movement and turnover, and vaccine development.

Results

Construction and characterization of reporter replicons

To establish a sensitive reporter system for measuring the level of cap-dependent translation of TBEV replicon RNA, we made plasmid constructs for use as templates for *in vitro* synthesis of capped RNA in which most of the region of the TBEV genome encoding the structural proteins C, prM, and E was replaced in-frame by a luciferase reporter gene. In these constructs, the natural translation initiation site of the viral polyprotein was retained together with the first 17, 27, or 37 amino acids of the capsid protein fused to the reporter (Fig. 1). The rest of the C gene, the entire prM gene, and all of the E gene except for the second transmembrane region (TM2) were deleted. The TM2 portion of E was retained because it also serves as an internal signal sequence for establishing the proper topology of the polyprotein in the ER membrane and targeting of the nonstructural protein NS1 to the secretory pathway (Lindenbach et al., 2007). The sequence was preceded by a recognition sequence (Arg-Arg-Ser) for the replicon-encoded viral NS2B/3 protease

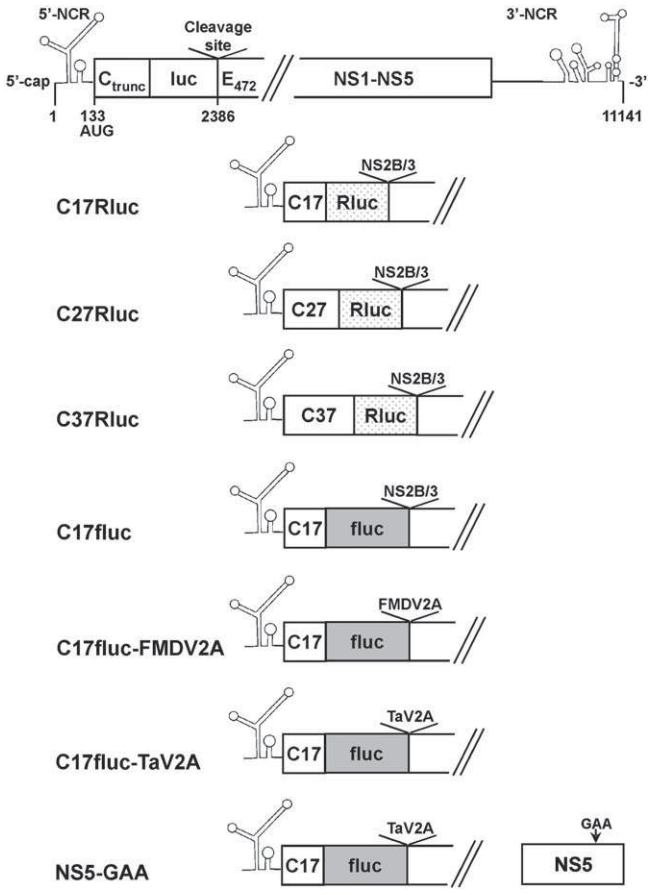

Fig. 1. Schematic diagram of TBEV reporter replicons. A generalized scheme showing the common features of all of the replicons (not to scale) is shown at the top of the figure, and the specific features of the individual constructs are illustrated below it. 5′-NCR, 5′-noncoding region; 3′-NCR, 3′-noncoding region; C_{truc}, truncated capsid gene; luc, luciferase gene; E_{472}, codon 472 of the E protein gene; NS1–NS5, the coding region for nonstructural proteins 1–5; C17, C27, and C37, truncated C genes containing only the first 17, 27, and 37 codons, respectively; Rluc, the *Renilla* luciferase gene; fluc, the firefly luciferase gene; NS2B/3, cleavage site for TBEV NS2B/3 protease; FMDV2A, foot-and-mouth disease virus 2A site; TaV2A, Thosea asigna virus 2A site; GAA, site of GDD-GAA mutation in the NS5 polymerase active site.

to allow the luciferase to be liberated posttranslationally from the polyprotein precursor. In some constructs, a 2A sequence from foot-and-mouth disease virus or from Thosea asigna virus was inserted in order to compare the efficiency of these different systems. In these experiments, two different luciferase genes were tested as reporter genes: *Renilla* luciferase (Rluc) and firefly luciferase (fluc).

When BHK-21 cells were transfected by electroporation with capped replicon RNA made by *in vitro* transcription of a construct containing the first 17 codons of the C region fused to firefly luciferase (C17fluc, Fig. 1), there was a biphasic pattern of luciferase activity over a time course of 72 h (Fig. 2A). The first peak, which appeared within the first 2 h after transfection, shows that the initial input RNA was translated in the cell, yielding a functional luciferase enzyme. After a subsequent decrease in luciferase activity indicative of a decrease in translation (probably due to degradation of the input RNA), a second, higher peak of luciferase activity was detected which began to increase around 12 h after transfection. This second peak represents luciferase that was expressed from newly synthesized sense-strand RNA after replication of the input RNA. Similar biphasic profiles have been observed previously with reporter replicon systems derived from mosquito-borne flaviviruses (Alvarez et al., 2005; Filomatori et al., 2006; Holden et al., 2006; Lo et al., 2003).

Surprisingly, in contrast to the C17fluc construct, an analogous construct that instead contained the luciferase gene from *Renilla*, C17Rluc (Fig. 1), did not yield a biphasic profile, giving rise to only the first peak, corresponding to translation of the input RNA (Fig. 2B). This observation indicates that although the C17Rluc RNA is competent for cap-dependent translation and expression of functional *Renilla* luciferase, this RNA, unexpectedly, is not able to replicate efficiently in BHK-21 cells. This lack of efficient replication was also reflected by a lack of detectable NS1 protein in immunofluorescence assays carried out three days after transfection (Fig. 2C).

We speculated that the C17Rluc fusion might have resulted in a fortuitous disruption of the local RNA secondary structure that interfered with RNA replication. We therefore made additional constructs in which the Rluc gene was inserted at a position farther downstream, reasoning that increasing the distance between the luciferase gene and the putative RNA secondary structure element in the 5′ portion of the genome might alleviate this problem. The first of these, C27Rluc, contained the first 27 amino acids of C fused to the reporter gene, and the second, C37Rluc, contained 37 amino acids (Fig. 1). Interestingly, RNA replication competence was indeed observed when capped RNA derived from each of these constructs was used to transfect BHK-21 cells, with both constructs yielding a biphasic profile similar to the one obtained with C17fluc (Fig. 2B). Both of these also yielded positive results in the immunofluorescence assay with anti-NS1 antibody, in contrast to C17Rluc (Fig. 2C). This demonstrates that although insertion of the Rluc gene is tolerated in some contexts, the C17Rluc fusion apparently interferes with replication of the replicon RNA.

For reasons of consistency and comparability of data, we chose to use C17fluc constructs in all of the experiments discussed below, because the C17 replicon used for constructing C17fluc had been extensively characterized in an earlier study (Kofler et al., 2006).

Because the constructs described above rely on the viral NS2B/3 protease encoded in the replicon itself for release of the luciferase reporter enzyme from the polyprotein precursor, we decided to test whether the efficiency of reporter expression (and thus the sensitivity of the system) could be improved by introducing alternative processing sites after the reporter gene that would free the replicon from the constraint of having to provide its own processing enzyme. This approach has been used successfully in earlier studies with other flavivirus reporter replicons (Alvarez et al., 2005). For this purpose, two different sites were engineered into the region of C17fluc between the C-terminus of the fluc gene and the NS1 signal peptide (see Materials and methods for details). The first of these was the 2A site from foot-and-mouth disease virus (FMDV2A), which introduces a gap in the polyprotein during translation by a "topGo" mechanism rather than a proteolytic cleavage event (Atkins et al., 2007; de Felipe et al., 2003; Donnelly et al., 2001b). The second was the analogous 2A site from Thosea asigna virus (TaV2A) (Donnelly et al., 2001a).

As shown in Fig. 3A, when the relative amounts of fluc activity were compared 3 h after transfection of BHK-21 cells with capped RNA made from these constructs, the FMDV2A and the TaV2A replicons both yielded considerably higher levels of luminescence than did the original C17fluc construct containing the TBEV NS2B/3 cleavage site. The luminescence intensity was more than two-fold higher with the FMDV2A construct and about three-fold higher with the TaV2A construct. Furthermore,

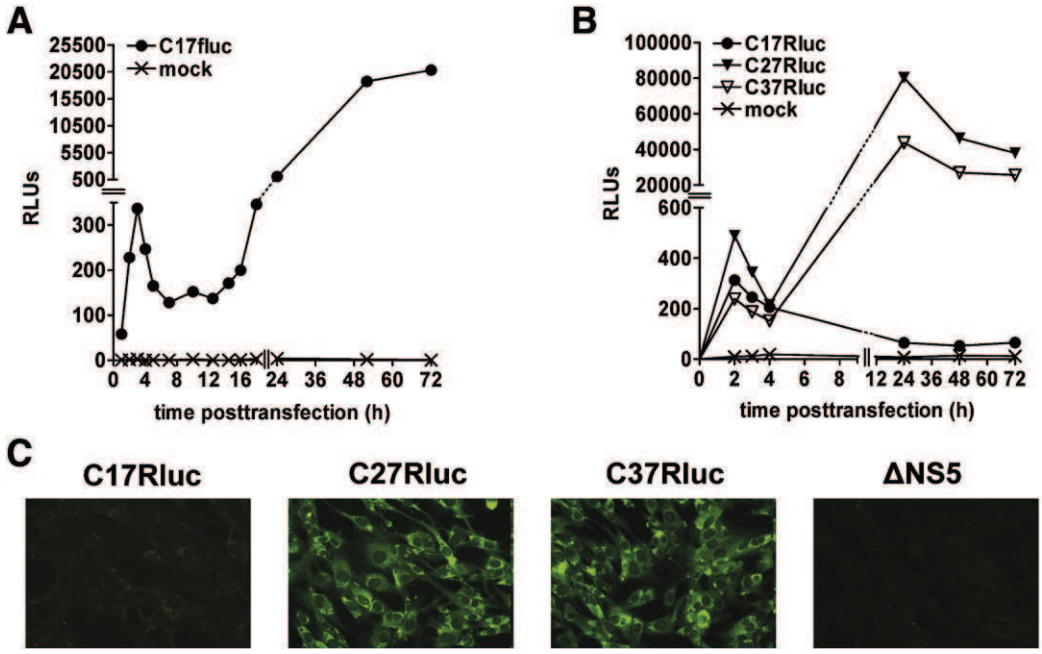

Fig. 2. (A) Kinetics of firefly luciferase activity in BHK-21 cells transfected with C17fluc. Mock, mock-transfected cells; RLUs, relative light units. (B) Kinetics of *Renilla* luciferase activity in BHK-21 cells transfected with C17Rluc, C27Rluc, or C37Rluc. (C) NS1 expression measured by immunofluorescence with an NS1-specific monoclonal antibody three days after transfection with replicon C17Rluc, C27Rluc, or C37Rluc, or a replication-deficient mutant, ΔNS5 (Kofler et al., 2006), which was used as a control.

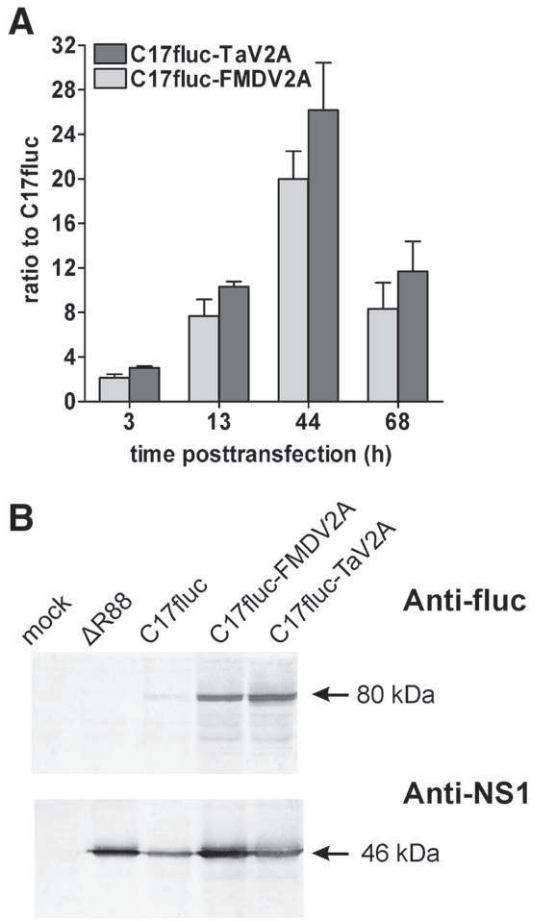

Fig. 3. Effect of different processing sites at the C-terminus of the firefly luciferase gene. (A) Relative luciferase activity at different time points in BHK-21 cells transfected with C17fluc-TaV2A or C17fluc-FMDV2A expressed as a ratio to that of C17fluc (using the NS2B/3 protease site) at the corresponding time point. Error bars represent the standard deviation from a minimum of two independent experiments. (B) Relative processing efficiency of C17fluc, C17fluc-FMDV2A, and C17fluc-TaV2A. Cells harvested 48 h after transfection were analyzed by immunoblotting using specific antibodies against firefly luciferase (Anti-luc) or the TBEV NS1 protein (Anti-NS1). "Mock" is a mock-transfected control, and "ΔR88" is a prM-cleavage-deficient TBEV mutant (Elshuber and Mandl, 2005) used as a positive control for NS1 expression and processing.

significant differences in luminescence intensity were observed at later time points, after RNA replication had taken place. As shown in Fig. 3A, the luminescence yield 44 h after transfection was about 20 times higher with the FMDV2A construct and more than 25 times higher with the TaV2A construct than with the original construct containing the NS2B/3 cleavage site. This result was confirmed by immunoblotting 48 h after transfection with antibodies specific for fluc or the TBEV NS1 protein (Fig. 3B). Significantly more fluc was present in the cells at this time point when the gene was followed by the TaV2A or the FMDV2A site instead of the NS2B/3 site suggesting a more efficient release of fluc. It seems reasonable to conclude that the faster processing of the fluc-NS1 junction region greatly increases the sensitivity of this reporter system. We therefore chose the more efficient of these two, C17fluc-TaV2A, for use in further experiments investigating the effect of changes in the TBEV 3′-NCR on translation and RNA replication.

Standardization for quantitative comparisons

Luciferase reporter systems are very sensitive tools that can be used to make quantitative comparisons of translation and replication levels with different constructs, but for such comparisons, proper standardization is needed to normalize factors such as transfection efficiency. This is typically accomplished by using two different luciferase enzymes that use different substrates — one as the main reporter and the other, provided by cotransfection with a control construct, to provide a quantitative measure of transfection efficiency (Schagat et al., 2007). In the experiments described below, firefly luciferase was used as the reporter in the C17fluc-TaV2A replicon, and this was used together with either RNA or DNA containing the *Renilla* luciferase gene as a transfection control for normalization. For experiments examining early time points corresponding to the translation of input RNA (up to 12 h posttransfection), capped mRNA transcribed *in vitro* from the Rluc expression plasmid phRL-SV40 (Promega) was used as the transfection control, whereas for measuring translation of replicated RNA at later time points, after most of the input RNA had already been degraded, the expression plasmid itself (DNA instead of RNA) was used as the control. In our hands, Rluc expression in cells transfected with plasmid phRL-SV40 was detectable at 6 h after transfection and for the entire time thereafter that expression was monitored (70–96 h) (data not shown).

In order to confirm the correlation of the first and the second peak to translation and replication, respectively, fluc activity was monitored in BHK-21 cells transfected with C17fluc-TaV2A replicon RNA and compared to a replication-deficient variant of this replicon, NS5-GAA, and an *in vitro*-transcribed but uncapped C17fluc-TaV2A control RNA. NS5-GAA was identical to C17fluc-TaV2A except that it contained a mutated active-site motif (GDD-to-GAA) in the polymerase domain of NS5. This experiment demonstrated that the GDD-to-GAA mutation, which abolishes viral RNA replication, but not the ability of the RNA to be translated, yielded a profile in which the first (translation) peak was unchanged but the second (replication) peak was absent. Conversely, the uncapped replicon control, which initially was translated inefficiently due to the lack of a 5′-cap, produced only the later peak after new capped copies of this RNA had been produced in the cells (Chiu et al., 2005). This result could be reproduced in an experiment in which different time points were analyzed (not shown). The reporter replicon system therefore allows alterations affecting viral RNA replication to be distinguished from those affecting translation.

The correlation between luciferase activity and RNA replication was confirmed in a separate kinetics experiment in which the fluc activity of cells transfected with capped C17fluc-TaV2A and NS5-GAA RNA closely paralleled the number of copies of the RNA genome measured at different time points by quantitative PCR (Fig. 4B).

Effect of deletions in the variable region of the 3′-NCR

We next used the C17fluc-TaV2A reporter replicon to examine whether the variable region of the 3′-NCR plays a role in the efficiency of cap-dependent translation or replication of the viral genomic RNA. Some natural isolates of TBEV contain large internal poly(A) tracts in this region, whereas others may contain either short poly(A) stretches or none at all (Mandl et al., 1991; Wallner et al., 1995). Although some studies have shown that the poly(A) element can be deleted and is therefore not essential (Mandl et al., 1998), it has not been clear whether it might nevertheless provide a subtle advantage in either RNA replication or translation efficiency.

To test this question, we made three additional constructs in which different amounts of the variable region were removed from the reporter replicon, which initially contained a stretch of 49 adenines derived from the original infectious clone of TBEV prototype strain Neudoerfl (Mandl et al., 1997). In the first of these (replicon 9A), all but 9 adenines were removed, in the second (replicon ΔpolyA), all of the poly(A) tract was removed, and in the third (replicon Δvar), the entire variable region (nucleotides 10378 to 10795) was deleted (Fig. 5A). These constructs were used to make capped RNA transcripts *in vitro*, which were then used together with the appropriate Rluc control RNA or plasmid for transfection of BHK-21 cells. For comparison of translation efficiency of the different constructs, fluc activity was measured 3 h after transfection and normalized using the Rluc RNA

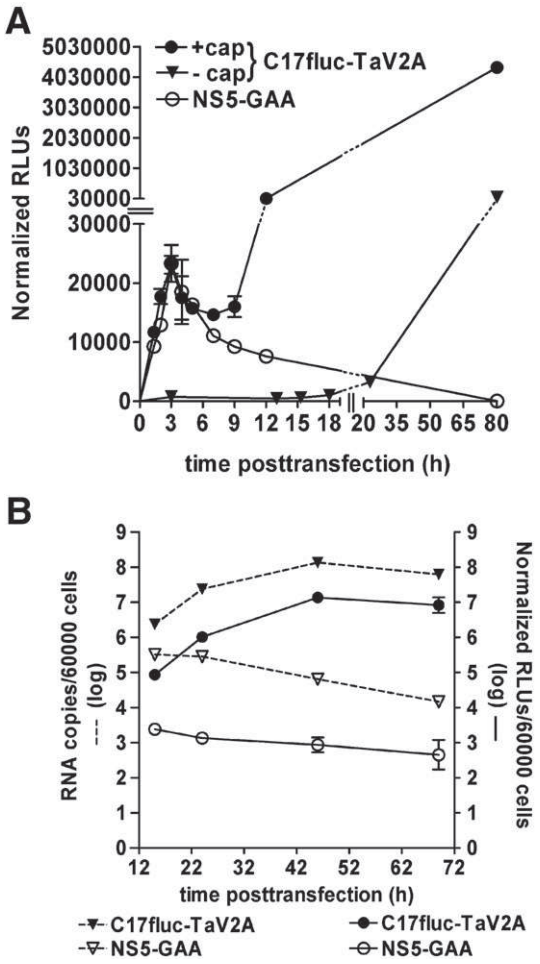

Fig. 4. Normalization and biphasic kinetics of firefly luciferase activity in BHK-21 cells transfected with C17fluc-TaV2A. (A) BHK-21 cells were transfected with capped (+cap) or uncapped (−cap) C17fluc-TaV2A RNA or capped NS5-GAA RNA. Luciferase values were normalized to an internal RNA control. (B) Comparison of luciferase activity (dashed lines with triangles) with RNA copy number as measured by quantitative PCR (solid lines with circles) at different time points. For the luciferase data, logarithmic means from two separate experiments are shown. Error bars represent the standard deviation from two independent experiments.

standard. RNA from the replication-defective NS5-GAA construct described in the previous section was included as a control.

As shown in Fig. 5B, the level of expression of luciferase from the input RNA was essentially identical for all of the constructs, indicating that the presence or absence of the poly(A) tract does not significantly affect the efficiency of cap-dependent translation from the viral polyprotein start site. Although the somewhat lower luciferase values obtained with Δvar do suggest that deletion of the entire variable region might have caused a slight reduction, this difference was within the error range of our test system. When luciferase levels were examined at later time points (13–68 h after transfection), it was again observed that none of these deletions had any observable effect on fluc expression (Fig. 5C), indicating that neither translation nor RNA replication efficiency is affected by removing part or all of the variable region.

Effect of replacing the variable region with expression cassettes

In earlier studies investigating the use of TBEV replicons for making bicistronic expression systems, it was observed that insertion of expression cassettes containing an internal ribosome entry site from encephalomyocarditis virus (EMCV IRES) into the variable region of the 3′-NCR resulted in reduced levels of RNA replication and expression of viral genes from the natural cap-dependent translation start site

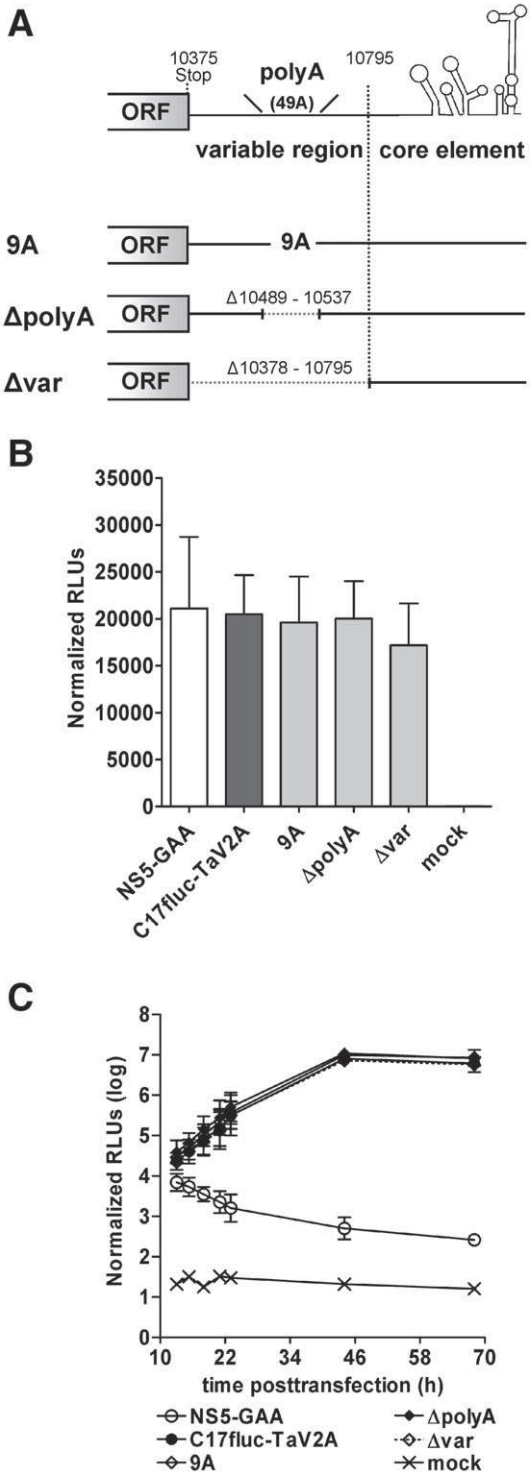

Fig. 5. Lack of effect of deletions in the variable region of the 3′-NCR on translation and replication. (A) Schematic diagram showing the positions of the deletions. The original construct contained 49 adenine residues, of which all but nine were deleted in replicon 9A. All 49 adenines (nucleotides 10489–10537) were deleted in replicon ΔpolyA, and the entire variable region (nucleotides 10378–10795) was deleted in replicon Δvar. (B) Comparison of levels of translation of input RNA from the different constructs using normalized luciferase data obtained 3 h posttransfection. The error bars show the standard deviation from at least three different experiments, and the scale of the *y*-axis is linear. (C) Normalized luciferase activity (log scale) at later time points (10–70 h posttransfection), corresponding to the kinetics of RNA replication. Capped NS5-GAA RNA, which can be translated (see panel B) but cannot replicate because its RNA polymerase is nonfunctional, was used as a control.

(Orlinger et al., 2006) and that certain point mutations and small insertions in the IRES element that decreased the translation efficiency of the IRES itself mitigated these effects (Gehrke et al., 2005; Orlinger et al., 2007). In these studies it was speculated that binding of a ribosome to the IRES in the 3′-NCR might interfere with translation of the cap-dependent cistron by a different ribosome, block the synthesis of minus-strand RNA by the viral polymerase, or possibly both. Here, we were able to address this question using the newly established reporter replicon system.

The following expression cassettes from earlier studies were used for these experiments: 1) IRES-eGFP (Gehrke et al., 2005), which encodes an enhanced green fluorescent protein (eGFP) under the control of an EMCV IRES, 2) IRES-ME (Orlinger et al., 2006), which contains the region encoding the TBEV prM and E proteins under the control of an EMCV IRES, and 3) $IRES_{(A771C)}ME$ and 4) $IRES_{(26A)}ME$ (Orlinger et al., 2007), which are variants of IRES-ME that were selected during propagation of a self-replicating artificial bicistronic TBEV genome, TBE-bc. The first of these contains an A–C substitution at nucleotide position 771 in the oligo(A) loop of the JK stem–loop structure of the IRES element, and the second contains an insertion of 19 additional adenines in this same oligo(A) loop, thus increasing the total number in the original loop from 7 to 26. In the context of the artificial bicistronic TBEV, both of these were shown to provide a growth advantage over the parental construct while weakening the translation capacity of the IRES itself (Orlinger et al., 2007).

Each of the expression cassettes described above was cloned into the C17fluc-TaV2A reporter replicon (Fig. 6A) as described in Materials and methods, and the resulting cDNAs were used as templates for *in vitro* synthesis of capped RNA. Equimolar amounts of each RNA were used for transfection of BHK-21 cells, together with the appropriate Rluc standard for normalization, as discussed above, and fluc and Rluc activity were measured at different time points after transfection. As controls, the parental reporter replicon and the replication-defective mutant NS5-GAA were also used.

As shown in Figs 6B and C the normalized fluc activity at 3 h posttransfection was similar for all of the constructs examined, indicating that, similar to what was observed with the deletions in the variable region, the expression cassettes tested here clearly did not have a strong effect on the efficiency of cap-dependent translation. Furthermore, the IRES mutations that had been selected previously (A771C and 26A) did not demonstrate significantly increased efficiency of translation of the input RNA (Fig. 6C). This means that the hypothesis that mutations causing weaker binding of the ribosome to the IRES had increased the fitness of the original bicistronic RNA by reducing competition for ribosomes between the IRES and cap cistrons is not supported.

In contrast to the 3-hour time point, significant differences were found at later time points, suggesting differences in the rate of accumulation of RNA in the cell. As shown in Fig. 6B, the reporter replicons containing the IRES-eGFP cassette and the IRES-ME cassette both displayed reduced luciferase expression compared to the parental replicon: with the IRES-eGFP construct it was 10–50-fold (1–1.7 log) lower, and with IRES-ME it was 10–440-fold (1-2.6 log) lower. Furthermore, in both of these cases, replication proceeded with a delay when compared to the replicon without an insertion. Interestingly, reporter replicons containing the IRES-ME cassette with the IRES mutations A771C or 26A had about 10 times higher luciferase levels than the IRES-ME construct with a normal IRES, suggesting that these

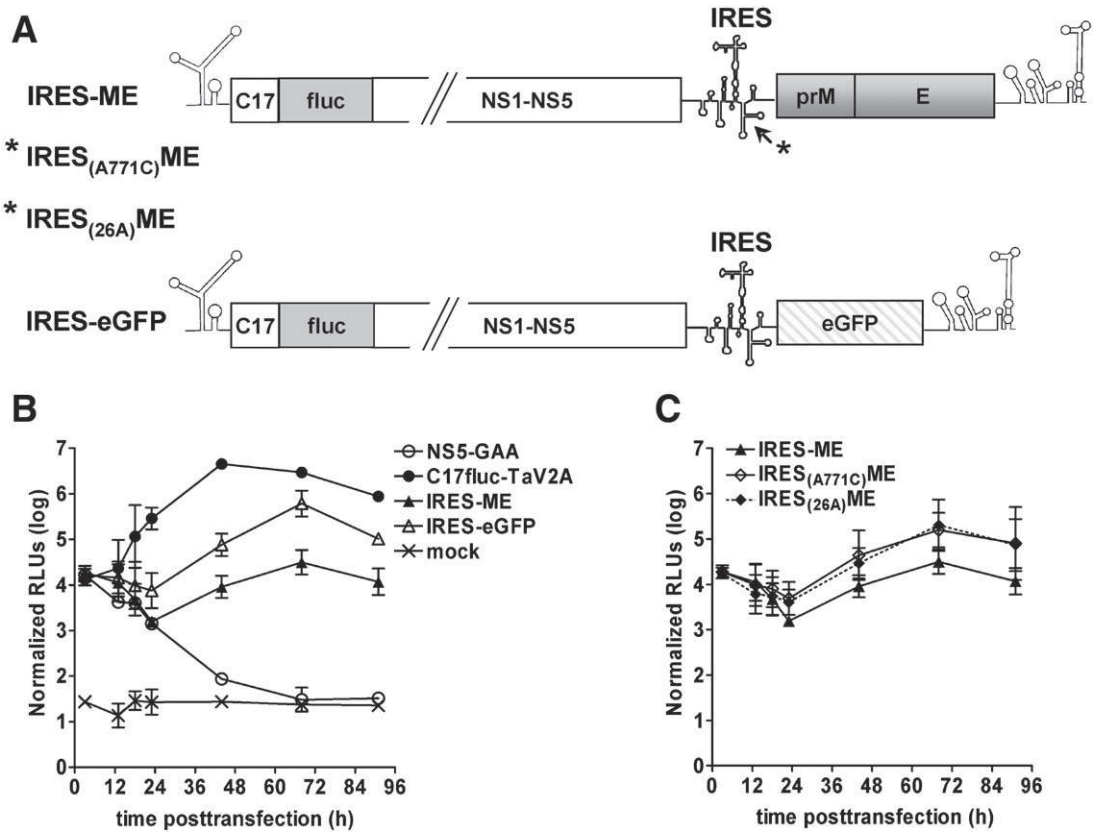

Fig. 6. Effect of IRES-containing expression cassettes in the 3′-NCR on cap-dependent translation and RNA replication. (A) Schematic diagram of the C17fluc-TaV2A derivatives IRES-ME and IRES-eGFP. The position of the EMCV IRES in each construct is indicated, and its secondary structure is depicted. The position of the A771C and 26A mutations within the IRES is indicated by an asterisk. IRES-ME, $IRES_{(A771C)}ME$ and $IRES_{(26A)}ME$ contain the region encoding the TBEV prM and E proteins, and IRES-eGFP contains the gene for the enhanced green fluorescent protein (eGFP). (B) Kinetics of reporter expression in BHK-21 cells transfected with IRES-ME, mutant $IRES_{(A771C)}ME$, or mutant $IRES_{(26A)}ME$, shown on a logarithmic scale. (C) Kinetics of reporter expression in BHK-21 cells transfected with IRES-ME, IRES-eGFP, C17fluc-TaV2A, or replication-deficient NS5-GAA, shown on a logarithmic scale. Error bars represent the standard deviation from a minimum of three independent experiments.

mutations had a positive effect on RNA replication efficiency (Fig. 6C). These results together imply that the presence of an expression cassette in the 3′-NCR, and probably the IRES itself, interferes with RNA replication, but it does not influence translation from the cap-dependent start site at the 5′ end.

Effect of replacing the variable region with protein-binding elements

In addition to its previously demonstrated usefulness as a site for inserting genes for foreign protein expression, the variable region of the TBEV 3′-NCR also has the potential to be used as a site for inserting a specific RNA–protein interaction sequence for GFP-tagged cognate ligands. In fact, it has been reported that insertion of recognition elements from the bacteriophage MS2 coat protein allows RNA molecules to be detected in cells expressing an MS2 coat protein fused to the green fluorescent protein (GFP) (Bertrand et al., 1998). This method allowed for the first time the study of mRNA biogenesis in real time in live cells (Boireau et al., 2007; Darzacq et al., 2007). We therefore made constructs in which the variable region of the TBEV reporter replicon was replaced by 12 or 24 copies of the 19-nucleotide MS2 repeat element to study the effect of these elements, both in the presence and absence of the EYFP-MS2 (enhanced yellow fluorescence protein) fusion protein, on translation and replication of the replicon RNA using the luciferase reporter assay (Fig. 7A). As in the previous experiments, capped RNA was made *in vitro* and used together with the transfection standard for electroporation of BHK-21 cells, but in addition, some of the cells were also simultaneously transfected with plasmid pEYFP-MS2, which contains the gene for the bacteriophage MS2 core protein fused to EYFP driven by the CMV promoter (see accompanying paper by Miorin et al., submitted). As shown in Fig. 7B, neither the 12- nor the 24-repeat insertion had a significant effect on translation of the input RNA, and normalized luciferase levels 3 h after transfection were similar for these constructs and the controls. At later time points, however, luciferase levels remained somewhat lower (about ten-fold) in cells transfected with RNAs containing the repeats than in cells transfected with the parental C17fluc-TaV2A construct (Fig. 7B), suggesting a modest effect of these elements on RNA replication. This effect does not appear to be proportional to the size of the inserted sequence, since 12xMS2 and 24xMS2 yielded essentially identical curves.

In cells in which 12xMS2, 24xMS2, or the parental construct were cotransfected with the plasmid encoding the EYFP-MS2 protein, no additional effect was observed at any of the time points (Fig. 7C). There is therefore no indication from this set of experiments that EYFP-MS2, when expressed in this manner, interferes at all with translation or replication of the replicon RNA, regardless of whether or not there are copies of its target sequences present in the 3′-NCR of the replicon. Together, these results support the potential use of TBE virus or replicon RNA containing MS2 repeats to study viral RNA in living cells using the EYFP-MS2 reporter.

Discussion

In this study, a functional analysis of the variable region of the TBEV 3′-NCR was performed using a simple and sensitive system to measure both replication and primary translation of self-replicating RNA. The variable region of most strains of TBEV is significantly longer than in mosquito-borne flavivirus genomes (Bryant et al., 2005; Gritsun et al., 1997; Ma et al., 2003; Mandl et al., 1998, 1991; Markoff, 2003; Yang et al., 2004). Some strains, such as the prototypic strain Neudoerfl, carry an internal poly(A) region of variable length which may further elongate during viral growth (unpublished observation).

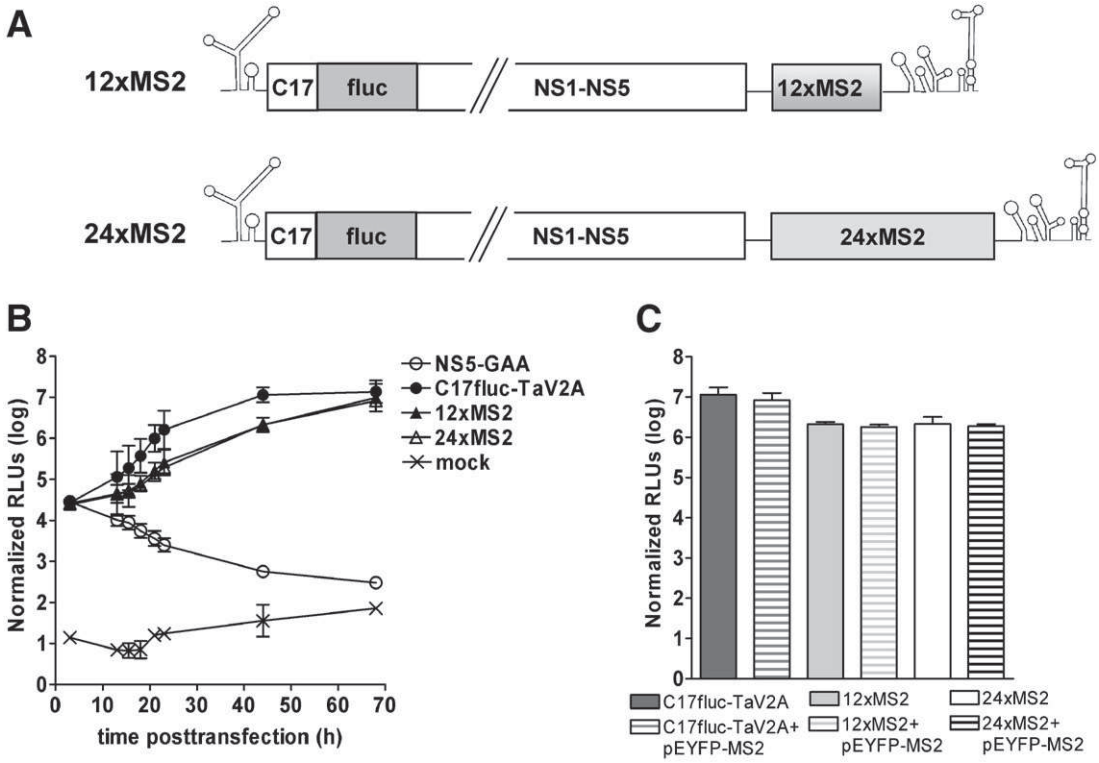

Fig. 7. Effect of insertion of MS2 coat protein-binding sites into the 3′-NCR on cap-dependent translation and RNA replication. (A) Schematic diagram of C17fluc-TaV2A derivatives 12xMS2 and 24xMS2, which contain 12 and 24 copies, respectively, of the MS2 recognition site. (B) Kinetics of reporter expression in BHK-21 cells transfected with 12xMS2, 24xMS2, C17fluc-TaV2A, or replication-deficient NS5-GAA, shown on a logarithmic scale. Error bars represent the standard deviation from a minimum of three independent experiments. (C) Lack of interference of enhanced yellow fluorescent protein-tagged MS2 coat protein (EYFP-MS2) with luciferase expression from reporter constructs containing binding sites for this protein. BHK-21 cells were either transfected with C17fluc-TaV2A, 12xMS2, or 24xMS2 alone or cotransfected with a mixture of replicon RNA and plasmid pEYFP-MS2, as indicated below the figure. The data, shown on a logarithmic scale, are normalized luciferase values measured 44 h after transfection. A similar lack of effect of coexpression with pEYFP-MS2 was also observed at 13, 15, 18, 21, 23 and 68 h posttransfection (data not shown).

On the other hand, repeated passages can also result in spontaneous deletions of parts of the variable region, including the poly(A) tract (Mandl et al., 1998). Strains with shorter variable regions, or that entirely lack this region, were previously found to maintain viability in cell culture and virulence in mice (Mandl et al., 1998). Here, we wanted to find out whether the presence and length of the variable region and its poly(A) tract had a measurable influence on the efficiency of translation and/or RNA replication of TBEV. We did not find any such influence in our experiments, indicating that these elements are entirely dispensable in BHK-21 cells. This finding contrasts with recent results obtained with dengue viruses 1 and 2 (Alvarez et al., 2005; Tajima et al., 2007). Deletion of the variable region of these mosquito-borne flaviviruses was shown to impair viral growth in mammalian cells such as BHK-21 cells. Our findings were unexpected also with regard to the fact that the 3′-terminal poly(A) stretches of cellular mRNAs are targeted by specific cellular factors (Grange et al., 1987; Mangus et al., 2003; Sachs et al., 1997; Tarun and Sachs, 1996) and influence translation efficiency (Jacobson and Favreau, 1983; Sachs et al., 1997). Furthermore, hepatitis C virus, another member of the family *Flaviviridae* possesses within the 3′-NCR a poly(U/UC) tract. The length of which is decisive for achieving maximal RNA amplification (You and Rice, 2008). Apparently, no such role is played by the internal poly(A) stretch of TBEV, at least when tested in BHK-21 cells. We have also tried to investigate the properties of our replicons in a tick cell line, but we were unable to establish an adequate RNA transfection protocol for these cells.

The observed lack of function of the TBEV variable region is a very welcome finding with respect to the potential of this viral genome to accept foreign genetic information. We and others have previously demonstrated that expression cassettes under the control of a heterologous IRES element can be inserted in place of this element in the context of infectious genomes or replicons (Gehrke et al., 2005; Hayasaka et al., 2004; Orlinger et al., 2006, 2007; Yoshii et al., 2005). Using constructs in which the TBEV surface proteins required the foreign IRES for their translation, we were recently able to select mutations in the IRES itself that enhanced the fitness of such bicistronic viruses (Orlinger et al., 2007). In that study, the normal IRES sequence was found to interfere with viral replication, but it remained unclear whether this was primarily due to an inhibition of RNA replication or competition of the IRES with cap-dependent translation. The results obtained with the luciferase reporter indicate that cap-dependent translation is not affected by the insertion of the IRES, but RNA replication is significantly impaired. The results also suggest that the disturbance of RNA replication is even stronger with longer expression cassettes. The previously identified IRES mutations lessen the impact of the IRES on RNA replication but, unexpectedly, have no influence on cap translation. One may hypothesize that IRES-mediated binding of the input RNA to the ribosome may prevent the RNA from entering compartments in which RNA replication can take place, but does not impair its cap-dependent translation.

The utility of replacing the variable region with foreign genetic elements is not restricted to expression cassettes. We also inserted repetitive sequence elements that serve as specific recognition sequences for a phage MS2 capsid protein. Again, these insertions did not interfere with cap-dependent translation. Notably, they had significantly less of a negative impact on RNA replication than the IRES expression cassettes. Moreover, in the case of these noncoding sequences, there was no relationship observed between the length of the insert and disturbance of RNA replication. A sequence of 1484 nucleotides caused a moderate reduction in replication that was equal to that of a 742-nucleotide-long sequence. Thus, the capacity of the TBEV genome to accept foreign sequence elements in place of the variable region appears to be high. This is in good agreement with the fact that some TBEV strains have very long variable regions, which in the light of our results may be regarded as neither necessary nor harmful for translation and replication. Maybe this indicates an important functional difference between TBEV and the mosquito-borne flaviviruses, which generally have shorter variable regions. Co-expression of an EYFP-MS2 protein did not cause a further reduction of RNA replication, although FACS analysis demonstrated that at least 40% of the cells expressed this protein, and in a separate study, the EYFP-MS2 fusion protein has been found to bind efficiently to the TBEV replicons containing the specific repeat sequence insertions (Miorin et al., submitted, and unpublished data). Apparently, binding of a cytoplasmic, soluble protein such as MS2 is well tolerated, suggesting that such systems can be used to localize and quantify RNA synthesis *in vivo*.

In addition to the exploration of the role of the TBEV variable region and its potential to be substituted by various foreign genetic elements, this study yielded several methological insights which may be of more general importance for the generation and optimization of replicating RNA reporter systems:

(i) The choice of the reporter gene, firefly luciferase versus *Renilla* luciferase, can cause a dramatic difference in the replicative ability of the system. The different outcomes obtained with constructs containing the two luciferases, which are usually thought to be functionally equivalent, were striking and unexpected. Whereas the firefly construct replicated well, the *Renilla* construct essentially did not replicate. Great care was taken to exclude that any unintended mutations elsewhere in the genome were responsible for this. Remarkably, primary translation was not affected at all by the introduction of the *Renilla* gene. *In silico* RNA folding analysis yielded no explanation for these observations. No significant changes in the formation of RNA secondary structure or the cyclization of the genome were predicted to be caused by the insertion of the *Renilla* gene (C. Thurner, unpublished observation). When 30 nucleotides (10 codons) of the originally deleted capsid protein sequence were re-inserted into the construct (the C27-Rluc construct), RNA replication was restored, suggesting that not the insertion of the *Renilla* gene *per se*, but its proximity to the 5′-terminus was causing the problem. Possibly, an RNA structure present in the *Renilla* coding sequence interferes with the RNA replication mechanism, but not translation, if it is in spatial proximity to the 5′-NCR. This unexplained inhibitory effect observed with this gene may be relevant for other systems as well and should be considered by researchers working with similar self-replicating RNA constructs.

(ii) The sensitivity of the system depends strongly on the choice of the cleavage mechanism by which the reporter protein is separated from the polyprotein. The direct comparison between the cleavage site for the viral protease NS2B/3 and the FMDV2A and TaV2A sites indicated that the highest reporter gene expression was achieved with the TaV2A site. The TaV2A sequence turned out to be somewhat more efficient than the FMDV2A sequence, which is widely used in various expression systems. These two sites very rapidly introduce a break in the growing polypeptide chain by a “StopGo” mechanism, as demonstrated recently for the FMDV2A sequence (Atkins et al., 2007). In contrast, cleavage of the NS2B/3 site depends on prior translation and accumulation of the protease. Furthermore, in some cases the site may not be efficiently recognized by the protease, resulting, as demonstrated in our experiments, not only in release of low levels of the reporter gene, but also in reduced formation of protein NS1, which may in turn impair the formation of replication complexes. While different cleavage mechanisms may perform best in different expression systems, our observations illustrate the necessity to evaluate this process in order to achieve optimal sensitivity of the system.

(iii) Standardization of firefly luciferase assays to study flavivirus translation and replication is critical to obtain a comparable set

of data. However, the reporter gene expression needs to be monitored for 96 h. Therefore, it is not possible to rely only on the use of *in vitro*-transcribed *Renilla* luciferase RNA because it becomes undetectable after a few hours, whereas expression from a plasmid construct becomes detectable only at later times. The use of both RNA and DNA as internal standards resolves this issue and provides a convenient method to study early time points after transfection, using *Renilla* luciferase RNA, as well as late time points, using an expression plasmid.

In conclusion, the TBEV reporter replicon has proven to be a valuable tool for the investigation of specific sequence elements that govern RNA translation and replication. Future studies will target the stem–loop structures and the embedded circularization elements close to the genomic termini. Analysis of viral mutants has revealed that a variety of specific genomic determinants that attenuate the virulence of TBEV, and self-replicating, but non-infectious TBEV RNAs that produce subviral particles have been developed (Kofler et al., 2004). Both of these approaches may be useful for the development of new and safe live, replicating flavivirus vaccines. Finally, TBEV shows good potential as a backbone for the generation of infectious or non-infectious gene vectors. For all of these approaches it is very important to better define, understand and distinguish from each other molecular elements and specific mutations that influence translation and/or RNA replication. Ultimately, a better definition of such determinants will lead to the ability to optimize and fine-tune new vaccines and vectors with respect to their replication and protein expression capacities.

Materials and methods

Reporter replicon construction

All of the replicon constructs described in this study are derivatives of pTNd/c, an infectious cDNA clone of TBEV strain Neudoerfl (GenBank accession number U27495), the prototype of the Western subtype (Mandl et al., 1997), and were constructed by making modifications to a previously described replicon construct, C17 (Kofler et al., 2006). This construct contains the first 17 codons of the N-terminal region of the capsid protein, corresponding to nucleotides 133–183 (numbering according to the full-length sequence of strain Neudoerfl), followed by a large deletion extending from the beginning of the prM gene through most of the region coding for the E protein (nucleotides 184–2386). The deleted region was replaced by a small artificial multiple cloning site (MCS) followed by a short recognition sequence for the TBEV protease NS2B/3. C17 and all of its derivatives contain a T7 promoter upstream of the viral sequence to enable *in vitro* transcription of the replicon RNA.

The sequences of the oligonucleotide primers used in this study are given in Supplementary Table 1, and the different replicon constructs are depicted in Fig. 1.

The reporter replicon C17Rluc was made by first amplifying the *Renilla* luciferase (Rluc) gene (933 nts) from plasmid phRL-SV40 (Promega) by PCR using primers F-PacI_Rluc and R-NotI_Rluc, trimming the PCR product with PacI and NotI, and inserting it into the MCS of C17.

Replicons C27Rluc and C37Rluc were made by replacing a portion of C17Rluc, extending from a SalI site upstream of the T7 promoter to the PacI site between the truncated capsid gene and the luciferase gene, with an otherwise identical fragment containing a longer extension of the C gene at its 3′ end. This was accomplished by amplifying a region of a related replicon construct containing all of the capsid protein except for the 16 carboxy-terminal codons (pTNd/ΔME) (Gehrke et al., 2003) using the forward primer F-SalI together with the reverse primer R-C27_PacI (for C27Rluc) or R-C37_PacI (for C37Rluc) to generate the appropriate PCR product, which was then trimmed with SalI and PacI and inserted in place of the shorter SalI–PacI fragment of C17Rluc.

To generate C17fluc, the region containing the *Renilla* luciferase gene was removed from the C17Rluc plasmid by digestion with PacI and NotI and then replaced by a firefly luciferase (fluc) gene (1649 nts) that had been amplified by PCR from plasmid pGL3 (Promega) using the forward and reverse primers (F-PacI_fluc and R-NotI_fluc) containing restriction sites for PacI and NotI, respectively.

To construct C17fluc-FMDV2A, a 60-nt region encoding the 2A site of foot-and-mouth disease virus was amplified by PCR from plasmid MSCV-GFP2AHOXB4 (Klump et al., 2001) using the primers F-NotI_FMDV and R-NotI_FMDV. The PCR product was then trimmed with NotI and inserted into the NotI site of C17fluc. C17fluc-TaV2A was made in the same way as C17fluc-FMDV2A, using the retroviral vector dsRed-2A-CDX4 (friendly gift from H. Klump) and primers F-NotI_TaV and R-NotI_TaV to amplify a 60-nt region containing the Thosea asigna virus 2A site (Donnelly et al., 2001a), which was likewise inserted into the NotI site of C17fluc.

The replication-negative mutant of C17fluc-TaV2A, NS5-GAA, was generated by changing the conserved GDD motif (9652–9660) in the polymerase active site of NS5 to GAA using a GeneTailor Site-Directed Mutagenesis System (Invitrogen) with mutagenic forward primer F-mutGDD and a wild-type reverse primer.

Deletions and insertions in the variable region of the 3′-NCR

To create variants that either completely lacked the poly(A) tract in the 3′-NCR or contained only 9 of the original 49 adenines, appropriate forward primers (F-Dra-2 and F-Dra-3, respectively) were designed that contained the desired sequence preceded by a DraI site. Each of these forward primers was used together with the reverse primer R-AgeI for PCR amplification of the corresponding region of a plasmid clone, pTNd/3′ (Mandl et al., 1997), containing the 3′ portion of the TBEV strain Neudoerfl genome. The PCR products were trimmed with DraI and AgeI and inserted in place of a DraI/AgeI fragment in pTNd/3′ extending from nucleotides 10484 to 10796. Primers F-XbaI and R-AatII were then used to amplify the region containing the modified poly(A) tract (nucleotides 9163–11145), and the PCR product was trimmed with XbaI and AatII and inserted in place of the corresponding region of C17fluc-TaV2A to create the replicon constructs ΔpolyA and A9.

Replicon Δvar, lacking the entire variable region, was constructed in the same way as ΔpolyA and A9, with the same primers (F-XbaI and R-AatII) and restriction enzymes, but using the previously described plasmid clone pNd/3′Δ10795 (Mandl et al., 1998), which has a deletion from nucleotide 10378 to 10795, as template.

The reporter replicons in this study that contained expression cassettes in the 3′-NCR, (IRES-eGFP, IRES-ME, $IRES_{(A771C)}$ME and $IRES_{(26A)}$ME) were obtained by taking previously described plasmids containing these cassettes and replacing a fragment extending from a SalI site preceding the T7 promoter to a ClaI site at nucleotide 3155 (in the NS1 coding region) with the corresponding region from C17fluc-TaV2A. The following plasmids were used as backbones for these constructs: pTNd/ΔME-EGFP (Gehrke et al., 2005), TBEV-bc (Orlinger et al., 2006), TBEV-$bc_{(A771C)}$ and TBEV-$bc_{(26A)}$ (Orlinger et al., 2007).

To obtain the replicons 12xMS2 and 24xMS2, we took advantage of the plasmids pTNd/ΔME_12xMS2 and pTNd/ΔME_24xMS2, in which the variable region of the 3′-NCR within the previously described plasmid pTNd/ΔME (Gehrke et al., 2003) had been replaced by cassettes containing 12 or 24 repeats of a stem–loop RNA structure (19 nucleotides each) that is specifically recognized by the MS2 bacteriophage coat protein (Bertrand et al., 1998). Construction of the plasmids pTNd/ΔME_12xMS2 and pTNd/ΔME_24xMS2 is described in detail in an accompanying paper by Miorin et al. (submitted). The 3′-NCR containing the repeats was substituted for the corresponding fragment in the C17fluc-TaV2A construct using restriction sites for ClaI (position 3155) and NheI (at the 3′ end).

All plasmids were propagated in *E. coli* strain HB101, and preparations were made using commercial purification systems (Qiagen).

The sequences of the constructs were confirmed using an automated DNA sequencing system (PE Applied Biosystems, GA3100).

In vitro RNA synthesis and transfection

Procedures for *in vitro* transcription and transfection of BHK-21 cells by electroporation were performed as reported in previous studies (Mandl et al., 1997). Uncapped and capped RNA with m7GpppG cap analogue were synthesized using reagents from the T7 Megascript kit (Ambion) according to the manufacturer's protocol. After the transcription reaction, template DNA was digested with DNAseI, purified, and separated from unincorporated nucleotides using an RNeasy® Mini Kit (Qiagen). The integrity of the RNA was checked by electrophoresis in a 1% agarose gel containing 6% formalin. RNA was quantified by spectrophotometric measurement, and equal amounts of RNA (corresponding to approximately 1.9×10^{12} copies) were used for all transfections.

RNA for expression of *Renilla* luciferase as a cotransfection control was made by first linearizing plasmid phRL-SV40 with BamHI and purifying it by phenol-chloroform treatment. A 6-µg aliquot of this DNA was then used to make capped RNA, using the same procedures for synthesis, purification, and quantitation that were used for the replicon RNA.

BHK-21 cells (ATCC CL10) were grown at 37 °C with 5% CO_2 in Eagle's minimal essential medium (EMEM) (Sigma) supplemented with 5% fetal calf serum (FCS), 1% glutamine, and 0.5% neomycin. The cells were electroporated using a GenePulser apparatus (Bio-Rad) as described previously (Mandl et al., 1997). After transfection, the growth medium was replaced by a maintenance medium consisting of EMEM without phenol red (Cambrex), containing 1% FCS.

Luciferase assays

A Dual-Glo™ Luciferase Assay System (Promega) was used according to the manufacturer's instructions to simultaneously measure both firefly and *Renilla* luciferase activity. After electroporation of BHK-21 cells with RNA and/or DNA, cells were washed once with growth medium (EMEM without phenol red, Cambrex) containing 5% FCS and counted. A maximum of 60,000 cells were seeded onto 96-well plates (Perkin Elmer), and triplicate wells were lysed at individual time points, followed by measurement with a Victor Light Luminometer (Perkin Elmer). The primary data are given in relative light units (RLUs).

For normalization of the firefly luciferase values, replicon RNA (1.9×10^{12} copies) containing the firefly luciferase gene was cotransfected with either 6 µg of RNA that had been transcribed *in vitro* from phRL-SV40 (encoding *Renilla* luciferase) as a standard for the early time points (3 hours) (h), or 6 µg of phRL-SV40 DNA for later time points (13–96 h). In addition, a separate "control standard" consisting of BHK-21 cells transfected with the control nucleic acid alone was included in each experiment, and the mean value of the *Renilla* luciferase activity of these cells was determined at each time point. The ratio of the uncorrected luciferase activity measured for the RNA versus the DNA controls differed less than two-fold between individual transfection experiments indicating that only little variability was introduced due to the usage of two different controls within a single time course experiment. The same electroporation conditions were used for DNA and RNA samples and yielded consistently high efficiencies between 50 and almost 100% of the transfected cells as determined by immunofluorescence or FACS. To calculate the normalized firefly luciferase activity, the measured *Renilla* luciferase activity from each cotransfected sample was divided by the corresponding control standard value to obtain a normalization factor by which the measured firefly luciferase value of that well was divided. To correct for variability between different plates, the control standards from each plate were normalized to a single standard to obtain a factor by which the firefly luciferase values for that plate were then multiplied. In this way, corrections could be made for differences in transfection efficiency as well as total cell count at different time points. The corrected data are presented as "normalized RLUs".

Immunofluorescence assay

Approximately 1×10^5 cells were seeded onto individual glass cover slips in 24-well plates and supplied with growth medium supplemented with 5% FCS. The growth medium was replaced 20 h posttransfection with maintenance medium with the FCS content reduced to 1% to slow cell growth. Immunofluorescence staining was performed on day 3 after electroporation. Cells were permeabilized by acetone–methanol (1:1) fixation, and the presence of NS1 protein was visualized by incubation with a mouse anti-NS1 monoclonal antibody (Iacono-Connors et al., 1996) and FITC-conjugated anti-mouse IgG antibody (Sigma). The evaluation of the immunofluorescence staining was performed by visual inspection using a Nikon Microphot microscope.

Immunoblotting

Cells grown in 12-well plates were harvested 48 h after electroporation, washed twice with PBS, lysed in 100 µl lysis buffer (1 M Tris, 2% SDS, 10% glycerin and 0.05% bromophenol blue), and boiled for 7 min at 95 °C. Ten-microliter aliquots of the cell lysates were separated under SDS-denaturating conditions on a 15% polyacrylamide gel, and proteins were blotted onto a PVDF membrane (Bio-Rad), which was then blocked overnight at 4 °C using PBS containing 1% BSA and 0.2% Tween-20 (PBS-T). The membranes were probed with primary antibodies to TBEV NS1 (1:1000 in PBS-T) or anti-luciferase polyclonal antibody (Promega) (1:1000) for 2 h at room temperature (RT). Both peroxidase-conjugated rabbit anti-mouse IgM (1:3000) (Amersham Biosciences) and donkey anti-goat (1:7500) (Promega) secondary antibodies were used, and FAST™ 3,3-diaminobenzidine tablets (Sigma) were used for detection.

Quantitative PCR

Intracellular RNA levels were monitored by quantitative real-time PCR as described previously (Kofler et al., 2006). Briefly, BHK-21 cells were electroporated with equimolar amounts of RNA. Then, to remove noninternalized RNA, cells were washed twice with growth medium containing 5% FCS and seeded into 25-cm^2 tissue culture flasks. Cells were harvested at different time points and counted using a Casy 1 TT cell counter (Schärfe system). Cytoplasmic RNA was extracted from a defined number of cells using an RNeasy® Mini Kit (Qiagen) and subjected to quantitative PCR (PE Applied Biosystems), as described elsewhere (Kofler et al., 2006).

Acknowledgments

We are grateful to Steven L. Allison for his invaluable assistance during data evaluation and preparation of the manuscript. We thank Caroline Thurner for her helpful discussion concerning RNA folding. We also thank Hannes Klump (Hannover Medical School, Germany) for kindly providing us plasmids coding for FMDV and TaV 2A sites as well as for the valuable advice. Paul Breit is gratefully acknowledged for the photographic artwork. We thank Katharina Huszar and Markus Mandl for their participation in mutant construction, which was performed as part of a laboratory course. Finally, we are grateful to the staff of the molecular biology laboratory of the Children's Cancer Research Institute (Vienna) for the help with setting up the luciferase detection system.

This project was funded in part of by the Austrian "Fonds zur Förderung der wissenschaftlichen Forschung" (FWF), grant number P17584-B14 and P19411-B11, as well as by a HFSP Young Investigators Grant to AM and by the ICGEB intramural funding scheme.

Appendix A. Supplementary data

Supplementary data associated with this article can be found, in the online version, at doi:10.1016/j.virol.2008.04.035.

References

Alvarez, D.E., De Lella Ezcurra, A.L., Fucito, S., Gamarnik, A.V., 2005. Role of RNA structures present at the 3′ UTR of dengue virus on translation, RNA synthesis, and viral replication. Virology 339, 200–212.

Atkins, J.F., Wills, N.M., Loughran, G., Wu, C.Y., Parsawar, K., Ryan, M.D., Wang, C.H., Nelson, C.C., 2007. A case for "StopGo": reprogramming translation to augment codon meaning of GGN by promoting unconventional termination (Stop) after addition of glycine and then allowing continued translation (Go). RNA 13, 803–810.

Bertrand, E., Chartrand, P., Schaefer, M., Shenoy, S.M., Singer, R.H., Long, R.M., 1998. Localization of ASH1 mRNA particles in living yeast. Mol. Cell 2, 437–445.

Boireau, S., Maiuri, P., Basyuk, E., de la Mata, M., Knezevich, A., Pradet-Balade, B., Backer, V., Kornblihtt, A., Marcello, A., Bertrand, E., 2007. The transcriptional cycle of HIV-1 in real-time and live cells. J. Cell Biol. 179, 291–304.

Bryant, J.E., Vasconcelos, P.F., Rijnbrand, R.C., Mutebi, J.P., Higgs, S., Barrett, A.D., 2005. Size heterogeneity in the 3′ noncoding region of South American isolates of yellow fever virus. J. Virol. 79, 3807–3821.

Chiu, W.W., Kinney, R.M., Dreher, T.W., 2005. Control of translation by the 5′ - and 3′ -terminal regions of the dengue virus genome. J. Virol. 79, 8303–8315.

Chu, P.W., Westaway, E.G., 1985. Replication strategy of Kunjin virus: evidence for recycling role of replicative form RNA as template in semiconservative and asymmetric replication. Virology 140, 68–79.

Darzacq, X., Shav-Tal, Y., de Turris, V., Brody, Y., Shenoy, S.M., Phair, R.D., Singer, R.H., 2007. *In vivo* dynamics of RNA polymerase II transcription. Nat. Struct. Mol. Biol. 14, 796–806.

de Felipe, P., Hughes, L.E., Ryan, M.D., Brown, J.D., 2003. Co-translational, intraribosomal cleavage of polypeptides by the foot-and-mouth disease virus 2A peptide. J. Biol. Chem. 278, 11441–11448.

Deas, T.S., Binduga-Gajewska, I., Tilgner, M., Ren, P., Stein, D.A., Moulton, H.M., Iversen, P.L., Kauffman, E.B., Kramer, L.D., Shi, P.Y., 2005. Inhibition of flavivirus infections by antisense oligomers specifically suppressing viral translation and RNA replication. J. Virol. 79, 4599–4609.

Donnelly, M.L., Hughes, L.E., Luke, G., Mendoza, H., ten Dam, E., Gani, D., Ryan, M.D., 2001a. The 'cleavage' activities of foot-and-mouth disease virus 2A site-directed mutants and naturally occurring '2A-like' sequences. J. Gen. Virol. 82, 1027–1041.

Donnelly, M.L., Luke, G., Mehrotra, A., Li, X., Hughes, L.E., Gani, D., Ryan, M.D., 2001b. Analysis of the aphthovirus 2A/2B polyprotein 'cleavage' mechanism indicates not a proteolytic reaction, but a novel translational effect: a putative ribosomal 'skip'. J. Gen. Virol. 82, 1013–1025.

Edgil, D., Diamond, M.S., Holden, K.L., Paranjape, S.M., Harris, E., 2003. Translation efficiency determines differences in cellular infection among dengue virus type 2 strains. Virology 317, 275–290.

Elshuber, S., Mandl, C.W., 2005. Resuscitating mutations in a furin cleavage-deficient mutant of the flavivirus tick-borne encephalitis virus. J. Virol. 79, 11813–11823.

Filomatori, C.V., Lodeiro, M.F., Alvarez, D.E., Samsa, M.M., Pietrasanta, L., Gamarnik, A.V., 2006. A 5′ RNA element promotes dengue virus RNA synthesis on a circular genome. Genes Dev. 20, 2238–2249.

Gehrke, R., Ecker, M., Aberle, S.W., Allison, S.L., Heinz, F.X., Mandl, C.W., 2003. Incorporation of tick-borne encephalitis virus replicons into virus-like particles by a packaging cell line. J. Virol. 77, 8924–8933.

Gehrke, R., Heinz, F.X., Davis, N.L., Mandl, C.W., 2005. Heterologous gene expression by infectious and replicon vectors derived from tick-borne encephalitis virus and direct comparison of this flavivirus system with an alphavirus replicon. J. Gen. Virol. 86, 1045–1053.

Grange, T., de Sa, C.M., Oddos, J., Pictet, R., 1987. Human mRNA polyadenylate binding protein: evolutionary conservation of a nucleic acid binding motif. Nucleic Acids Res 15, 4771–4787.

Gritsun, T.S., Venugopal, K., Zanotto, P.M., Mikhailov, M.V., Sall, A.A., Holmes, E.C., Polkinghorne, I., Frolova, T.V., Pogodina, V.V., Lashkevich, V.A., Gould, E.A., 1997. Complete sequence of two tick-borne flaviviruses isolated from Siberia and the UK: analysis and significance of the 5′ and 3′ -UTRs. Virus Res. 49, 27–39.

Gubler, D.J., Kuno, G., Markoff, R., 2007. Flaviviruses, In: Knipe, D.M., Howley, P.M. (Eds.), Fields Virology, 5th ed. Lippincott Williams & Wilkins Co., Philadelphia, PA., pp. 1154–1252.

Hahn, C.S., Hahn, Y.S., Rice, C.M., Lee, E., Dalgarno, L., Strauss, E.G., Strauss, J.H., 1987. Conserved elements in the 3′ untranslated region of flavivirus RNAs and potential cyclization sequences. J. Mol. Biol. 198, 33–41.

Hayasaka, D., Yoshii, K., Ueki, T., Iwasaki, T., Takashima, I., 2004. Sub-genomic replicons of Tick-borne encephalitis virus. Arch. Virol. 149, 1245–1256.

Holden, K.L., Harris, E., 2004. Enhancement of dengue virus translation: role of the 3′ untranslated region and the terminal 3′ stem-loop domain. Virology 329, 119–133.

Holden, K.L., Stein, D.A., Pierson, T.C., Ahmed, A.A., Clyde, K., Iversen, P.L., Harris, E., 2006. Inhibition of dengue virus translation and RNA synthesis by a morpholino oligomer targeted to the top of the terminal 3′ stem-loop structure. Virology 344, 439–452.

Iacono-Connors, L.C., Smith, J.F., Ksiazek, T.G., Kelley, C.L., Schmaljohn, C.S., 1996. Characterization of Langat virus antigenic determinants defined by monoclonal antibodies to E, NS1 and preM and identification of a protective, non-neutralizing preM-specific monoclonal antibody. Virus Res. 43, 125–136.

Jacobson, A., Favreau, M., 1983. Possible involvement of poly(A) in protein synthesis. Nucleic Acids Res 11, 6353–6368.

Jones, C.T., Patkar, C.G., Kuhn, R.J., 2005. Construction and applications of yellow fever virus replicons. Virology 331, 247–259.

Khromykh, A.A., 2000. Replicon-based vectors of positive strand RNA viruses. Curr. Opin. Mol. Ther. 2, 555–569.

Khromykh, A.A., Westaway, E.G., 1997. Subgenomic replicons of the flavivirus Kunjin: construction and applications. J. Virol. 71, 1497–1505.

Klump, H., Schiedlmeier, B., Vogt, B., Ryan, M., Ostertag, W., Baum, C., 2001. Retroviral vector-mediated expression of HoxB4 in hematopoietic cells using a novel coexpression strategy. Gene Ther. 8, 811–817.

Kofler, R.M., Aberle, J.H., Aberle, S.W., Allison, S.L., Heinz, F.X., Mandl, C.W., 2004. Mimicking live flavivirus immunization with a noninfectious RNA vaccine. Proc. Natl. Acad. Sci. U. S. A. 101, 1951–1956.

Kofler, R.M., Hoenninger, V.M., Thurner, C., Mandl, C.W., 2006. Functional analysis of the tick-borne encephalitis virus cyclization elements indicates major differences between mosquito-borne and tick-borne flaviviruses. J. Virol. 80, 4099–4113.

Lindenbach, B.D., Thiel, H.-J., Rice, C.M., 2007. *Flaviviridae*: the viruses and their replication, In: Knipe, D.M., Howley, P.M. (Eds.), Fields Virology, 5th ed. Lippincott Williams & Wilkins Co., Philadelphia, PA., pp. 1101–1152.

Lo, M.K., Tilgner, M., Bernard, K.A., Shi, P.Y., 2003. Functional analysis of mosquito-borne flavivirus conserved sequence elements within 3′ untranslated region of West Nile virus by use of a reporting replicon that differentiates between viral translation and RNA replication. J. Virol. 77, 10004–10014.

Ma, S.P., Yoshida, Y., Makino, Y., Tadano, M., Ono, T., Ogawa, M., 2003. Short report: a major genotype of Japanese encephalitis virus currently circulating in Japan. Am. J. Trop. Med. Hyg. 69, 151–154.

Mandl, C.W., Ecker, M., Holzmann, H., Kunz, C., Heinz, F.X., 1997. Infectious cDNA clones of tick-borne encephalitis virus European subtype prototypic strain Neudoerfl and high virulence strain Hypr. J. Gen. Virol. 78, 1049–1057.

Mandl, C.W., Kunz, C., Heinz, F.X., 1991. Presence of poly(A) in a flavivirus: significant differences between the 3′ noncoding regions of the genomic RNAs of tick-borne encephalitis virus strains. J Virol 65, 4070–4077.

Mandl, C.W., Holzmann, H., Kunz, C., Heinz, F.X., 1993. Complete genomic sequence of Powassan virus: evaluation of genetic elements in tick-borne versus mosquito-borne flaviviruses. Virology 194, 173–184.

Mandl, C.W., Holzmann, H., Meixner, T., Rauscher, S., Stadler, P.F., Allison, S.L., Heinz, F.X., 1998. Spontaneous and engineered deletions in the 3′ noncoding region of tick-borne encephalitis virus: construction of highly attenuated mutants of a flavivirus. J. Virol. 72, 2132–2140.

Mangus, D.A., Evans, M.C., Jacobson, A., 2003. Poly(A)-binding proteins: multifunctional scaffolds for the post-transcriptional control of gene expression. Genome Biol. 4, 223.

Markoff, L., 2003. 5′ - and 3′ -noncoding regions in flavivirus RNA. Adv. Virus Res. 59, 177–228.

Orlinger, K.K., Hoenninger, V.M., Kofler, R.M., Mandl, C.W., 2006. Construction and mutagenesis of an artificial bicistronic tick-borne encephalitis virus genome reveals an essential function of the second transmembrane region of protein e in flavivirus assembly. J. Virol. 80, 12197–12208.

Orlinger, K.K., Kofler, R.M., Heinz, F.X., Hoenninger, V.M., Mandl, C.W., 2007. Selection and analysis of mutations in an encephalomyocarditis virus internal ribosome entry site that improve the efficiency of a bicistronic flavivirus construct. J. Virol. 81, 12619–12629.

Pletnev, A.G., 2001. Infectious cDNA clone of attenuated Langat tick-borne flavivirus (strain E5) and a 3′ deletion mutant constructed from it exhibit decreased neuroinvasiveness in immunodeficient mice. Virology 282, 288–300.

Rauscher, S., Flamm, C., Mandl, C.W., Heinz, F.X., Stadler, P.F., 1997. Secondary structure of the 3′ -noncoding region of flavivirus genomes: comparative analysis of base pairing probabilities. RNA 3, 779–791.

Sachs, A.B., Sarnow, P., Hentze, M.W., 1997. Starting at the beginning, middle, and end: translation initiation in eukaryotes. Cell 89, 831–838.

Schagat, T., Paguio, A., Kopisch, K., Promega Cooperation, 2007. Normalizing genetic reporter assays: approaches and considerations for increasing consistency and statistical significance. Cell notes 17, 9–12.

Scholle, F., Girard, Y.A., Zhao, Q., Higgs, S., Mason, P.W., 2004. trans-Packaged West Nile virus-like particles: infectious properties *in vitro* and in infected mosquito vectors. J. Virol. 78, 11605–11614.

Shi, P.Y., Tilgner, M., Lo, M.K., 2002. Construction and characterization of subgenomic replicons of New York strain of West Nile virus. Virology 296, 219–233.

Tajima, S., Nukui, Y., Takasaki, T., Kurane, I., 2007. Characterization of the variable region in the 3′ non-translated region of dengue type 1 virus. J. Gen. Virol. 88, 2214–2222.

Tarun Jr., S.Z., Sachs, A.B., 1996. Association of the yeast poly(A) tail binding protein with translation initiation factor eIF-4G. EMBO J. 15, 7168–7177.

Tilgner, M., Shi, P.Y., 2004. Structure and function of the 3′ terminal six nucleotides of the west nile virus genome in viral replication. J. Virol. 78, 8159–8171.

Tilgner, M., Deas, T.S., Shi, P.Y., 2005. The flavivirus-conserved penta-nucleotide in the 3′ stem-loop of the West Nile virus genome requires a specific sequence and structure for RNA synthesis, but not for viral translation. Virology 331, 375–386.

Wallner, G., Mandl, C.W., Kunz, C., Heinz, F.X., 1995. The flavivirus 3′ -noncoding region: extensive size heterogeneity independent of evolutionary relationships among strains of tick-borne encephalitis virus. Virology 213, 169–178.

Wengler, G., 1981. Terminal sequences of the genome and replicative-from RNA of the flavivirus West Nile virus: absence of poly(A) and possible role in RNA replication. Virology 113, 544–555.

Wengler, G., Gross, H.J., 1978. Studies on virus-specific nucleic acids synthesized in vertebrate and mosquito cells infected with flaviviruses. Virology 89, 423–437.

Yang, D.K., Kim, B.H., Kweon, C.H., Kwon, J.H., Lim, S.I., Han, H.R., 2004. Molecular characterization of full-length genome of Japanese encephalitis virus (KV1899) isolated from pigs in Korea. J. Vet. Sci. 5, 197–205.

Yoshii, K., Hayasaka, D., Goto, A., Kawakami, K., Kariwa, H., Takashima, I., 2005. Packaging the replicon RNA of the Far-Eastern subtype of tick-borne encephalitis virus into single-round infectious particles: development of a heterologous gene delivery system. Vaccine 23, 3946–3956.

You, S., Rice, C.M., 2008. 3′ RNA elements in hepatitis C virus replication: kissing partners and long poly(U). J. Virol. 82, 184–195.

4 MANUSCRIPT 2

Functional microRNA generated from a cytoplasmic RNA virus

Harald Rouha[a], Caroline Thurner[a,b] and Christian W. Mandl[a,c,†]

submitted to "Nucleic Acids Research"

[a]Department of Virology, Medical University of Vienna, Vienna, Austria.
[b]Present address: Institute for Theoretical Chemistry, University of Vienna, Vienna, Austria.
[c]Present address: Novartis Vaccines and Diagnostics, Inc., Cambridge, MA, USA.
[†]Corresponding author. Mailing address: Department of Virology, Medical University of Vienna, Kinderspitalgasse 15, A-1095 Vienna, Austria. FAX: +43 1 40490 9795.
email address: christian.mandl@meduniwien.ac.at

Abstract

MicroRNAs (miRNAs) are a class of small, non-coding RNAs that play a pivotal role in the regulation of post-transcriptional gene expression in a wide range of eukaryotic organisms. Although DNA viruses have been shown to encode miRNAs and exploit the cellular RNA silencing machinery as a convenient way to regulate viral and host gene expression, it is generally believed that this pathway is not available to RNA viruses that replicate in the cytoplasm of the cell because miRNA biogenesis is initiated in the nucleus. In fact, among the more than 100 viral miRNAs that have been experimentally verified so far, none is derived from an RNA virus. Here, we show that a cytoplasmic RNA virus can indeed encode and produce a functional miRNA. We introduced a heterologous miRNA-precursor stem-loop sequence element into the RNA genome of the flavivirus tick-borne encephalitis virus, and this led to the production of a functional miRNA during viral infection without impairing viral RNA replication. These findings demonstrate that miRNA biogenesis can be used by cytoplasmic RNA viruses to produce regulatory molecules for the modulation of the transcriptome.

Introduction

MicroRNAs (miRNAs) are a class of short (~21-25 nucleotides), single-stranded noncoding RNA molecules that play a critical role in many cellular processes, such as cell development, differentiation, apoptosis and oncogenesis (1-3). They exert their suppressive activity on gene expression by guiding the RNA-induced silencing complex (RISC) to complementary RNA stretches within a specific messenger RNA. The biosynthesis of the vast majority of microRNAs involves the sequential action of two RNAse III enzymes, Drosha and Dicer (4). A larger RNA precursor containing a characteristic miRNA hairpin structure is transcribed in the nucleus. This so-called primary microRNA is recognized by Drosha (acting

with cofactor DGCR8) and cleaved into a ~70-nt stem-loop RNA intermediate (precursor-miRNA, pre-miRNA), which is then transported by exportin-5 to the cytoplasm, where it undergoes processing by Dicer, and gives rise to a mature, single-stranded microRNA (5-11).

The number of identified microRNAs in plants and animals is rapidly increasing, and more than 700 miRNAs are known so far in humans (12). The first microRNAs expressed from human viruses were discovered in 2004 (13). Since then, more than 100 viral microRNAs have been described, but up to now, all of them have been derived from viruses with a nuclear DNA stage in their replication cycle, mainly of the herpesvirus family (12,14). Although computer algorithms have also predicted the existence of microRNA hairpins in viruses with RNA genomes (15), a study involving the cloning of small RNAs from cells infected with two positive-strand RNA viruses, hepatitis C virus (HCV) and yellow fever virus (YFV), did not result in the identification of any RNA virus-derived small interfering RNAs (siRNAs) or miRNAs (16). However, Parameswaran *et al.* quite recently identified virus derived smallRNAs (vsRNAs) in a wide range of vertrebrate cells infected with RNA viruses, such as Dengue, West Nile and Hepatitis C virus (17). Although the experimental high-troughput approach taken in that study did neither elucidate the exact precursor structures of the discovered vsRNAs nor provide evidence for their functionality, it raised the possibilty that these vsRNAs might also include virus-derived microRNAs.

In the present study, we investigated whether RNA viruses are fundamentally capable of producing functional miRNA, by inserting a known miRNA element into the genome of an RNA virus whose life cycle is confined to the cytoplasm of the host cell. Thereby we show that a functional microRNA can indeed be produced during infection without imparing viral RNA replication.

Material and Methods

Viruses and cells

Western subtype TBEV strain Neudoerfl, which has been characterized in detail, including the determination of its entire genomic sequence (18,19), (GenBank accession no. U27495), was used as the wild-type control in all infection experiments, and all mutants described in this study were derived from this strain.

The EBV miR-BART2 sequence was obtained from genomic DNA of human herpesvirus 4 (Epstein-Barr virus (20), GenBank accession no. V01555).

BHK-21 cells were grown at 37 °C with 5% CO_2 in Eagle's minimal essential medium (Sigma) supplemented with 5% fetal calf serum (FCS), 1% glutamine, and 0.5% neomycin (growth medium) and were maintained in Eagle's minimal essential medium supplemented with 1% FCS, 1% glutamine, 0.5% neomycin, and 15 mM HEPES, pH 7.4 (maintenance medium).

Mutant construction

All viral constructs described in this study are derivatives of pTNd/c, an infectious cDNA clone of TBEV strain Neudoerfl (21). To create variants containing the miR-BART2 precursor stem-loop and flanking EBV sequence, DNA was amplified from EBV B95-8 genomic DNA using primers 5'-ATCGACCGGTATGCCACCTCCCTGCCTG-3' and 5'-CGATACCGGTGCGTGGCCCGTGGATCTG-3'. The PCR product was digested with AgeI and ligated with AgeI-digested reporter replicon construct C17, yielding C17 BART(+) or C17 BART(-), depending on the orientation of the insert. C17 is a modified version of the previously described construct C17fluc-TaV2A (22) in which the firefly luciferase start codon ATG was deleted. C17 matBART(+) was constructed by first annealing oligonucleotides 5'-CCGGACTATTTTCTGCATTCGCCCTTGCGT-3' and 5'-CCGGACGCAAGGGCGAATGCAGAAAATAGT -3', resulting in a double-stranded DNA fragment with AgeI overhangs, and then ligating this fragment with AgeI-digested C17

plasmid DNA. Full-length infectious cDNA clones were constructed by excising an XbaI/NheI fragment from each C17 replicon and inserting it into the corresponding site of XbaI/NheI-digested pTNd/c.

The non-replicating C17 variant C17 BART(+)GAA was constructed by replacement of the NS5 coding sequence of C17 BART(+) with an KpnI/XbaI-digested fragment of the previously described reporter replicon mutant NS5-GAA. The sequences of all constructs in this study were confirmed using an automated DNA sequencing system (PE Applied Biosystems, GA3100).

Reporter constructs and luciferase assays

To construct the luciferase reporter plasmids psiCHECK1-BART2 and psiCHECK2-BART2, oligonucleotides 5'-TCGAGCGCAAGGGCGAATGCAGAAAATAGT-3' and 5'-GGCCACTATTTTCTGCATTCGCCCTTGCGC-3', containing XhoI and NotI overhangs, were annealed and ligated into the multiple cloning site of psiCHECK^{TM}-1 and psiCHECK^{TM}-2 (Promega).

The Dual-Glo^{TM} Luciferase Assay System (Promega) was used according to the manufacturer's instructions to measure both firefly and *Renilla* luciferase activity simultaneously. For experiments with infectious viruses, cells were electroporated with 6 µg psiCHECK2-BART2 plasmid DNA using a Gene Pulser apparatus (Bio-Rad). One day after electroporation, 60,000 cells/well were seeded in 96-well plates for subsequent infection in triplicate with wild-type and mutant virus at an MOI of 10. *Renilla* and firefly luciferase levels were determined immediately after infection and at 24 and 48 hours postinfection. For experiments using non-infectious replicons, cells were coelectroporated with equimolar amounts of *in vitro*-transcribed replicon RNA (corresponding to approximately 1.2 x 10^{12} RNA copies) and 6 µg psiCHECK1-BART2 plasmid DNA. Procedures for RNA *in vitro* transcription and electroporation of BHK-21 cells were performed as reported in previous studies (21,22).

Immunofluorescence assay

Approximately 1 x 10^5 cells were seeded onto individual glass cover slips in 24-well plates prior to infection (TNd/c mutant set) or after transfection (C17 mutant set). Immunofluorescence staining was performed 24 hours after infection with TNd/c mutants or 48 hours after transfection with replicon RNA. Cells were permeabilized by acetone-methanol (1:1) fixation, and viral proteins were detected by incubation with rabbit anti-TBEV serum and a fluorescein-isothyocyanate-conjugated anti-rabbit antibody (Jackson ImmunoResearch Laboratories).

Northern blot analysis

miRNA-BART2 northern blotting: Total RNA was extracted using a *mir*Vana miRNA Isolation Kit (Ambion) following the vendor's recommendations. 20 µg of total RNA per sample was electrophoresed through a 12% urea-polyacrylamide gel, which was stained with ethidium bromide for visualization of bands and then electroblotted to Hybond XL nylon membranes (GE Healthcare). A *mir*Vana miRNA Probe Construction Kit (Ambion) and [alpha-^{32}P] CTP (Hartmann Analytic) were used to construct a radioactive RNA probe (5'-GCAAGGGCGAAUGCAGAAAAUA-3') complementary to EBV miR-BART2-5p. Blots were hybridized overnight in PerfectHyb™ Plus (Sigma) hybridization buffer at 50°C and then washed twice with 5x SSC + 1% SDS and twice for 15 min with 1x SSC + 1% SDS prior to signal detection on a phosphorimager. Cells electroporated with synthetic miRNA (Pre-miR™ miRNA Precursor Molecules, Ambion) at a concentration of 30 nm were used as positive controls.

Northern blot of subgenomic RNA: One µg of total RNA, extracted from BHK-21 cells using an *mir*Vana miRNA Isolation Kit (Ambion), was subjected to denaturing gel electrophoresis using a Northern MaxGly Kit (Ambion) and transferred to a positively charged nylon membrane (BrightStar Plus, Ambion) according to the manufacturer's recommendations. Two different probes were constructed by *in vitro* transcription (MAXIscript T7 Kit, Ambion) using biotinylated UTP (Ambion). Templates for *in vitro*

transcription were generated by PCR amplification of pTNd/c-BART(+) DNA using the following T7 promoter primers: 5'- CAGGGGTGAGGAATGCCCCCAGA-3' and 5'-TAATACGACTCACTATAGGGCGGGTGTTTTTCCGAGTCAC-3', yielding a probe complementary to the core 3'-NCR of TBEV, and 5'-ATGCCACCTCCCTGCCTGGTGGAC-3' and 5'-TAATACGACTCACTATAGGGCGTGGCCCGTGGATCTGTGAA-3', yielding a probe specific for the miR-BART2 sequence insertion, including the EBV flanking regions. Hybridization and washing steps were performed according to the manual, and these were followed by a non-isotopic detection procedure (Bright Star Biodetect Kit, Ambion).

Real-time RT PCR

Total RNA from infected cells was extracted using a *mir*Vana miRNA Isolation Kit (Ambion). TaqMan MicroRNA Assays (Applied Biosystems) specific for EBV BART2-5p and U6 snRNA (endogenous control) were performed according to the manufacturer's protocol using an ABI 7300 Real-Time PCR System (PE Applied Biosystems).

Relative quantitation was carried out using the $2^{-\Delta\Delta T}$ method (23) for infected versus uninfected cells.

Virus production, passaging and focus assay

For the production of infectious virus particles, BHK-21 cells were transfected with equal amounts of *in vitro*-transcribed full-length RNA. The supernatant from the transfected cells was collected 48 hours postinfection and cleared by centrifugation. Various dilutions were applied to confluent cell monolayers to determine the number of focus-forming units (ffu). Fifty hours postinfection, cells were fixed with acetone-methanol (1:1) and treated with polyclonal rabbit anti-TBEV serum. Antibody-labeled cells were detected using an immunoenzymatic reaction consisting of successive incubations with goat anti-rabbit immunoglobulin G-alkaline phosphatase and the corresponding enzyme substrate (SigmaFast Red TR/Naphtol AS-MX tablets). To analyze the genomic stability of the viral

mutants and to increase the titer, viruses for infection experiments were passaged at least 5 times, using a 1:5,000 dilution of the supernatant.

Results

Construction of a cytoplasmic RNA virus encoding a viral miRNA.

For these experiments, we used tick-borne encephalitis virus (TBEV), a human pathogen of the genus *Flavivirus*, family *Flaviviridae*. Like all members of this family of positive-strand RNA viruses, the replication cycle of TBEV takes place in the cytoplasm. Its genome consists of a single RNA molecule of approximately 11 kb in length, which also serves as a messenger RNA, encoding a single polyprotein precursor that is processed to form three structural proteins (C, prM, E), which together with the genomic RNA compose the virion, and seven nonstructural proteins (NS1, NS2A, NS2B, NS3, NS4A, NS4B, NS5) that are necessary for replication (Fig. 1A) (24-26).

The 3'-noncoding region (3'-NCR) of TBEV has been shown to tolerate the insertion of heterologous sequence elements (22). We took advantage of this flexibility to insert the miR-BART2 hairpin precursor from the herpesvirus Epstein-Barr virus (EBV) between the variable and core regions of the 3'-NCR of a wild-type TBEV strain (TNd/c, Fig. 1B,C). MiR-BART2 downregulates expression of the EBV DNA polymerase BALF5, and this is thought to prevent the transition from latent to lytic replication (16,27,28). To favor proper formation of the stem-loop secondary structure, which is crucial for recognition by the classical miRNA-processing machinery (6,29,30), we decided to add flanking EBV sequence on either side of the hairpin. We generated three different BART mutants. The EBV miR-BART2 precursor was introduced in the plus-strand (messenger-sense) orientation (TNd/c BART(+)) and also as the reverse complement (TNd/c BART(-)) to allow a potentially functional miRNA precursor to be formed at the 5'end of the negative-strand (antisense) copy of the viral RNA during replication. Bioinformatic secondary structure analysis prior to construction of these mutants prompted us to add 30 nt of original genomic EBV sequence on either side of the

hairpin, resulting in a tolerable maximum of 128 nt for the full-hairpin insertions. In a third construct, only the “mature” miR-BART2 sequence, devoid of any EBV-derived flanking sequences or hairpin structure elements, was inserted (TNd/c matBART(+)). To assess the capability of these TBEV BART mutants to replicate and be translated, RNA from the mutants and wild-type TBEV was made by *in vitro* transcription and introduced into BHK-21 cells by electroporation. Immunofluorescence staining with an anti-TBEV serum 24 hours after transfection showed that all three mutants were able to replicate and express viral proteins (Fig. 1C), indicating that the inserted microRNA hairpin structure elements did not impair viral RNA replication or protein expression.

Next, we examined the stability of the heterologous sequence elements in a passage experiment on BHK-21 cells. After five rounds of sequential infection with diluted supernatant from the previous passage, no sequence changes could be detected in the inserted miR-BART2 sequences or the flanking elements. The only mutations observed were ones that occurred in the viral envelope protein E and were of a type previously associated with cell culture adaptations (Table S1) (31,32). Taken together, these results demonstrated that the insertion of a microRNA hairpin precursor in either orientation into the RNA genome of this flavivirus was genetically stable and compatible with viral growth.

Functional activity of the inserted miRNA.

As a tool to measure the functional activity of miR-BART2, we established a dual-luciferase reporter assay. The original miR-BART2 target sequence was inserted downstream of the translational stop codon of the *Renilla* luciferase (Rluc) coding sequence of the siRNA evaluation vector psiCHECK^{TM}-2, yielding a construct encoding an Rluc mRNA fused to a BART2 target site, termed psiCHECK2-BART2 (Fig. 1D). Firefly luciferase (fluc) on the same plasmid, driven from a second promoter, served as an internal control. As expected, Rluc expression from this construct was suppressed in a dose-dependent manner upon transfection with synthetic miR-BART2 (Fig. S1A). To investigate whether the viral mutants TNd/c BART(+), TNd/c BART(-) and TNd/c matBART(+) were able to downregulate

reporter gene expression, BHK-21 cells were transfected with psiCHECK2-BART2 and 24 hours thereafter infected with BART mutants or wild-type virus. TNd/c BART(+) strongly suppressed reporter gene expression at 24 and 48 hours postinfection (Fig. 2A). The observed reduction by approximately 50% is equal to the effect seen with the natural miR-BART2 target BALF5 protein in EBV-infected cells with forced miR-BART2 expression (27). In contrast, infection of cells with TNd/c BART(-) or TNd/c matBART(+) did not decrease reporter gene expression.

Time course of miR-BART2 generation during infection.

To obtain direct evidence for the formation of miR-BART2, total RNA was isolated from infected cells and subjected to northern blot analysis 24 hours after infection (Fig. 2B). Consistent with the data from the luciferase assay, mature miRNA and the corresponding pre-miR were readily detected in cells infected with TNd/c BART(+), but not in samples of the other mutants or wild-type virus. To establish a time course of miRNA formation in infected cells, we performed a TaqMan^{TM} MicroRNA Assay (Fig. 2C). In cells infected with TNd/c BART(+), levels of miR-BART2 increased within 24 hours to a maximum plateau level, whereas the signal detected for TNd/c BART(-) and TNd/c matBART(+) remained at or close to background levels.

Dependence of miRNA production on replication of viral RNA.

The experiments described above consistently indicated that significant amounts of functional miR-BART2 were generated with TNd/c BART(+) and prompted a more detailed investigation of the relationship between RNA replication and miRNA formation. For this purpose, we prepared an analogous set of replicons (C17 BART(+), C17 BART(-) and C17 matBART(+)) based on the TBEV reporter replicon C17fluc-TaV2A, a construct in which the viral structural proteins had been replaced by an in-frame insertion of the firefly luciferase gene (Fig. 3A) (22). Additionally, we designed a replication-negative variant of C17 BART(+) with a GDD-to-GAA mutation in the active site of the viral polymerase, termed C17

BART(+)GAA (Fig. 3A). Immunofluorescence staining with an anti-TBEV antiserum 48 hours after transfection confirmed that all of the replicons encoding a functional RNA polymerase were able to replicate and express viral proteins (Fig. 3A, bottom).

Replication of these replicons was monitored by measurement of fluc activity in transfected BHK-21 cells, and this revealed that the insertion of the miRNA sequence (in either orientation or in its mature form) did not alter the level of RNA replication relative to the parental C17 replicon (Fig. 3B). As expected, and consistent with the immunofluorescence results, C17 BART(+)GAA was negative for RNA replication. To confirm that miRNA formation from these replicons mirrored the findings with infectious virus, functional miR-BART2 activity was assayed by measuring Rluc reporter gene repression (Fig. 3C; Fig S2 for a complete data set) using a modified reporter plasmid lacking firefly luciferase, psiCHECK1-BART2 (Fig. 3D). C17 BART(+) clearly suppressed reporter gene activity, and the presence of the miRNA was additionally confirmed in a northern blot assay (Fig. 3E). In contrast, no activity and no miRNA was observed for C17 BART(-), C17 matBART(+) or the parental control C17. Notably, the replication-deficient control C17 BART(+)GAA also did not suppress Rluc expression or generate detectable miRNA (Fig. 3C,E).

Discussion

This is the first study that describes the generation of a functional microRNA from a cytoplasmic RNA virus. This observation is unexpected since two theoretical barriers are generally thought to impede miRNA biogenesis for this class of viruses: First, in contrast to DNA and retroviruses, the replication cycle of cytoplasmic RNA viruses takes place in the cytoplasm, away from the nucleus where Drosha resides and initiates the processing of the miRNA hairpin structure for a majority of all known microRNAs. Secondly, even if the microRNA precursor could be liberated from an RNA virus genome, this excision event would be expected to destroy copies of the viral genome and thereby reduce RNA replication efficiency.

A detailed follow-up study has to be carried out now, to clarify, how and where the microRNA is generated in our system, and which key players of the classical microRNA biogenesis pathway are involved in this process. Regardless of the mechanism, however, our results demonstrate that these barriers are not absolute and that they can eventually be circumvented.

One possible way in which this could occur is that viral infection might lead to a partial breakup of cellular compartmentalization or to protein retrafficking, allowing the Drosha complex to act in the cytoplasm. Another possibility is that a fraction of the flavivirus RNA containing the miRNA-BART2 precursor enters the nucleus. Many positive- and negative-strand RNA viruses with a cytoplasmic replication cycle have been reported to alter nuclear-cytoplasmic trafficking to expedite viral growth (33), and the presence of flaviviral RNA in the nucleus has been suggested in a recent study (34). It therefore seems justifiable to speculate that Drosha and a fraction of the viral RNA containing the microRNA hairpin structure are present in the same cellular compartment at some point during infection. First experiments, performed to unravel the role of Drosha, point in this direction and do not suggest a Drosha-independent pathway (data not shown). As it is becoming clear since recently that also non-canonical pathways can lead to the generation of functional microRNAs (5), it remains possible, however, that the activity of this enzyme is bypassed. One such pathway, in which miRNA precursors are fed into the miRNA maturation pathway without a contribution of Drosha, is the mirtron pathway (35-37). In this case, pre-miRNAs are formed from debranched introns during mRNA splicing.

One of the most important findings of our study is that while active viral replication was required for production of miRNA-BART2, the presence of the functional miRNA precursor element in the TBEV genome did not have a measurable negative impact on RNA replication. Remarkably, in a recent study, it was found that several flaviviruses produce a 3'-terminal noncoding RNA fragment that accumulates in infected cells due to incomplete degradation of viral genomic RNA (38). This highly structured, nuclease-resistant RNA was shown to increase both virus replication and virus-induced cytopathogenicity, although the

reason for this is still unknown. This observation supports the idea that fragmentation processes can also be beneficial and that RNA viruses can indeed use such mechanisms to generate smaller RNA molecules with biological activity without the need for subgenomic promoters. In further experiments, we found that TBEV-infected cells also contain relatively large amounts of a 3'-terminal subgenomic RNA and that the amount of this RNA present in the cell is not altered by the insertion of the BART2 sequence element (Fig. S3).

We also found that although insertion of the natural miRNA-BART2 hairpin precursor, with flanking sequences from the EBV genome, into the TBEV 3'-NCR in the plus-strand (messenger-sense) orientation led to production of a mature, functional miRNA, insertion of only the portion corresponding to mature miRNA-BART2 did not. This further emphasizes that the resulting mature microRNA was not simply a remaining piece of randomly degraded viral RNA but indeed the product of an active miRNA processing pathway.

Interestingly, the insertion of the same miRNA-BART2 precursor in the antisense orientation did not result in miRNA production. Since all of the constructs tested were genetically stable over multiple passages and apparently had no effect on the efficiency of viral RNA replication, we conclude that there must be specific mechanistic reasons for the requirement of the precursor element to be in the positive-sense orientation. First, the replication of flaviviruses is asymmetrical, meaning that viral plus-strands accumulate in around tenfold excess over the corresponding genome-length minus-strands (24). Second, the minus-strand RNA template may be inaccessible to the microRNA machinery when it is in the ER-associated viral replication complex. Recent biochemical analysis has suggested that the flavivirus replication complex resides in virus-induced double-layered membrane compartments (39). Therefore, it seems reasonable that the minus-strand remains shielded from other cellular compartments and enzymes. The plus-strand, in contrast, is forced to leave the site of replication to gain access to the cellular translation machinery.

The results of this study demonstrate that, contrary to current assumptions, RNA viruses, at least under some circumstances, can carry functional microRNA elements. It is therefore not unlikely that among the vast assortment of diverse RNA viruses found in

nature, some will be found that encode miRNAs and even use them as part of their replication strategy to regulate viral or host gene expression. The recent discovery of RNA virus-derived small RNAs in a wide range of host cells (17) is in good agreement with this hypothesis and it is tempting to speculate that at least some of them represent such RNA virus-derived miRNAs.

We hope that our report stimulates a more comprehensive search for natural microRNAs in many different RNA viruses. But regardless of whether or not microRNAs are found to play a physiological role in their biology, our study provides first direct evidence that their generation is mechanistically possible. This knowledge opens up new avenues for the rational design of RNA virus mutants and vectors encoding this important class of regulatory molecules.

Funding

This project was supported by the Austrian “Fonds zur Foerderung der wissenschaftlichen Forschung (FWF)”, grant number P19411-B11.

Acknowledgments

We are grateful to F.A. Graesser and T. Pfuhl (Homburg, Germany) for introduction to miRNA northern blotting, and U. Blaesi and A. Resch (MFPL, Vienna) for providing their radioactive facility. We thank Franz X. Heinz for stimulating discussions, G. O’Riordain for participation in mutant construction, C. Taucher, V.M. Hoenninger and K. Ramsauer for critical review of the manuscript, and S. L. Allison for his invaluable assistance in manuscript preparation.

References

1. Ambros, V. (2004) The functions of animal microRNAs. *Nature*, **431,** 350-355.

2. Bartel, D.P. (2004) MicroRNAs: genomics, biogenesis, mechanism, and function. *Cell*, **116,** 281-297.
3. Bushati, N. and Cohen, S.M. (2007) microRNA functions. *Annu Rev Cell Dev Biol*, **23,** 175-205.
4. Lee, Y., Jeon, K., Lee, J.T., Kim, S. and Kim, V.N. (2002) MicroRNA maturation: stepwise processing and subcellular localization. *Embo J*, **21,** 4663-4670.
5. Kim, V.N., Han, J. and Siomi, M.C. (2009) Biogenesis of small RNAs in animals. *Nat Rev Mol Cell Biol*, **10,** 126-139.
6. Han, J., Lee, Y., Yeom, K.H., Nam, J.W., Heo, I., Rhee, J.K., Sohn, S.Y., Cho, Y., Zhang, B.T. and Kim, V.N. (2006) Molecular basis for the recognition of primary microRNAs by the Drosha-DGCR8 complex. *Cell*, **125,** 887-901.
7. Lee, Y., Ahn, C., Han, J., Choi, H., Kim, J., Yim, J., Lee, J., Provost, P., Radmark, O., Kim, S. *et al.* (2003) The nuclear RNase III Drosha initiates microRNA processing. *Nature*, **425,** 415-419.
8. Lund, E., Guttinger, S., Calado, A., Dahlberg, J.E. and Kutay, U. (2004) Nuclear export of microRNA precursors. *Science*, **303,** 95-98.
9. Yi, R., Qin, Y., Macara, I.G. and Cullen, B.R. (2003) Exportin-5 mediates the nuclear export of pre-microRNAs and short hairpin RNAs. *Genes Dev*, **17,** 3011-3016.
10. Hutvagner, G., McLachlan, J., Pasquinelli, A.E., Balint, E., Tuschl, T. and Zamore, P.D. (2001) A cellular function for the RNA-interference enzyme Dicer in the maturation of the let-7 small temporal RNA. *Science*, **293,** 834-838.
11. Ketting, R.F., Fischer, S.E., Bernstein, E., Sijen, T., Hannon, G.J. and Plasterk, R.H. (2001) Dicer functions in RNA interference and in synthesis of small RNA involved in developmental timing in C. elegans. *Genes Dev*, **15,** 2654-2659.
12. Griffiths-Jones, S., Saini, H.K., van Dongen, S. and Enright, A.J. (2008) miRBase: tools for microRNA genomics. *Nucleic Acids Res*, **36,** D154-158.
13. Pfeffer, S., Zavolan, M., Grasser, F.A., Chien, M., Russo, J.J., Ju, J., John, B., Enright, A.J., Marks, D., Sander, C. *et al.* (2004) Identification of virus-encoded microRNAs. *Science*, **304,** 734-736.
14. Umbach, J.L. and Cullen, B.R. (2009) The role of RNAi and microRNAs in animal virus replication and antiviral immunity. *Genes Dev*, **23,** 1151-1164.
15. Li, S.C., Shiau, C.K. and Lin, W.C. (2008) Vir-Mir db: prediction of viral microRNA candidate hairpins. *Nucleic Acids Res*, **36,** D184-189.
16. Pfeffer, S., Sewer, A., Lagos-Quintana, M., Sheridan, R., Sander, C., Grasser, F.A., van Dyk, L.F., Ho, C.K., Shuman, S., Chien, M. *et al.* (2005) Identification of microRNAs of the herpesvirus family. *Nat Methods*, **2,** 269-276.

17. Parameswaran, P., Sklan, E., Wilkins, C., Burgon, T., Samuel, M.A., Lu, R., Ansel, K.M., Heissmeyer, V., Einav, S., Jackson, W. *et al.* Six RNA viruses and forty-one hosts: viral small RNAs and modulation of small RNA repertoires in vertebrate and invertebrate systems. *PLoS Pathog*, **6,** e1000764.
18. Mandl, C.W., Heinz, F.X. and Kunz, C. (1988) Sequence of the structural proteins of tick-borne encephalitis virus (western subtype) and comparative analysis with other flaviviruses. *Virology*, **166,** 197-205.
19. Mandl, C.W., Heinz, F.X., Stockl, E. and Kunz, C. (1989) Genome sequence of tick-borne encephalitis virus (Western subtype) and comparative analysis of nonstructural proteins with other flaviviruses. *Virology*, **173,** 291-301.
20. Baer, R., Bankier, A.T., Biggin, M.D., Deininger, P.L., Farrell, P.J., Gibson, T.J., Hatfull, G., Hudson, G.S., Satchwell, S.C., Seguin, C. *et al.* (1984) DNA sequence and expression of the B95-8 Epstein-Barr virus genome. *Nature*, **310,** 207-211.
21. Mandl, C.W., Ecker, M., Holzmann, H., Kunz, C. and Heinz, F.X. (1997) Infectious cDNA clones of tick-borne encephalitis virus European subtype prototypic strain Neudoerfl and high virulence strain Hypr. *J Gen Virol*, **78 (Pt 5),** 1049-1057.
22. Hoenninger, V.M., Rouha, H., Orlinger, K.K., Miorin, L., Marcello, A., Kofler, R.M. and Mandl, C.W. (2008) Analysis of the effects of alterations in the tick-borne encephalitis virus 3'-noncoding region on translation and RNA replication using reporter replicons. *Virology*, **377,** 419-430.
23. Schmittgen, T.D. and Livak, K.J. (2008) Analyzing real-time PCR data by the comparative C(T) method. *Nat Protoc*, **3,** 1101-1108.
24. Lindenbach, B.D., Thiel, H.-J., Rice, C.M. (2007) In Knipe, D. M., Howley, P.M. (ed.), *Fields Virology, 5th ed. Lippincott Williams & Wilkins Co., Philadelphia, PA.*, Philadelphia, pp. 1101-1152.
25. Wengler, G. and Wengler, G. (1981) Terminal sequences of the genome and replicative-from RNA of the flavivirus West Nile virus: absence of poly(A) and possible role in RNA replication. *Virology*, **113,** 544-555.
26. Wengler, G., Wengler, G. and Gross, H.J. (1978) Studies on virus-specific nucleic acids synthesized in vertebrate and mosquito cells infected with flaviviruses. *Virology*, **89,** 423-437.
27. Barth, S., Pfuhl, T., Mamiani, A., Ehses, C., Roemer, K., Kremmer, E., Jaker, C., Hock, J., Meister, G. and Grasser, F.A. (2008) Epstein-Barr virus-encoded microRNA miR-BART2 down-regulates the viral DNA polymerase BALF5. *Nucleic Acids Res*, **36,** 666-675.

28. Cai, X., Schafer, A., Lu, S., Bilello, J.P., Desrosiers, R.C., Edwards, R., Raab-Traub, N. and Cullen, B.R. (2006) Epstein-Barr virus microRNAs are evolutionarily conserved and differentially expressed. *PLoS Pathog*, **2,** e23.

29. Zeng, Y. and Cullen, B.R. (2005) Efficient processing of primary microRNA hairpins by Drosha requires flanking nonstructured RNA sequences. *J Biol Chem*, **280,** 27595-27603.

30. Zeng, Y., Yi, R. and Cullen, B.R. (2005) Recognition and cleavage of primary microRNA precursors by the nuclear processing enzyme Drosha. *Embo J*, **24,** 138-148.

31. Kroschewski, H., Allison, S.L., Heinz, F.X. and Mandl, C.W. (2003) Role of heparan sulfate for attachment and entry of tick-borne encephalitis virus. *Virology*, **308,** 92-100.

32. Mandl, C.W., Kroschewski, H., Allison, S.L., Kofler, R., Holzmann, H., Meixner, T. and Heinz, F.X. (2001) Adaptation of tick-borne encephalitis virus to BHK-21 cells results in the formation of multiple heparan sulfate binding sites in the envelope protein and attenuation in vivo. *J Virol*, **75,** 5627-5637.

33. Hiscox, J.A. (2003) The interaction of animal cytoplasmic RNA viruses with the nucleus to facilitate replication. *Virus Res*, **95,** 13-22.

34. Uchil, P.D., Kumar, A.V. and Satchidanandam, V. (2006) Nuclear localization of flavivirus RNA synthesis in infected cells. *J Virol*, **80,** 5451-5464.

35. Berezikov, E., Chung, W.J., Willis, J., Cuppen, E. and Lai, E.C. (2007) Mammalian mirtron genes. *Mol Cell*, **28,** 328-336.

36. Okamura, K., Hagen, J.W., Duan, H., Tyler, D.M. and Lai, E.C. (2007) The mirtron pathway generates microRNA-class regulatory RNAs in Drosophila. *Cell*, **130,** 89-100.

37. Ruby, J.G., Jan, C.H. and Bartel, D.P. (2007) Intronic microRNA precursors that bypass Drosha processing. *Nature*, **448,** 83-86.

38. Pijlman, G.P., Funk, A., Kondratieva, N., Leung, J., Torres, S., van der Aa, L., Liu, W.J., Palmenberg, A.C., Shi, P.Y., Hall, R.A. *et al.* (2008) A highly structured, nuclease-resistant, noncoding RNA produced by flaviviruses is required for pathogenicity. *Cell Host Microbe*, **4,** 579-591.

39. Uchil, P.D. and Satchidanandam, V. (2003) Architecture of the flaviviral replication complex. Protease, nuclease, and detergents reveal encasement within double-layered membrane compartments. *J Biol Chem*, **278,** 24388-24398

Figure legends

Figure 1.

TNd/c BART mutants and reporter plasmid psiCHECK2-BART2. **(A)** Genome organization of wild-type TBEV virus strain Neudoerfl (TNd/c). 5'-NCR, 5'-noncoding region; 3'-NCR, 3'-noncoding region. The positions of the "variable" and conserved "core" regions of the 3'-NCR are indicated. **(B)** EBV miR-BART2 precursor in the predicted secondary structure (miRBase accession number: MI0001068) flanked by 30 nt of EBV B95-8 sequence on either side. The sequence of the precursor of miR-BART2 is highlighted in red and blue, with the red region corresponding to the mature miR-BART2. **(C)** *Top.* Schematic diagram of the 3'-NCR of parental virus TNd/c and the derived TNd/c BART mutants. *Below.* Immunofluorescence (IF) staining of infected cells with rabbit anti-TBEV serum 24 hours postinfection. **(D)** Mature miR-BART2 (red) and the corresponding target sequence in the 3'-UTR of the EBV BALF5 mRNA (green) that was inserted into the 3'-UTR of the *Renilla* luciferase (Rluc) mRNA gene of the parental vector psiCHECK-2. Firefly luciferase (fluc) expressed from the HSV-TK promoter served as an internal standard. Promoters are indicated by flags: SV40, simian virus 40; HSV-TK, herpes simplex virus thymidine kinase. Diagrams are not drawn to scale.

Figure 2.

A functional miRNA is produced during infection with TBEV mutant TNd/c BART(+). **(A)** Relative Rluc activity after infection with TNd/c BART mutants. BHK-21 cells were transfected with psiCHECK2-BART2 and 24 hours thereafter infected with viral mutants at an MOI of 10. Values represent Rluc expression levels relative to the infection with wild-type virus. Error bars indicate standard deviations of three experiments, each measured in triplicate. **(B)** Northern blot analysis of intracellular RNA 24 hours after infection using a radioactive complementary RNA probe specific for the mature miR-BART2 sequence. Cells electroporated (EP) with synthetic miRNA-BART2 (syn. miRNA) served as a positive control.

(C) Time course analysis of miR-BART2 expression in BHK-21 cells infected at an MOI of 10. At the indicated time points, total RNA of infected cells was isolated and subjected to a TaqMan™ MicroRNA Assay specific for mature miR-BART2. U6 snRNA served as an endogenous control. The ΔC_T value of uninfected cells at time point 0 was used as a base value to calculate fold change in expression by the comparative CT method.

Figure 3.

RNA replication is necessary for but not affected by miRNA biogenesis. **(A)** *Top.* Schematic diagram of parental luciferase reporter replicon C17, which contains the first 17 aa of the capsid protein and has the rest of the structural proteins replaced by firefly luciferase (fluc). The 3'-NCR of each replicon is identical to that of the corresponding TNd/c virus mutant (Fig. 1C). Replication-negative C17 BART(+)GAA differs from C17 BART(+) by a GDD-to-GAA mutation in the polymerase active site of the viral NS5 protein. *Below*. Immunofluorescence (IF) staining with rabbit anti-TBEV serum 48 hours posttransfection. **(B)** Replication efficiencies of the C17 BART mutant set monitored by firefly luciferase activity in BHK-21 cells. Error bars represent the standard deviation of three independent experiments, each measured in triplicate. **(C)** Relative Rluc activity in BHK-21 cells co-transfected with miR-BART2 reporter plasmid psiCHECK1-BART2 and the C17 BART mutants C17 BART(+) and C17 BART(+)GAA. Rluc levels are shown as a percentage of the level obtained with the parental replicon C17. Error bars represent the standard deviation calculated from a minimum of three independent experiments, each measured in triplicate. **(D)** Schematic diagram of the reporter plasmid psiCHECK1-BART2, which contains the miR-BART2 target sequence fused to the *Renilla* luciferase coding sequence under the control of an SV40 promoter. **(E)** Relative Rluc activity of C17 BART mutants at 48 hours posttransfection (*top*) and northern blot analysis (*below)* of the same intracellular RNA preparation used in the Rluc assay. The positions of the precursor and the mature miRNA are indicated by arrows. Total RNA of cells electroporated with synthetic miR-BART2 (syn. miRNA) served as a control. Diagrams (A) and (D) are not to scale.

Figure legends – Supplementary Material

Figure S1.

miR-BART2 specifically downregulates the expression of reporter mRNAs fused to the corresponding miR-BART2 target site. Time course of *Renilla* luciferase (Rluc) activity in cells transfected with the reporter constructs psiCHECK2-BART2 **(A)** and psiCHECK1-BART2 **(B)**, either individually or together with synthetic pre-miR-BART2 precursor molecules at a concentration of 1mM or 30 nM. In the case of psiCHECK2-BART2, the Rluc light units were normalized to those of firefly luciferase (fluc) expressed from a different promoter on the same plasmid as an internal standard (Fig. 1D). psiCHECK-1-BART2 does not contain the fluc cistron (Fig. 3D). Data from control experiments using the parental vectors without miR-BART2 are shown at the right. Error bars represent the standard deviation of one experiment, measured in triplicate.

Figure S2.

Downregulation of Renilla luciferase in cells co-transfected with psiCHECK1-BART2 and the C17 BART mutants (complete data set). Rluc levels are shown as a percentage of the level obtained with the parental replicon C17. Error bars represent the standard deviation from a minimum of three independent experiments, each measured in triplicate.

Figure S3.

A subgenomic RNA is produced from the 3'-terminal region of TNd/c and TNd/c BART(+) (A), but the miR-BART2 sequence insertion is not contained on this fragment (B). BHK-21 cells were infected with the indicated viruses at an MOI of 10, and total RNA was subjected to northern blot analysis using two biotinylated probes, one specific for the conserved "core" region of the 3'-NCR (probe A) and one specific for the miR-BART2 sequence insertion including the flanking EBV elements (probe B). gRNA, genomic RNA; sgRNA, subgenomic RNA.

Figures

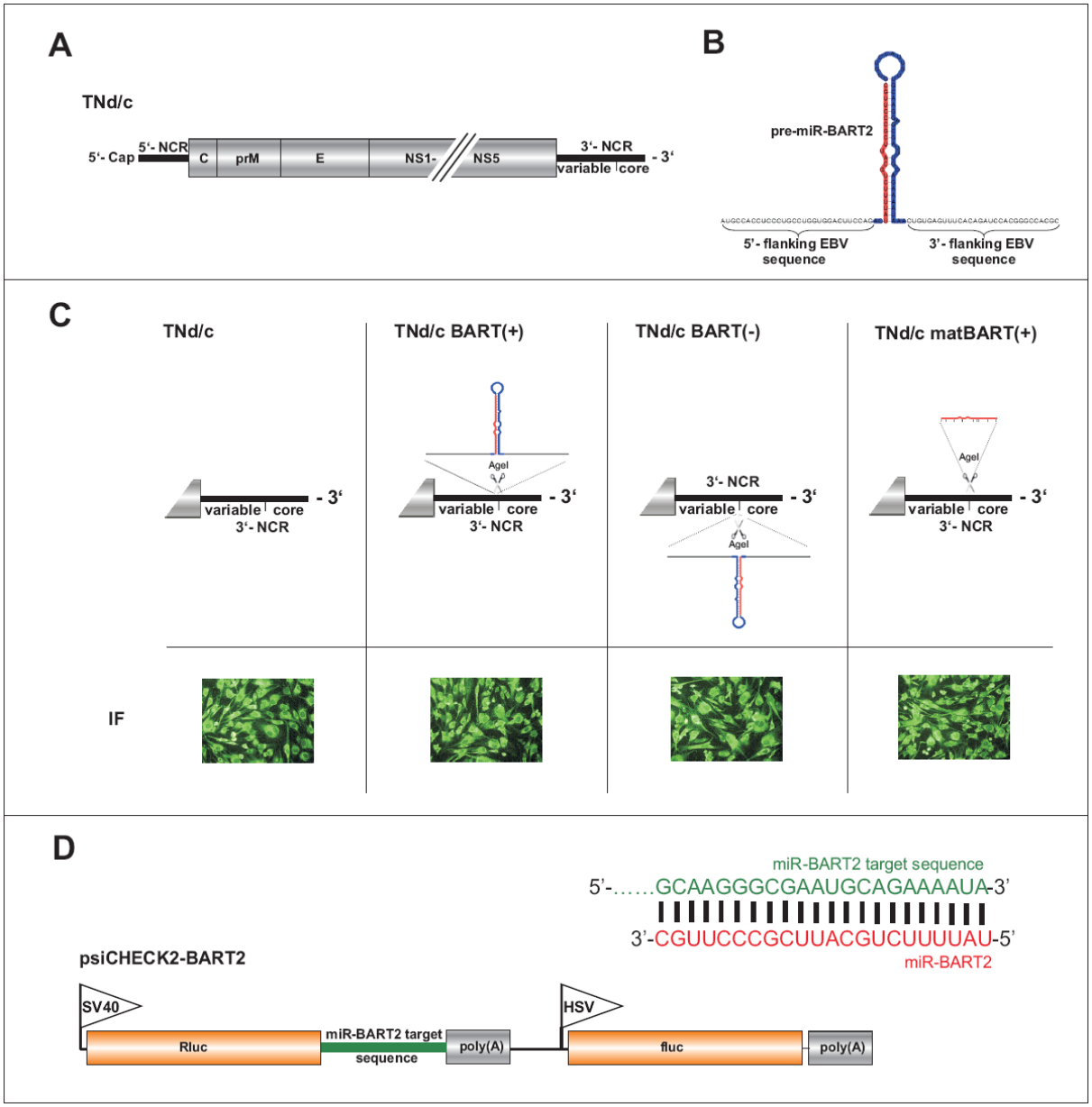

Figure 1

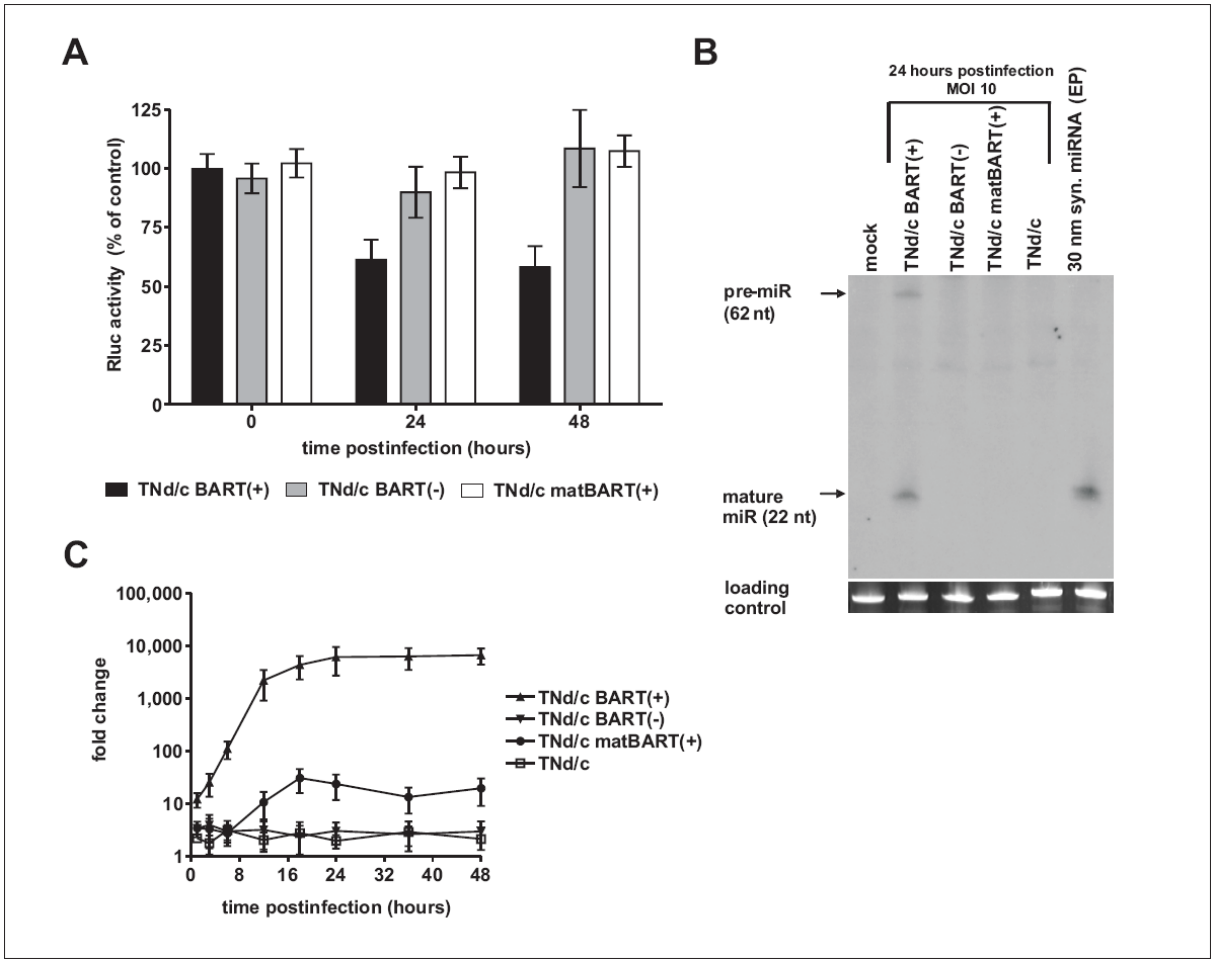
A
Rluc activity (% of control)
125
100
75
50
25
0
0
24
48
time postinfection (hours)
TNd/c BART(+)
TNd/c BART(-)
TNd/c matBART(+)
B
24 hours postinfection
MOI 10
mock
TNd/c BART(+)
TNd/c BART(-)
TNd/c matBART(+)
TNd/c
30 nm syn. miRNA (EP)
pre-miR
(62 nt)
mature
miR (22 nt)
loading
control
C
fold change
100,000
10,000
1,000
100
10
1
0
8
16
24
32
40
48
time postinfection (hours)
TNd/c BART(+)
TNd/c BART(-)
TNd/c matBART(+)
TNd/c

Figure 2

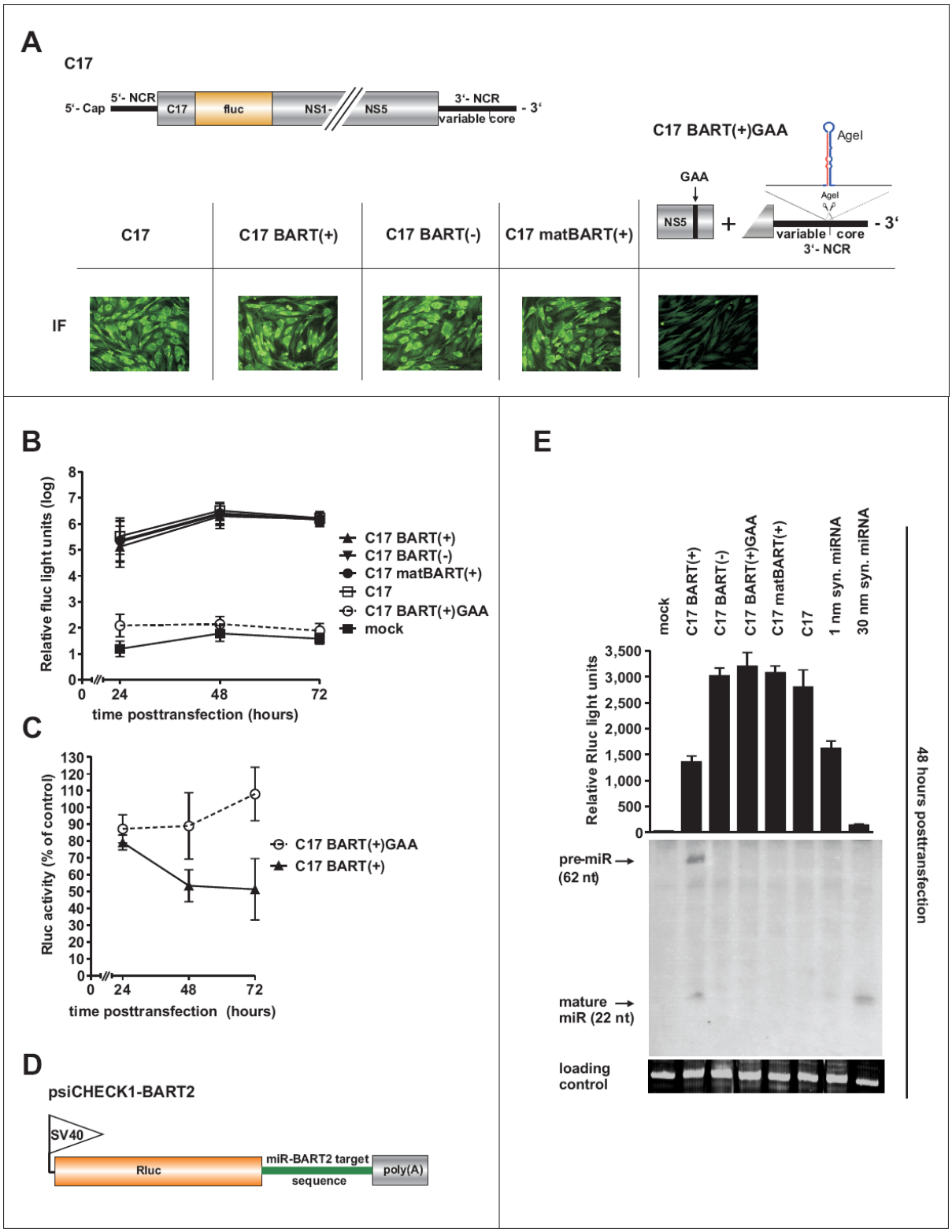
A
C17
5'- Cap
5'- NCR
C17
fluc
NS1-
NS5
3'- NCR
variable core
- 3'
C17 BART(+)GAA
AgeI
GAA
NS5
+
variable
core
3'- NCR
- 3'
C17
C17 BART(+)
C17 BART(-)
C17 matBART(+)
IF
B
Relative fluc light units (log)
time posttransfection (hours)
C17 BART(+)
C17 BART(-)
C17 matBART(+)
C17
C17 BART(+)GAA
mock
C
Rluc activity (% of control)
time posttransfection (hours)
C17 BART(+)GAA
C17 BART(+)
D
psiCHECK1-BART2
SV40
Rluc
miR-BART2 target sequence
poly(A)
E
mock
C17 BART(+)
C17 BART(-)
C17 BART(+)GAA
C17 matBART(+)
C17
1 nm syn. miRNA
30 nm syn. miRNA
Relative Rluc light units
pre-miR (62 nt)
mature miR (22 nt)
loading control
48 hours posttransfection

Figure 3

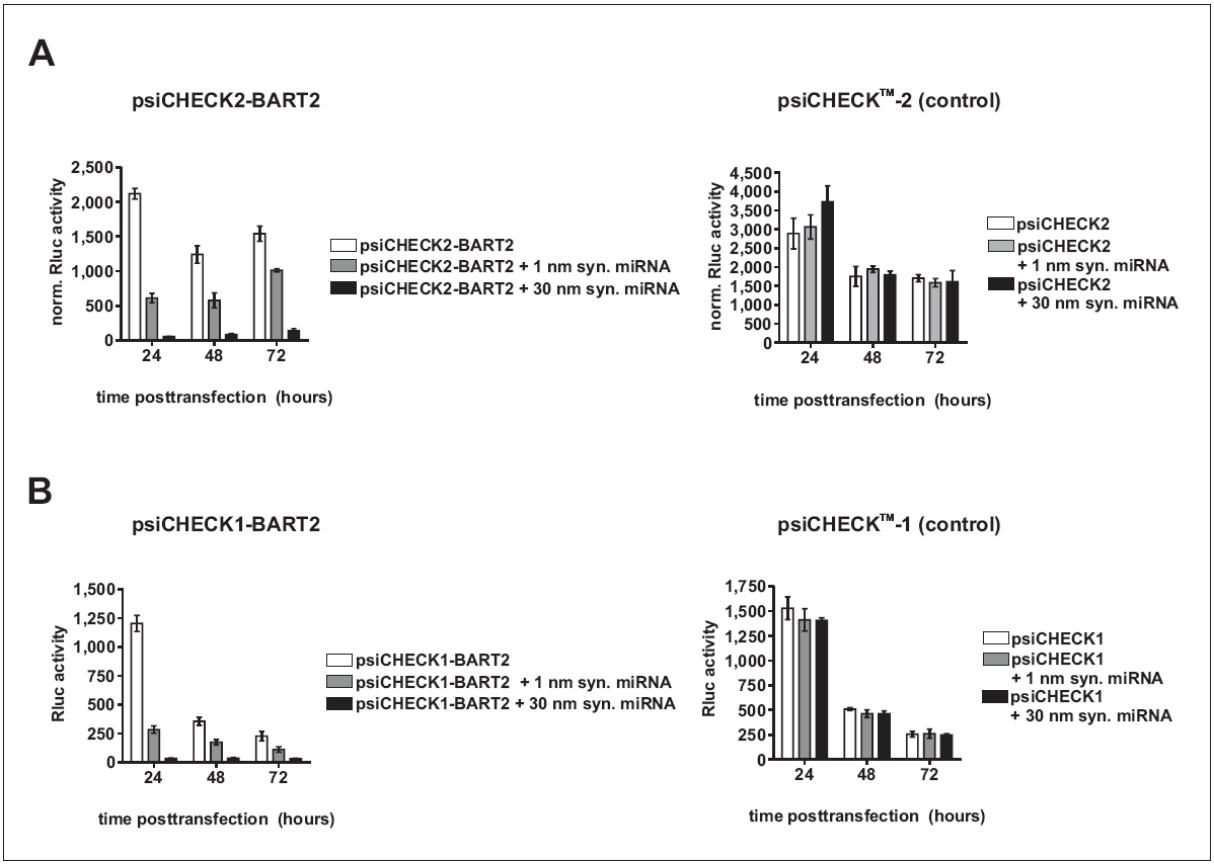

Supplementary Figure 1

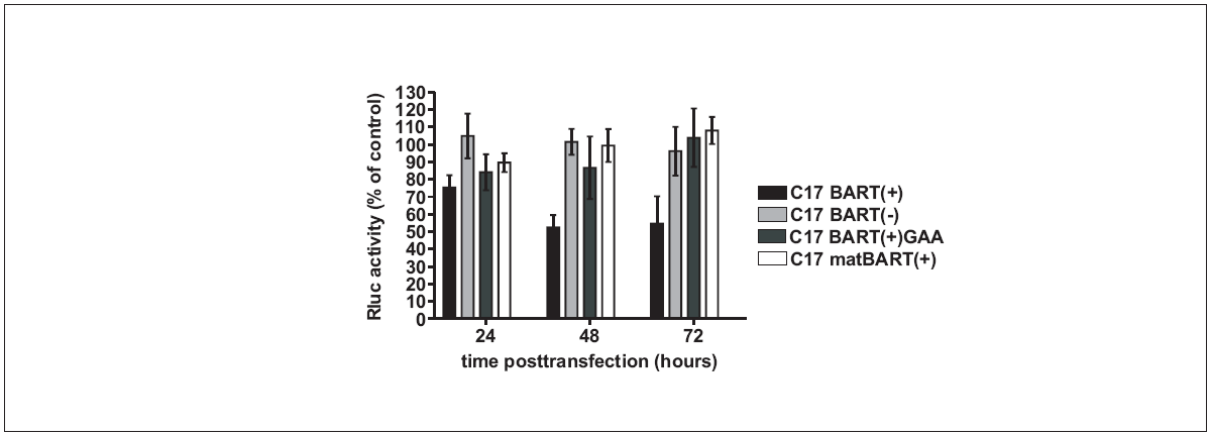

Supplementary Figure 2

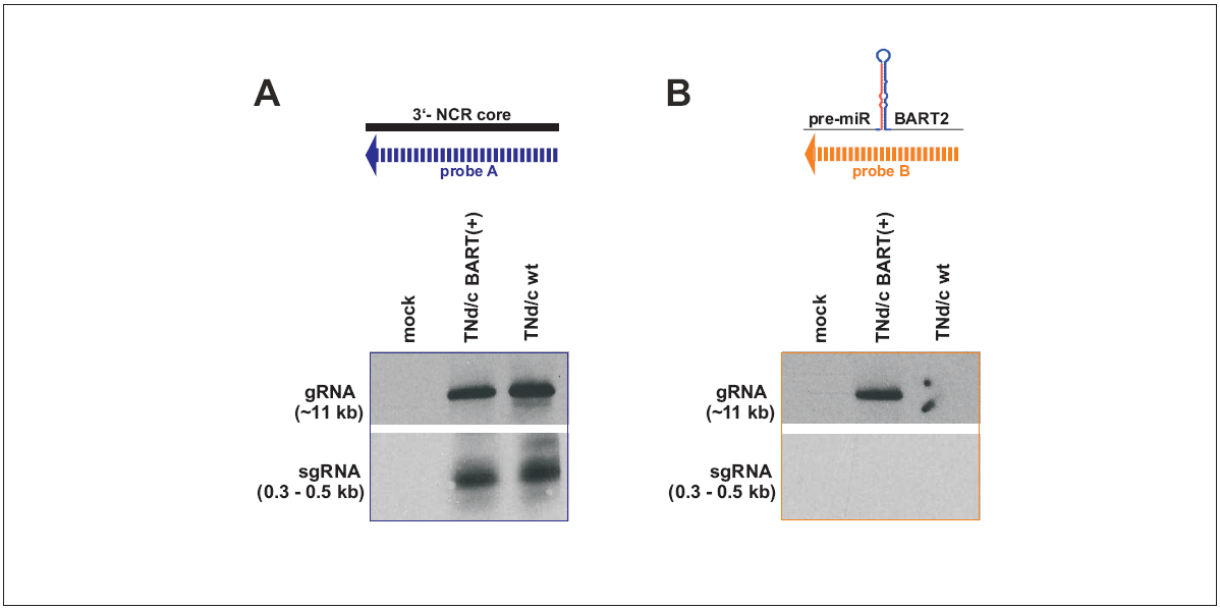

Supplementary Figure 3

5 MANUSCRIPT 3

Mutational analysis of three tick-borne encephalitis virus 5'-proximal stem-loop structures indicates different roles in RNA replication and translation

Harald Rouha[a,‡], Verena M. Hoenninger [a,‡],

Caroline Thurner [a,b] and Christian W. Mandl[a,c,†]

[a]Department of Virology, Medical University of Vienna, Vienna, Austria.

[b]Present address: Institute for Theoretical Chemistry, University of Vienna, Vienna, Austria.

[c]Present address: Novartis Vaccines and Diagnostics, Inc., Cambridge, MA, USA.

[†]Corresponding author. Mailing address: Department of Virology, Medical University of Vienna, Kinderspitalgasse 15, A-1095 Vienna, Austria. FAX: +43 1 40490 9795.

email address: christian.mandl@meduniwien.ac.at

[‡]These authors contributed equally to this work.

Abstract

The RNA genomes of flaviviruses encode important cis-acting elements that are involved in the modulation of viral gene expression. A majority of these elements are located within the 5'- and 3'-terminal untranslated regions. In spite of their functional importance, sequence and secondary structures of these regulatory elements vary considerably among different members of the genus. Computer assisted prediction of the tick-borne encephalitis virus (TBEV) RNA secondary structure suggested the formation of 4 characteristic stem-loop (SL) elements in the first 180 nts of the viral genome, 5'-SL1, 5'-SL2, 5'-SL3 and 5'-SL4. Here, we applied a recently developed sensitive luciferase-based TBEV reporter system to unravel the role of 5'-SL2, 5'-SL3 and 5'-SL4 in viral input RNA translation and RNA replication. Mutations were introduced to manipulate the thermodynamic stability of these SL elements. We found that a balanced stability equilibrium of the 5'-SL2 element, which had previously been shown to contain the 5'-part of the TBEV genome cyclization sequence, was required for efficient viral RNA replication. In addition our data suggest that the formation of the 5'-SL3 element is critical for viral RNA replication. Although this structure contains the AUG start codon, its formation was not or only to a very small extent required for viral input RNA translation, whereas stabilization even had a negative effect on translation. Finally, our data indicate that 5'-SL4 may facilitate RNA translation and replication similar to the previously described cHP element in the genome of two mosquito-borne flaviviruses although it is situated at a different genomic position.

Introduction

Flaviviruses are small enveloped viruses with a positive-stranded ~11 kb RNA genome and comprise one of the three genera within the family *Flaviviridae* (1). The genus is further divided into three groups, based on the mode of transmission: mosquito-borne, tick-borne

and no-known-vector flaviviruses. The two major arthropod vector groups include important human pathogens such as West Nile virus (WNV), Dengue virus (DENV), yellow fever virus (YFV), Japanese encephalitis virus (JEV) - (all of them mosquito-borne) and tick-borne encephalitis virus (TBEV), the most important tick-transmitted flavivirus. TBEV is endemic in parts of Asia and Europe and causes thousands of cases of severe neurological illness every year (1,2).

The RNA genome of all flaviviruses is a multifunctional molecule that serves as the sole mRNA for the translation into a single polyprotein, as template for minus-strand synthesis and as genomic RNA for incorporation into viral particles (1,3). To meet these versatile demands, the flaviviral RNA molecule is assumed to change its overall secondary structure at specific stages of the viral life cycle. Specific RNA sequence motifs in the terminal regions of the flavivirus genome may mediate these essential rearrangements (4). A well characterized aspect of these processes involves “cyclization” of the linear RNA molecule, in which base-pairing of a set of complementary RNA stretches present in the terminal regions of the genome induce the formation of a so-called panhandle-like structure (4-6). The viral replicase which specifically binds to a structure at the 5’-end of the genome is thus brought into close proximity of the 3’-terminus where it initiates synthesis of the negative-strand RNA molecule. Thus genome cyclization is essential for RNA replication of both mosquito-borne and tick-borne flaviviruses.

Although genomes of both virus groups share a great deal of organizational similarity, there are significant differences in the sequence motifs that mediate cyclization. In mosquito-borne flaviviruses, a 5’-cyclization sequence (5’-CS) within the capsid coding region binds to a complementary and highly conserved 3’-CS element in the 3’-NCR (4,5,7-9). In addition, a second interaction, outside of the 5’-3’-CS, has been reported (5,10,11), termed 5’-3’-UAR (upstream AUG region, as the 5’-element is located upstream of translation initiator AUG in the 5’-UTR). In contrast, in tick-borne flaviviruses a different set of sequence motifs mediates this process. The tick-borne 5’-CS-A element is located upstream of the viral start codon rather than downstream, and the complementary 3’-CS-A is placed at the bottom of the

terminal stem-loop 3'-SL1. Therefore this part of the 3'-SL1 cannot form when the genome has assumed the circularized conformation (12). Different from mosquito-borne flaviviruses, no functionality in RNA replication has been assigned to a second set of inverted sequence motifs (termed 5'- and 3'-CS-B) that had been predicted to be involved in long-range interactions by computational calculation (8,13,12).

Furthermore, a small RNA hairpin element in the capsid-coding region (capsid-coding region hairpin element, cHP) was shown for mosquito-borne flaviviruses (DENV and WNV) to enhance translation start codon selection and to be required for viral replication in a sequence-independent manner (14,15). Although a hairpin resembling the mosquito-borne cHP element is predicted to be maintained in tick-borne flaviviruses (5'-SL4), this structure is somewhat more distant from the AUG start codon and no function in viral gene expression has so far been demonstrated (12).

Recently we have established a luciferase reporter replicon for TBEV which allows measurement and discrimination of mutational effects on RNA replication and/or translation (16). Here we applied this novel system to unravel the roles of three 5'-proximal TBEV secondary structure elements, termed 5'-SL2, 5'-SL3 and 5'-SL4 in viral translation and replication. We introduced stabilizing and destabilizing (as far as hairpin obviating) mutations in these conserved RNA stem-loop structures. In the case of 5'-SL2, which includes the 5'-CS-A motif, RNA replication was found to strongly depend on its thermodynamic stability. Increase of stability completely abrogated RNA replication, presumably because it prevented 5'-CS-A to induce genome cyclization. Surprisingly, destabilization of 5'-SL2 also impaired RNA replication without, however, affecting translation. Furthermore, a role in RNA replication was also revealed for 5'-SL3. Destabilization of 5'-SL3 impaired RNA replication. In contrast, stabilization of this structure, which contains the AUG start codon, diminished translation, but had only a minor effect, if any, on RNA replication. Finally, the data indicate an auxiliary function of the 5'-SL4 in viral translation initiation and RNA replication, reminiscent of the mosquito-borne cHP element.

Results and Discussion

To independently analyze the role of 5'-SL2, 5'-SL3 and 5'-SL4 of TBEV (Fig. 1A) in viral replication and translation we constructed a set of mutants in the TBEV reporter replicon C17 (Rouha *et al.*, submitted) which has the viral structural proteins replaced by an in-frame insertion of the firefly luciferase gene (Fig. 1B). C17 is a modified version of the previously described plasmid C17fluc-TaV2A, which has been proven to be a valuable tool for the investigation of specific sequence elements that govern RNA translation and replication (16). In addition to the mutants described and characterized in detail below, two replicons were used as control throughout this study: 5'-ΔAUG, a construct lacking the entire capsid coding sequence starting from nucleotide position 133 including the 5'-SL3 (the stem-loop containing the viral translational START codon, Fig. 1C). This construct was used as a negative control for viral translation. As a translation competent control that is unable to replicate we used NS5-GAA, a construct corresponding to the wild-type replicon but carrying a mutated active site motif (GDD to GAA) of the viral RNA-dependent RNA polymerase (NS5),(16).

Analysis of the 5' stem-loop structure 2 (5'-SL2)

The 5'-SL2 contains the 5'-part of the TBEV CS-A element (Fig. 1A, in green). This CS-A element has been characterized previously (12). It has been shown by the introduction of point mutations that the long range interaction with the CS-A element in the viral 3'-NCR is crucial for RNA replication. Mutations in the 5'-CS-A element that impede the long-range interaction with the viral 3'-end, can be counterbalanced by compensatory mutations in the 3'-part of CS-A (12).

To investigate the importance of the 5'-SL2 formation, we engineered mutants carrying point mutations outside the CS-A motif that would interfere with or stabilize the stem-loop structure. The mutants 5'-SL2mut3 and 5'-SL2mut6 contain three, and six nucleotide changes, respectively (Fig. 2A, upper panel), that affect internal base pairing of the 5'-SL2.

The new sequences were predicted to fold into a significantly different structure (not shown). For both mutants, however, the potential to establish long-range interactions with the 3'-CS-A element is fully maintained according to thermodynamic analysis (Fig. 2A, bottom). A further mutant destabilizing the 5'-SL2 but still allowing the formation of the stem was generated, i.e. 5'-SL2mut2 (Fig. 2A). In addition we sought to augment the stability of 5'-SL2 by extending its stem by three additional G-C base pairs at its bottom end (construct 5'-SL2stab, Fig. 2A). The calculated stability for the 5'-SL2 in 5'-SL2stab is strongly increased compared to C17 (Fig. 2A, bottom). As a consequence, long range interaction with the 3'-CS-A element are rendered thermodynamically unfavorable due to the inability of this stem to open up.

To determine the effects of 5'-SL2 stabilization and destabilization on RNA translation and replication, the parental C17 and the above described mutant replicon RNAs were transcribed *in vitro* and equimolar amounts of RNA were transfected into BHK-21 cells. *Renilla*-standard RNA for an early time point (3 hours) and *Renilla*-standard DNA for later time points (15.5 – 72 hours) respectively, were coelectroporated with the firefly constructs followed by the measurement of both luc activities. The normalized luc signal at 3 hours posttransfection was representative for the translation activity. To asses RNA replication, we analyzed luc activities from 15.5 to 72 hours.

Transfection with mutants destabilizing and stabilizing the 5'-SL2 exhibited fluc activities similar to those transfected with C17 3 hours posttransfection (Fig. 2B), indicating that the stability of this stem-loop did not have an effect on viral RNA translation. However, significant differences were seen at later time points (Fig. 2C) indicating that the mutations influenced RNA replication. Destabilization of 5'-SL2 led to impairment of RNA replication in an order corresponding to the degree of destabilization (mut6>mut3>mut2). Remarkably, the mutants 5'-SL2mut3 and 5'-SL2mut6 in which 5'-SL2 is predicted to not form at all, exhibited more than twenty fold less luciferase activity than the parental replicon C17 at 15.5 to 72 hours after electroporation (Fig. 2C). Furthermore, 5'-SL2stab was entirely negative for RNA replication, although translation was not impaired. This is in good agreement with

thermodynamic calculations which yielded a negative ΔΔG value indicative of an inability of this mutant to induce long range interactions of 5'-CS-A with the 3'-CS-A element.

Taken together these results demonstrate that stability and formation of 5'-SL2 does not affect RNA translation, but a balanced stability equilibrium of this motif is necessary for efficient RNA replication. Both formation of 5'-SL2 and its ability to open up are required, providing indirect but compelling evidence that the viral RNA molecule assumes different conformations during its replication cycle.

Analysis of the 5' stem-loop structure 3 (5'-SL3)

An obvious and important feature of the TBEV 5'-SL3 is the presence of the translational AUG start codon in the 5'-arm of this RNA secondary structure motif (Fig. 1A). The exact mechanisms for flaviviral input RNA translation are unknown. Different from mosquito-borne flaviviruses, the start codon of TBEV is in a strong Kozak initiation context suggesting that translation occurs by cap dependent initiation followed by ribosome scanning through the 5'-NCR. To analyze the role of 5'-SL3 we generated two mutants destabilizing the stem (5'-SL3mut2 and 5'-SL3mut5) and one construct with a stabilized and elongated hairpin (5'-SL3stab) as depicted in Fig. 3A. The destabilized hairpin of mutant 5'-SL3mut2 was constructed to maintain the strong Kozak sequence, whereas the overall potential to build the hairpin structure was lowered according to the calculated stem-loop base pairing probability (Fig. 3A, bottom). The five destabilizing mutations in 5'-SL3mut5 were predicted to induce formation of a significantly different stem-loop structure (structure not shown). However, the strong Kozak initiation context was preserved and the mutations did not alter the encoded amino acid sequence.

Surprisingly, the destabilized mutant 5'-SL3mut2 did not exhibit a difference in the translation of the viral input RNA compared to C17 but had a distinct defect in RNA replication (Fig. 3B, C). A more than twenty-fold reduction of fluc levels was observed for this mutant at the later time points. Complete breakup of the original hairpin element (5'-SL3mut5) resulted in a similar impairment of RNA replication as destabilization did in 5'-

SL3mut2. In addition, there also seemed to be a slight effect on RNA translation in 5'-SL3mut5. An even stronger negative effect on translation, however, was caused by the stabilization of the stem-loop element (5'-SL3stab). Compared to C17 the translational peak of the viral input RNA was reduced more than 40%. Noticeably, the stabilization did not interfere with RNA replication as much as destabilization did.

These data suggest that the formation of the 5'-SL3 is necessary for optimal RNA replication. This is, although somehow surprising as the 5'-SL3 of TBEV does not contain the viral 5'-cyclization sequence, not directly comparable to the situation in mosquito-borne flaviviruses (DENV, WNV), where the translational start codon is contained within the secondary structure motif that also bears the 5'-UAR cyclization element. Moreover these results indicate that the formation of the stem-loop is only of little if any importance for RNA translation and that it can actually even impair the translational process if the stability of the structure is artificially augmented (5'-SL3stab). The latter observation likely reflects a consequence of the incurred restriction of the stabilized structure to get unwound during the viral RNA translation process. As seen with 5'-SL2, a balanced stability equilibrium seems therefore to be required for optimal functionality of the 5'-SL3.

Analysis of the 5' stem-loop structure 4 (5'-SL4)

In contrast to TBEV and other tick-borne-flaviviruses, mosquito-borne flaviviruses generally lack a strong Kozak initiation context. Recently it has been demonstrated that a short hairpin structure element downstream of the translational start codon, the cHP element, directs start codon selection and is responsible for high efficiency translation initiation from this AUG (15). Furthermore it has been found that the cHP element has a role in DENV RNA replication and that it operates in a sequence independent manner (14,15).

A stable, highly conserved hairpin structure element, the 5'-SL4 (Fig. 1A), is also present in the capsid coding region of tick-borne flaviviruses and it has been speculated earlier that this hairpin represents the TBEV analog of the mosquito-borne cHP and has been maintained by sequence covariation (15). Notably, however, the spacing between the TBEV

AUG startcodon and the 5'-SL4 is larger than the distance between the mosquito-borne AUG and the cHP. Given the fact that the TBEV virus AUG is in a strong Kozak initiation context and considering that the 5'-SL4 is not situated in a distance from the startcodon that would correspond to a ribosomal footprint (12-15 nt), it remained so far unclear whether the 5'-SL4 has a similar function in TBEV RNA synthesis or RNA translation than the mosquito-borne cHP element.

To address this question, we first performed a thermodynamic analysis of the TBEV 5'-SL4 structure. Interestingly, the results revealed an exceptionally high potential of the stem-loop to form several slightly different variants, i.e. different from other structures such as 5'-SL2 or 5'-SL3 there is not a single overall dominating secondary structure formation. At least three different hairpins are likely to occur at this position in a pool of viral RNAs (Fig. 4A, 5'-SL4 wt).This "secondary-structure ensemble" is caused by a series of 6 consecutive Gs at the 5'-arm of the stem-loop, and a series of 5 consecutive Cs at its 3'-end, which allows the stem-loop to shift for one or two nucleotides in 5'- or 3'-direction without a significant change in thermodynamic stability. According to our computational analysis this feature is specific for the tick-borne 5'-SL4 element and does not apply to the mosquito-borne cHP element (unpublished observation). We then wanted to investigate the role of this conserved stem-loop ensemble in viral RNA replication and translation, and also unravel a potential relevance of its extraordinary structural flexibility in any of these processes. To this end, we generated three different mutants (Fig. 4A). In 5'-SL4mut3, three nucleotide changes were engineered that – according to thermodynamic analysis – abolished the flexibility of the hairpin element by the introduction of a G-C anchor in the middle of the stem region. Thus, although the flexibility of this mutant was predicted to be destroyed by enforcing the formation of a single variant, the overall stability of the resulting hairpin was largely unchanged, compared to the wild-type structure ensemble. An opposite outcome was achieved with mutant 5'-SL4stab. Three additional G-C pairs were introduced at the base of the stem, resulting in an elongation and strong stabilization of the resulting hairpin structures, whereas the potential of these stabilized hairpins to slide was retained similar to the wild-type structure. In mutant

C10, the entire 5'-SL4 sequence element was deleted (The mutant designation C10 indicates that only the first 10 amino acids of the capsid protein are encoded, whereas C17 and all derivatives encode the first 17 residues).

All three replicons were tested for translation and replication as described before. Deletion of 5'-SL4 significantly impaired RNA translation by approximately 50%. Interestingly, the reduction of its structural flexibility (as achieved in mutant 5'-SL4mut3) also reduced translation. Although this mutant maintains one structure of the original ensemble, the luciferase assay revealed a more than 30% diminished translation efficiency, compared to the wildtype control C17 (Fig. 4B). In contrast, the elongation and stabilization of 5'-SL4 did not affect translation of input RNA (5'-SL4stab, Fig. 4B). This indicated that the presence and, notably, also the structural flexibility of 5'-SL4 can augment TBEV virus RNA translation.

The subsequent analysis of viral RNA replication revealed a moderate reduction in fluc levels obtained with C10 and 5'-SL4mut3 (Fig. 4C) indicating that the 5'-SL4 might also be involved in TBEV RNA replication. This would support earlier work of Clyde *et al.*, who suggested that the mosquito-borne cHP element and the corresponding element in tick-borne flaviviruses originally arose as a replication element that was only later recruited for translation initiation site selection in viruses that lack a strong Kozak initiation context, such as DENV or WNV (14). Most interestingly, however, the stabilization of the TBEV 5'-SL4 seemed to increase viral replication levels compared to the wild-type control at any time point included in our measurements. In contrast to the results obtained with 5'-SL2 and 5'-SL3, where a stability equilibrium of the secondary structure elements was either important for translation or replication, stabilization of 5'-SL4 did not appear to have a detrimental effect on any of these processes. This finding is in good agreement with a recent observation in DENV infected cells: Although it was found that destabilization of the cHP-element drastically decreased the titer of infectious virus, a more stable cHP element did not impact viral output or affect the kinetics of viral infection in human and mosquito cells (14).

Collectively, our results suggest that the TBEV 5'-SL4 contributes to translation initiation and also assists in viral RNA replication, a role that might be closely related to the proposed function of the mosquito-borne cHP element.

Material and Methods

Plasmids and cells

Replicon constructs in this study are all derivates of the cDNA clone of TBEV Western subtype prototypic strain Neudoerfl (GenBank Accession no. U27495). As parental construct the C17 replicon (described in Rouha *et al., submitted*) was used. Briefly, C17 lacks most of the structural protein coding region, replaced by the insertion of a firefly luciferase (fluc) followed by a 60-nucleotide-long 2A processing site of Thosea asigna virus. The firefly luciferase start codon (AUG) was deleted. Replicon cDNAs of all constructs were driven by a T7 promoter for *in vitro* transcription.

Cell culture

BHK-21 cells (ATCC CL10) were grown in Eagle's minimal essential medium (EMEM) supplemented with 5% fetal calf serum (FCS). The cells were electroporated using a GenePulser apparatus (Bio-Rad) as described previously (17). After transfection, the growth medium was replaced by a maintenance medium consisting of EMEM without phenol red (Cambrex), containing 1% FCS.

Mutant construction (5'-terminal region)

The C17 replicon was generated by the deletion of the start codon at position 132-134 (numbering according to the full-length sequence of strain Neudoerfl) using the forward mutagenesis primer F-fluc-AUGdel (GCCTTAATTAAGGAAGACGCCAAAAACAT), reverse primer R-E1 (TCTCCACACGACCAGGCCCT) and C17fluc-TaV2A as template for PCR amplification (Rouha *et al*., submitted). Replicon ΔAUG, that contained a deletion of 130-183

nucleotides (nt) and C10fluc with a deletion of 163 to 183 nt, were constructed by PCR amplification with the forward primer F-SalIreg (GCATCGGTCGACTTAATACGA) and the reverse primer NS1_SS_R (GCTCATGGACATTGTAGGGTTTCT), using the previously described plasmid clones Δ5'-SL3 and C10. The PCR products were trimmed with SalI and PacI replacing a fragment extending from a SalI site preceding the T7 promoter to a PacI site at nucleotide 184 with the corresponding region from C17. The replicon 5'-SL4mut3 was created by amplification using as template a partial cDNA clone C17ΔCME (containing the region extending from a unique SalI restriction site to the unique ClaI site at position 3155 within the NS1 coding region) and primer SalIreg and mutagenic primer R-5'-SL4mut3 GGTC*TTAATTAA*TCGTCGAGGCGGCCCGCCGC (the SalI recognition site is in cursive and the mutations in bold letters).

Plasmid 5'-SL2stab was constructed by three-step PCR using the mutagenic primer R-3'-SL2stab 5'-GGGCAGCTCTTGTTCTCCTAAGCTGCCCTCTTTTTCTCAACACGTT-3' and F-5'-SL2stab 5'-GGGCAGCTTAGGAGAACAAGAGCTGCCCGGGATGGTCAAGAAGGC-3'. The mutants 5'-SL2mut2 and 5'-SL2mut3 were generated, using a GeneTailor Site-Directed Mutagenesis System (Invitrogen), with mutagenic forward primers F-5'-SLmut2 (5'-CGTGTTGAGAAAAAGACAGCCGAGGAGAACAA-3'), F-5'-SLmut3 (5'-ACGTGTTGAGAAAAAGACCCGTTAGGAGAA) and a wild type reverse primer.

To generate all other mutants, bearing various mutations at their 5'-termini, the region from SalI and PacI was synthesized by GeneArt (Germany) then inserted into the C17 replicon, taking advantage of the corresponding SalI and PacI restriction sites.

As replication negative control NS5-GAA was used containing a mutation within the RNA dependent RNA polymerase (RdRp) active site at position 9652-9660 (GDD to GAA) (Hoenninger *et al.*, 2008). All plasmids were amplified in *Escherichia coli* HB101 and purified with commercially available systems (Qiagen).

RNA *in vitro* transcription, transfection and luciferase assay

RNA was transcribed from 1 µg aliquots of the plasmid DNA by T7 polymerase transcription, using commercially available reagents (Ambion) and conditions described in detail elsewhere (17). Briefly, after the transcription reaction, template DNA was digested by DNAseI incubation, purified and separated by unincorporated nucleotides by using an RNeasy Mini-Kit (Qiagen). RNA was then spectrophotometrically quantified and equal amounts (corresponding to approximately 1.4 x 10^{12} copies) were introduced into BHK-21 cells by electroporation with a Bio-Rad Gene Pulser, as described previously (17). For standardization the hRLSV40 plasmid (Promega) and an RNA expressing the *Renilla* luciferase was made by first linearizing the plasmid phRL-SV40 (Promega) with BamHI, followed by *in vitro* transcription, using the same procedure as described for the mutant constructs, respectively. The luciferase assay and standardization was performed as described elsewhere (Hoenninger *et al.* 2008).

Folding predictions

For all calculations of secondary structures we used the “Vienna RNApackage” (18). Calculations of the complete sequence of the wt genome C17 as well as all mutant contructs in this study revealed long range interactions, that lead to a panhandle like overall genome structure. For calculation of 5'- and 3'-secondary structures as shown in Fig.1 we recalculatetd the complete sequence with the constraints, that nt 115-123 and nt 11060-11063, 11068-11071 were not allowed to participate in any secondary structure. We obtained the secondary structures as shown in Fig. 1A for 5'- and 3'-terminal regions of the genome respectively. As closer inspection of folding probabilities showed that there was no secondary structures starting at the first 194 nucleotides that folded towards sections of the genome more downstream, we decided that it was feasible to use the first 194 nts to be a long enough template for estimating the ΔG and $\Delta\Delta G$ values of the stem-loops 5’- SL2, 5’-SL3 and 5’-SL4. As a reference value for the Gibbs free energy of the stem-loops 5’-SL2, 5’-SL3 and 5’-SL4, we calculated the difference between the Gibbs free energies of the first 194

nts with and without the constraint that the respective stem loops were allowed to form. We repeated the same calculations using the mutant sequences and thus obtained the contribution of the mutated stem loops to the overall Gibbs free energy of the structure. The difference of the Gibbs free energy of the mutated stem loops and the respective wt version of the stem loop revealed an energy value $\Delta\Delta G$, indicating the degree of stabilization (positive values) or destabilization (negative values).

References

1. Lindenbach, B.D., Thiel H.-J., Rice C.M. (2007) Flaviviridae: the viruses and their replication. *In: Knipe, D.M., Howley, P.M. (Eds.), Fields Virology, (5th ed.) Lippincott Williams & Wilkins Co., Philadelphia, PA., pp. 1101-1152.*
2. Gubler, D.J., Kuno, G., Markoff, R. (2007) Flaviviruses. *In: Knipe, D.M., Howley, P.M. (Eds.), Fields Virology, (5th ed.) Lippincott Williams & Wilkins Co., Philadelphia, PA., pp. 1154-1252.*
3. Wengler, G. and Gross, H.J. (1978) Studies on virus-specific nucleic acids synthesized in vertebrate and mosquito cells infected with flaviviruses. *Virology*, 89, 423-437.
4. Markoff, L. (2003) 5'- and 3'-noncoding regions in flavivirus RNA. *Adv Virus Res*, 59, 177-228.
5. Hahn, C.S., Hahn, Y.S., Rice, C.M., Lee, E., Dalgarno, L., Strauss, E.G. and Strauss, J.H. (1987) Conserved elements in the 3' untranslated region of flavivirus RNAs and potential cyclization sequences. *J Mol Biol*, 198, 33-41.
6. Villordo, S.M. and Gamarnik, A.V. (2008) Genome cyclization as strategy for flavivirus RNA replication. *Virus Res*.
7. Alvarez, D.E., De Lella Ezcurra, A.L., Fucito, S. and Gamarnik, A.V. (2005) Role of RNA structures present at the 3'UTR of dengue virus on translation, RNA synthesis, and viral replication. *Virology*, 339, 200-212.
8. Khromykh, A.A., Meka, H., Guyatt, K.J. and Westaway, E.G. (2001) Essential role of cyclization sequences in flavivirus RNA replication. *J Virol*, 75, 6719-6728.
9. Lo, M.K., Tilgner, M., Bernard, K.A. and Shi, P.Y. (2003) Functional analysis of mosquito-borne flavivirus conserved sequence elements within 3' untranslated region of West Nile virus by use of a reporting replicon that differentiates between viral translation and RNA replication. *J Virol*, 77, 10004-10014.

10. Khromykh, A.A., Varnavski, A.N., Sedlak, P.L. and Westaway, E.G. (2001) Coupling between replication and packaging of flavivirus RNA: evidence derived from the use of DNA-based full-length cDNA clones of Kunjin virus. *J Virol*, 75, 4633-4640.
11. Thurner, C., Witwer, C., Hofacker, I.L. and Stadler, P.F. (2004) Conserved RNA secondary structures in Flaviviridae genomes. *J Gen Virol*, 85, 1113-1124.
12. Kofler, R.M., Hoenninger, V.M., Thurner, C. and Mandl, C.W. (2006) Functional analysis of the tick-borne encephalitis virus cyclization elements indicates major differences between mosquito-borne and tick-borne flaviviruses. *J Virol*, 80, 4099-4113.
13. Mandl, C.W., Holzmann, H., Kunz, C. and Heinz, F.X. (1993) Complete genomic sequence of Powassan virus: evaluation of genetic elements in tick-borne versus mosquito-borne flaviviruses. *Virology*, 194, 173-184.
14. Clyde, K., Barrera, J. and Harris, E. (2008) The capsid-coding region hairpin element (cHP) is a critical determinant of dengue virus and West Nile virus RNA synthesis. *Virology*, 379, 314-323.
15. Clyde, K. and Harris, E. (2006) RNA secondary structure in the coding region of dengue virus type 2 directs translation start codon selection and is required for viral replication. *J Virol*, 80, 2170-2182.
16. Hoenninger, V.M., Rouha, H., Orlinger, K.K., Miorin, L., Marcello, A., Kofler, R.M. and Mandl, C.W. (2008) Analysis of the effects of alterations in the tick-borne encephalitis virus 3'-noncoding region on translation and RNA replication using reporter replicons. *Virology*, 377, 419-430.
17. Mandl, C.W., Ecker, M., Holzmann, H., Kunz, C. and Heinz, F.X. (1997) Infectious cDNA clones of tick-borne encephalitis virus European subtype prototypic strain Neudoerfl and high virulence strain Hypr. *J Gen Virol*, 78 (Pt 5), 1049-1057.
18. Hofacker, I.L. (2003) Vienna RNA secondary structure server. *Nucleic Acids Res*, 31, 3429-3431.

Figure Legends

Figure 1

Genome secondary structure and organization of TBEV and derived replicon constructs. (A) TBEV. The stem-loop structures are shown as predicted for the linear form, without consideration of the long-range interaction of the cyclization sequence (depicted in green) in the viral 5'-SL2 and 3'-SL2. The viral start codon AUG in the 5'-SL3 is highlighted in grey. **(B)** Generalized scheme of the parental replicon C17 that has the structural protein region of TBEV replaced by an in-frame insertion of the firefly luciferase gene (fluc). C17, truncated Capsid coding gene; E472, codon 472 of the E protein gene; NS1-NS5, the coding region for the non-structural proteins 1-5; NCR, noncoding region. **(C)** Schematic diagram of mutant replicon ΔAUG that lacks the entire capsid coding sequence starting from nucleotide position 133 including the 5'-SL3, containing the viral start codon. Diagrams A-C are not drawn to scale.

Figure 2

Characterization of 5'-SL2. (A) *Top.* Schematic drawing of the predicted secondary structure for wild-type 5'-SL2 (bold letters) and engineered mutant replicons. Nucleotide changes are depicted in red. *Bottom.* Thermodynamic analysis of wild-type 5'-SL2 and the respective mutants. ΔG, Gibbs free energy of the secondary structure of a segment of the first 194 nucleotides of the viral genome; ΔG_{const}, Gibbs free energy of the same segment calculated with the constraint that SL2 is not allowed to form; $\Delta G_{rel,}$ difference of ΔG and ΔG_{const} and thus the energetic contribution of SL2 (wt, mut2, mut3, mut6 and stab respectively) to the overall energy of the calculated segment; ΔΔG, the difference of ΔG_{rel} of the respective stem to the ΔG_{rel} of the wt; positive values correspond to destabilization whereas negative values reflect stabilization of the stem-loop. **(B)** Translation level of viral input RNA 3 hours posttransfection into BHK-21 cells. Normalized luciferase levels are shown as percentage relative to the parental control C17. RNA of construct ΔAUG, lacking

the viral translational start codon AUG, was used as a negative control. Error bars represent standard deviation of at least two independent experiments **(C)** Viral RNA replication efficiencies of the parental C17 replicon and mutants derived from it, monitored by normalized firefly luciferase activity in BHK-21 cells 15.5 - 72 hours posttransfection. Capped NS5-GAA RNA, which can be translated but cannot replicate due to a GDD to GAA mutation in the viral RNA polymerase gene NS5, was used as a control. Error bars represent the standard deviation of two independent experiments, each measured in triplicate.

Figure 3

Characterization of 5'-SL3. (A) *Top.* Schematic drawing of the predicted secondary structure for wild-type 5'-SL3 (bold letters) and engineered mutant replicons. Nucleotide changes are depicted in red. Thermodynamic analysis of wild-type 5'-SL3 and the respective mutants. ΔG, Gibbs free energy of the secondary structure of a segment of the first 194 nucleotides of the viral genome; ΔG_{const}, Gibbs free energy of the same segment calculated with the constraint that SL3 is not allowed to form; $\Delta G_{rel,}$ difference of ΔG and ΔG_{const} and thus the energetic contribution of SL3 (wt, mut2, mut5 and stab respectively) to the overall energy of the calculated segment; $\Delta\Delta G$, the difference of ΔG_{rel} of the respective stem to the ΔG_{rel} of the wt; positive values correspond to destabilization whereas negative values reflect stabilization of the stem-loop. **(B)** Translation level of viral input RNA 3 hours posttransfection into BHK-21 cells. Normalized luciferase levels are shown in % relative to the parental control C17. RNA of construct ΔAUG, lacking the viral translational start codon AUG, was used as a negative control. Error bars represent standard deviation of at least two independent experiments **(C)** Viral RNA replication efficiencies of the parental C17 replicon and mutants derived from it, monitored by normalized firefly luciferase activity in BHK-21 cells 15.5 - 72 hours posttransfection. Capped NS5-GAA RNA, which can be translated but cannot replicate due to a GDD to GAA mutation in the viral RNA polymerase gene NS5, was used as a control. Error bars represent the standard deviation of two independent experiments, each measured in triplicate.

Figure 4

Characterization of 5'-SL4. (A) *Top.* Schematic drawing of the predicted secondary structures for wild-type 5'-SL4 (bold letters) and engineered mutant replicons. Nucleotide changes are depicted in red. Structures shown in the middle are the ones that have the highest probability to be formed in the structure ensemble. Arrows indicate a shift in another secondary structure of the same stem-loop element (see text for details). Hairpins which are not predicted to be formed any more as a result of the introduced mutations or hairpins that have been deleted (red cross) are shown in light grey. *Bottom.* Thermodynamic analysis of wild-type (C17) and the respective mutants. ΔG, Gibbs free energy of the secondary structure of a segment of the first 194 nucleotides of the viral genome; ΔG_{const}, Gibbs free energy of the same segment calculated with the constraint that SL4 is not allowed to form; $\Delta G_{rel,}$ difference of ΔG and ΔG_{const} and thus the energetic contribution of SL4 (wt, mut3 and stab respectively) to the overall energy of the calculated segment; $\Delta\Delta$G, the difference of ΔG_{rel} of the respective stem to the ΔG_{rel} of the wt; positive values correspond to destabilization whereas negative values reflect stabilization of the stem-loop. **(B)** Translation level of viral input RNA 3 hours posttransfection into BHK-21 cells. Normalized luciferase levels are shown in % relative to the parental control C17. RNA of construct ΔAUG, lacking the viral translational start codon AUG, was used as a negative control. Error bars represent standard deviation of at least two independent experiments **(C)** Viral RNA replication efficiencies of the parental C17 replicon and mutants derived from it, monitored by normalized firefly luciferase activity in BHK-21 cells 15.5-72 hours posttransfection. Capped NS5-GAA RNA, which can be translated but cannot replicate due to a GDD to GAA mutation in the viral RNA polymerase gene NS5, was used as a control. Error bars represent the standard deviation of two independent experiments, each measured in triplicate.

Figures

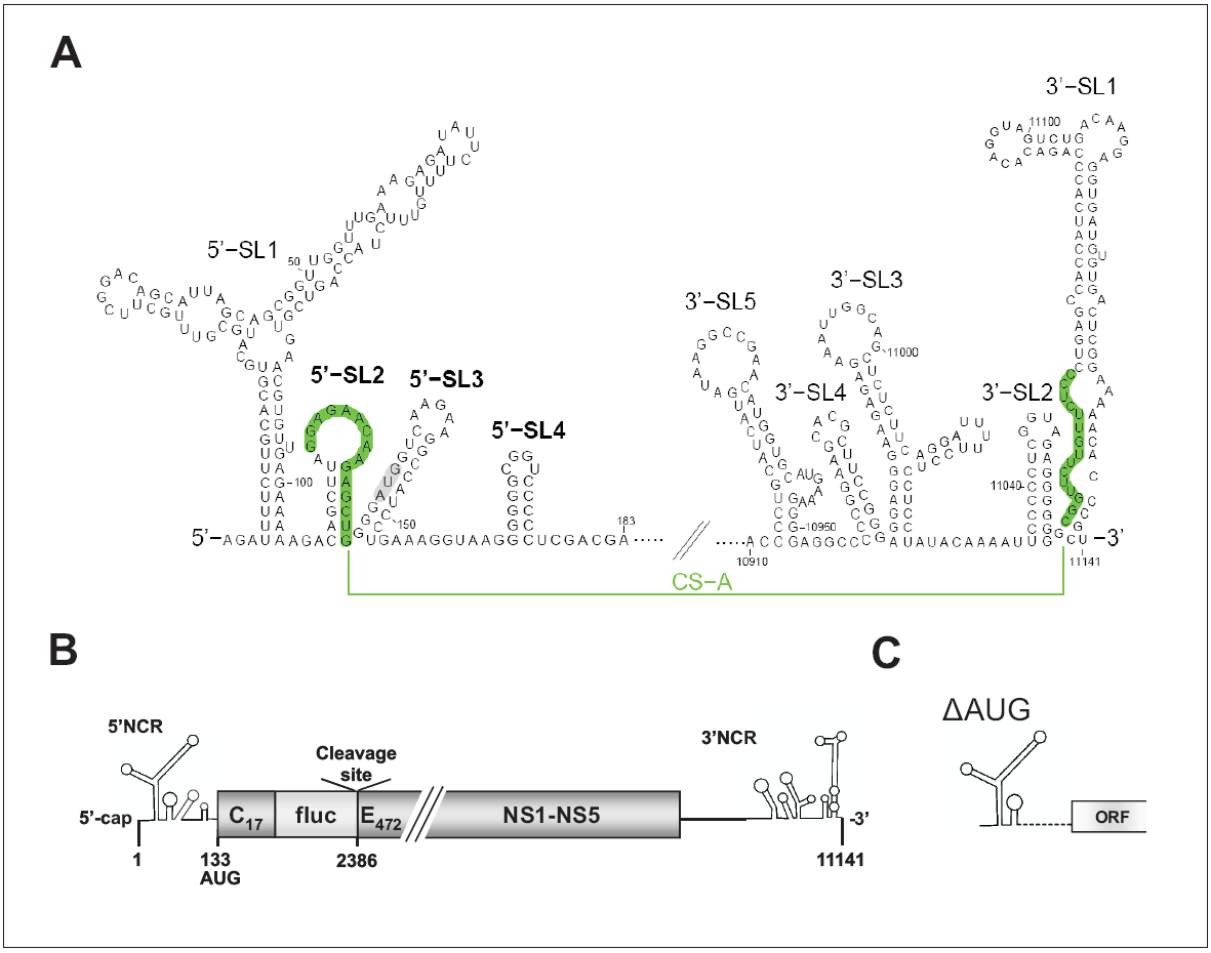

Figure 1

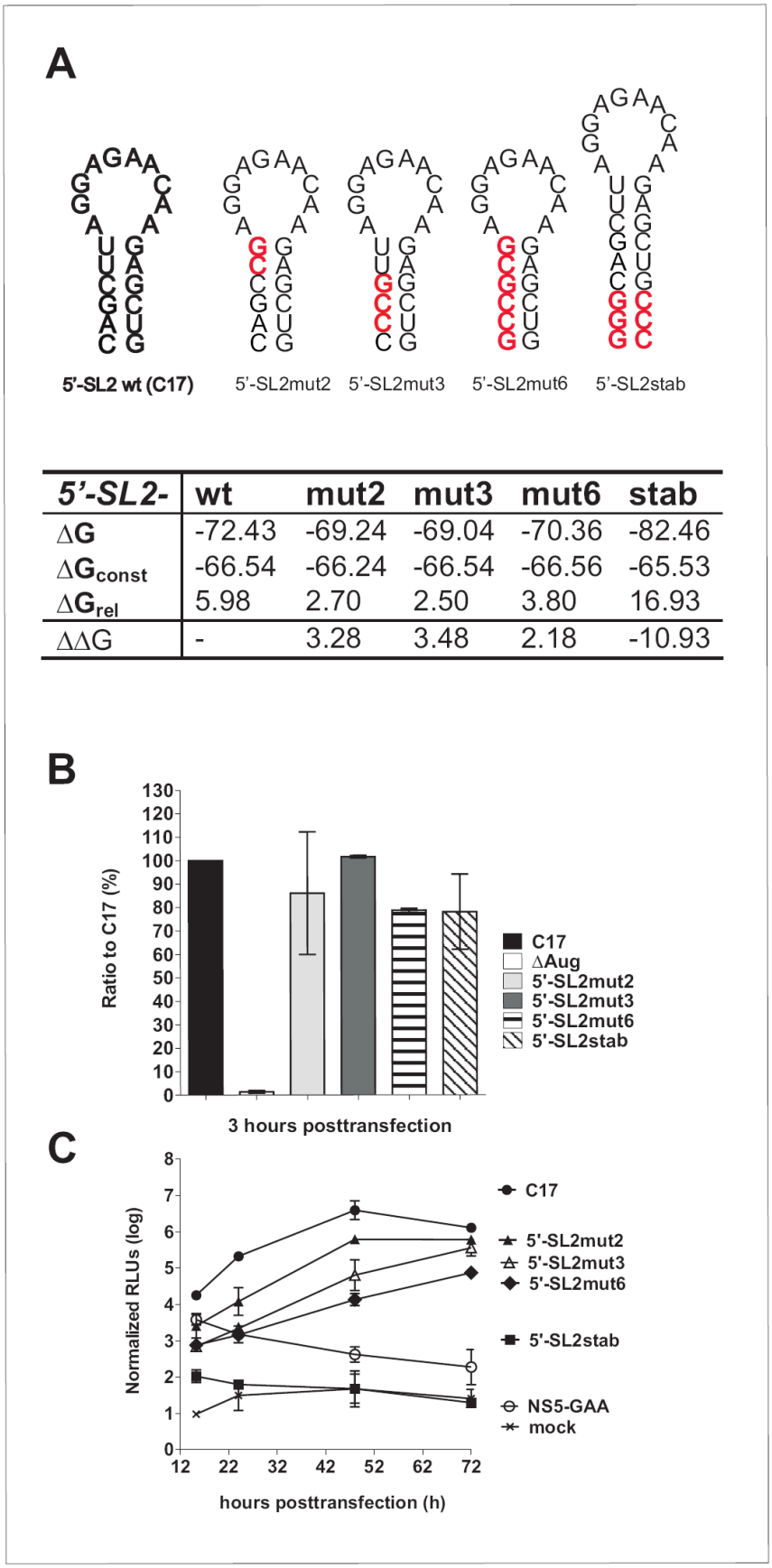

5'-SL2-	wt	mut2	mut3	mut6	stab
ΔG	-72.43	-69.24	-69.04	-70.36	-82.46
ΔG_{const}	-66.54	-66.24	-66.54	-66.56	-65.53
ΔG_{rel}	5.98	2.70	2.50	3.80	16.93
ΔΔG	-	3.28	3.48	2.18	-10.93

Figure 2

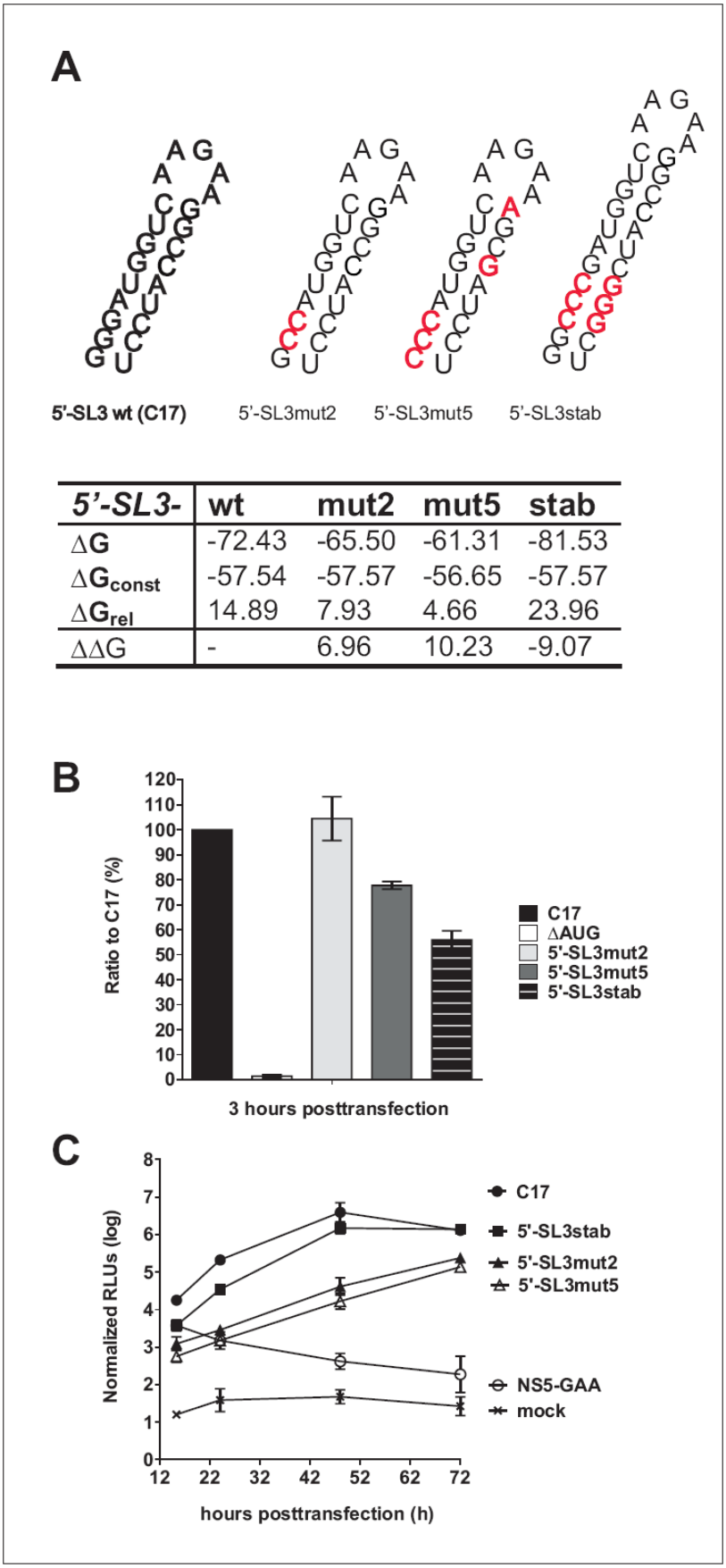

5'-SL3-	wt	mut2	mut5	stab
ΔG	-72.43	-65.50	-61.31	-81.53
ΔG_{const}	-57.54	-57.57	-56.65	-57.57
ΔG_{rel}	14.89	7.93	4.66	23.96
ΔΔG	-	6.96	10.23	-9.07

Figure 3

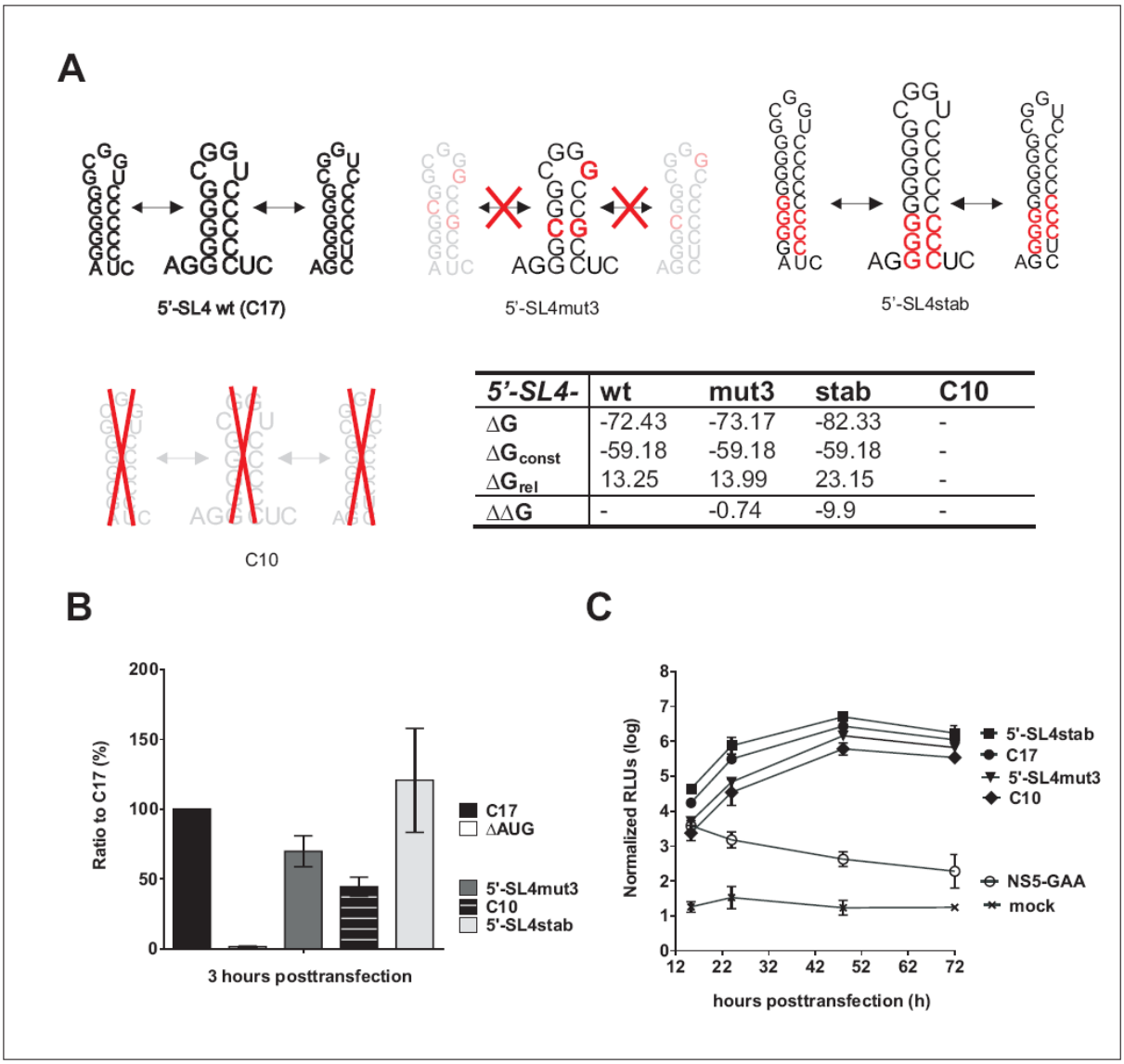
A
5'-SL4 wt (C17)
5'-SL4mut3
5'-SL4stab
C10
5'-SL4- | wt | mut3 | stab | C10
ΔG | -72.43 | -73.17 | -82.33 | -
ΔG const | -59.18 | -59.18 | -59.18 | -
ΔG rel | 13.25 | 13.99 | 23.15 | -
ΔΔG | - | -0.74 | -9.9 | -
B
Ratio to C17 (%)
200
150
100
50
0
C17
ΔAUG
5'-SL4mut3
C10
5'-SL4stab
3 hours posttransfection
C
Normalized RLUs (log)
8
7
6
5
4
3
2
1
0
12
22
32
42
52
62
72
hours posttransfection (h)
5'-SL4stab
C17
5'-SL4mut3
C10
NS5-GAA
mock

Figure 4

6 REFERENCES

1. Lindenbach, B.D., Thiel, H.-J., Rice, C.M. (2007) In Knipe, D. M., Howley, P.M. (ed.), *Fields Virology, 5th ed. Lippincott Williams & Wilkins Co., Philadelphia, PA.*, Philadelphia, pp. 1101-1152.
2. Calisher, C.H., Karabatsos, N., Dalrymple, J.M., Shope, R.E., Porterfield, J.S., Westaway, E.G. and Brandt, W.E. (1989) Antigenic relationships between flaviviruses as determined by cross-neutralization tests with polyclonal antisera. *J Gen Virol*, **70 (Pt 1),** 37-43.
3. Mukhopadhyay, S., Kuhn, R.J. and Rossmann, M.G. (2005) A structural perspective of the flavivirus life cycle. *Nat Rev Microbiol*, **3,** 13-22.
4. Gyure, K.A. (2009) West Nile virus infections. *J Neuropathol Exp Neurol*, **68,** 1053-1060.
5. Nash, D., Mostashari, F., Fine, A., Miller, J., O'Leary, D., Murray, K., Huang, A., Rosenberg, A., Greenberg, A., Sherman, M. *et al.* (2001) The outbreak of West Nile virus infection in the New York City area in 1999. *N Engl J Med*, **344,** 1807-1814.
6. Lindsey, N.P., Staples, J.E., Lehman, J.A. and Fischer, M. Surveillance for human West Nile virus disease - United States, 1999-2008. *MMWR Surveill Summ*, **59,** 1-17.
7. Dauphin, G. and Zientara, S. (2007) West Nile virus: recent trends in diagnosis and vaccine development. *Vaccine*, **25,** 5563-5576.
8. WHO. Dengue and dengue haemorrhagic fever, Fact sheet W.H.O., 2010. http://www.who.int/mediacentre/factsheets/fs117/en/, (accessed May 7, 2010).
9. Weaver, S.C. and Reisen, W.K. Present and future arboviral threats. *Antiviral Res*, **85,** 328-345.
10. Gould, E.A. and Solomon, T. (2008) Pathogenic flaviviruses. *Lancet*, **371,** 500-509.
11. Goncalvez, A.P., Engle, R.E., St Claire, M., Purcell, R.H. and Lai, C.J. (2007) Monoclonal antibody-mediated enhancement of dengue virus infection in vitro and in vivo and strategies for prevention. *Proc Natl Acad Sci U S A*, **104,** 9422-9427.
12. Kliks, S.C., Nimmanitya, S., Nisalak, A. and Burke, D.S. (1988) Evidence that maternal dengue antibodies are important in the development of dengue hemorrhagic fever in infants. *Am J Trop Med Hyg*, **38,** 411-419.
13. Webster, D.P., Farrar, J. and Rowland-Jones, S. (2009) Progress towards a dengue vaccine. *Lancet Infect Dis*, **9,** 678-687.
14. Hanna, J.N., Ritchie, S.A., Phillips, D.A., Shield, J., Bailey, M.C., Mackenzie, J.S., Poidinger, M., McCall, B.J. and Mills, P.J. (1996) An outbreak of Japanese encephalitis in the Torres Strait, Australia, 1995. *Med J Aust*, **165,** 256-260.
15. Mackenzie, J.S. (2005) Emerging zoonotic encephalitis viruses: lessons from Southeast Asia and Oceania. *J Neurovirol*, **11,** 434-440.
16. CDC. Japanese Encephalitis Fact Sheet CDC 2010, , http://www.cdc.gov/ncidod/dvbid/jencephalitis/facts.html, (accessed May 7, 2010).

17. CDC. Travelers' Health - Yellow Book: Chapter 2: Japanese Encephalitis. http://wwwnc.cdc.gov/travel/yellowbook/2010/chapter-2/japanese-encephalitis.aspx, (accessed May 7, 2010).
18. CDC. Yellow Fever Fact Sheet, 2010. http://www.cdc.gov/ncidod/dvbid/yellowfever/YF_FactSheet.html, (accessed May 7, 2010)
19. WHO. Yellow Fever Fact Sheet,. 2010. http://www.who.int/mediacentre/factsheets/fs100/en/ (accessed May 7, 2010)
20. Ravanfar, P., Satyaprakash, A., Creed, R. and Mendoza, N. (2009) Existing antiviral vaccines. *Dermatol Ther*, **22,** 110-128.
21. Ecker, M., Allison, S.L., Meixner, T. and Heinz, F.X. (1999) Sequence analysis and genetic classification of tick-borne encephalitis viruses from Europe and Asia. *J Gen Virol*, **80 (Pt 1),** 179-185.
22. Dumpis, U., Crook, D. and Oksi, J. (1999) Tick-borne encephalitis. *Clin Infect Dis*, **28,** 882-890.
23. Clarke, D.H. (1964) Further Studies on Antigenic Relationships among the Viruses of the Group B Tick-Borne Complex. *Bull World Health Organ*, **31,** 45-56.
24. Holzmann, H., Aberle, S.W., Stiasny, K., Werner, P., Mischak, A., Zainer, B., Netzer, M., Koppi, S., Bechter, E. and Heinz, F.X. (2009) Tick-borne encephalitis from eating goat cheese in a mountain region of Austria. *Emerg Infect Dis*, **15,** 1671-1673.
25. Lindquist, L. and Vapalahti, O. (2008) Tick-borne encephalitis. *Lancet*, **371,** 1861-1871.
26. Suss, J. (2008) Tick-borne encephalitis in Europe and beyond--the epidemiological situation as of 2007. *Euro Surveill*, **13**.
27. CDC. Travelers' Health - Yellow Book: Chapter 5: Tick-borne encephalitis. http://wwwnc.cdc.gov/travel/yellowbook/2010/chapter-5/tick-borne-encephalitis.aspx, (accessed May 7, 2010)
28. Heinz, F.X., Holzmann, H., Essl, A. and Kundi, M. (2007) Field effectiveness of vaccination against tick-borne encephalitis. *Vaccine*, **25,** 7559-7567.
29. Stiasny, K. and Heinz, F.X. (2006) Flavivirus membrane fusion. *J Gen Virol*, **87,** 2755-2766.
30. Wengler, G. and Wengler, G. (1981) Terminal sequences of the genome and replicative-from RNA of the flavivirus West Nile virus: absence of poly(A) and possible role in RNA replication. *Virology*, **113,** 544-555.
31. Kroschewski, H., Allison, S.L., Heinz, F.X. and Mandl, C.W. (2003) Role of heparan sulfate for attachment and entry of tick-borne encephalitis virus. *Virology*, **308,** 92-100.
32. Mandl, C.W., Kroschewski, H., Allison, S.L., Kofler, R., Holzmann, H., Meixner, T. and Heinz, F.X. (2001) Adaptation of tick-borne encephalitis virus to BHK-21 cells results in the formation of multiple heparan sulfate binding sites in the envelope protein and attenuation in vivo. *J Virol*, **75,** 5627-5637.
33. Allison, S.L., Schalich, J., Stiasny, K., Mandl, C.W., Kunz, C. and Heinz, F.X. (1995) Oligomeric rearrangement of tick-borne encephalitis virus envelope proteins induced by an acidic pH. *J Virol*, **69,** 695-700.

34. Westaway, E.G., Mackenzie, J.M. and Khromykh, A.A. (2002) Replication and gene function in Kunjin virus. *Curr Top Microbiol Immunol*, **267,** 323-351.
35. Uchil, P.D. and Satchidanandam, V. (2003) Architecture of the flaviviral replication complex. Protease, nuclease, and detergents reveal encasement within double-layered membrane compartments. *J Biol Chem*, **278,** 24388-24398.
36. Mandl, C.W. (2005) Steps of the tick-borne encephalitis virus replication cycle that affect neuropathogenesis. *Virus Res*, **111,** 161-174.
37. Stadler, K., Allison, S.L., Schalich, J. and Heinz, F.X. (1997) Proteolytic activation of tick-borne encephalitis virus by furin. *J Virol*, **71,** 8475-8481.
38. Liu, Y., Wimmer, E. and Paul, A.V. (2009) Cis-acting RNA elements in human and animal plus-strand RNA viruses. *Biochim Biophys Acta*, **1789,** 495-517.
39. Yocupicio-Monroy, M., Padmanabhan, R., Medina, F. and del Angel, R.M. (2007) Mosquito La protein binds to the 3' untranslated region of the positive and negative polarity dengue virus RNAs and relocates to the cytoplasm of infected cells. *Virology*, **357,** 29-40.
40. Ruiz-Linares, A., Bouloy, M., Girard, M. and Cahour, A. (1989) Modulations of the in vitro translational efficiencies of Yellow Fever virus mRNAs: interactions between coding and noncoding regions. *Nucleic Acids Res*, **17,** 2463-2476.
41. Markoff, L. (2003) 5'- and 3'-noncoding regions in flavivirus RNA. *Adv Virus Res*, **59,** 177-228.
42. Rice, C.M., Lenches, E.M., Eddy, S.R., Shin, S.J., Sheets, R.L. and Strauss, J.H. (1985) Nucleotide sequence of yellow fever virus: implications for flavivirus gene expression and evolution. *Science*, **229,** 726-733.
43. Gritsun, T.S. and Gould, E.A. (2007) Origin and evolution of flavivirus 5'UTRs and panhandles: trans-terminal duplications? *Virology*, **366,** 8-15.
44. Cahour, A., Pletnev, A., Vazielle-Falcoz, M., Rosen, L. and Lai, C.J. (1995) Growth-restricted dengue virus mutants containing deletions in the 5' noncoding region of the RNA genome. *Virology*, **207,** 68-76.
45. Dong, H., Ray, D., Ren, S., Zhang, B., Puig-Basagoiti, F., Takagi, Y., Ho, C.K., Li, H. and Shi, P.Y. (2007) Distinct RNA elements confer specificity to flavivirus RNA cap methylation events. *J Virol*, **81,** 4412-4421.
46. Lodeiro, M.F., Filomatori, C.V. and Gamarnik, A.V. (2009) Structural and functional studies of the promoter element for dengue virus RNA replication. *J Virol*, **83,** 993-1008.
47. Filomatori, C.V., Lodeiro, M.F., Alvarez, D.E., Samsa, M.M., Pietrasanta, L. and Gamarnik, A.V. (2006) A 5' RNA element promotes dengue virus RNA synthesis on a circular genome. *Genes Dev*, **20,** 2238-2249.
48. Villordo, S.M. and Gamarnik, A.V. (2009) Genome cyclization as strategy for flavivirus RNA replication. *Virus Res*, **139,** 230-239.
49. Kofler, R.M., Hoenninger, V.M., Thurner, C. and Mandl, C.W. (2006) Functional analysis of the tick-borne encephalitis virus cyclization elements indicates major differences between mosquito-borne and tick-borne flaviviruses. *J Virol*, **80,** 4099-4113.
50. Khromykh, A.A., Meka, H., Guyatt, K.J. and Westaway, E.G. (2001) Essential role of cyclization sequences in flavivirus RNA replication. *J Virol*, **75,** 6719-6728.

51. Zhang, B., Dong, H., Stein, D.A., Iversen, P.L. and Shi, P.Y. (2008) West Nile virus genome cyclization and RNA replication require two pairs of long-distance RNA interactions. *Virology*, **373,** 1-13.
52. Alvarez, D.E., De Lella Ezcurra, A.L., Fucito, S. and Gamarnik, A.V. (2005) Role of RNA structures present at the 3'UTR of dengue virus on translation, RNA synthesis, and viral replication. *Virology*, **339,** 200-212.
53. Lo, M.K., Tilgner, M., Bernard, K.A. and Shi, P.Y. (2003) Functional analysis of mosquito-borne flavivirus conserved sequence elements within 3' untranslated region of West Nile virus by use of a reporting replicon that differentiates between viral translation and RNA replication. *J Virol*, **77,** 10004-10014.
54. Edgil, D., Polacek, C. and Harris, E. (2006) Dengue virus utilizes a novel strategy for translation initiation when cap-dependent translation is inhibited. *J Virol*, **80,** 2976-2986.
55. Clyde, K. and Harris, E. (2006) RNA secondary structure in the coding region of dengue virus type 2 directs translation start codon selection and is required for viral replication. *J Virol*, **80,** 2170-2182.
56. Kozak, M. (1987) An analysis of 5'-noncoding sequences from 699 vertebrate messenger RNAs. *Nucleic Acids Res*, **15,** 8125-8148.
57. Kozak, M. (1990) Downstream secondary structure facilitates recognition of initiator codons by eukaryotic ribosomes. *Proc Natl Acad Sci U S A*, **87,** 8301-8305.
58. Pijlman, G.P., Funk, A., Kondratieva, N., Leung, J., Torres, S., van der Aa, L., Liu, W.J., Palmenberg, A.C., Shi, P.Y., Hall, R.A. *et al.* (2008) A highly structured, nuclease-resistant, noncoding RNA produced by flaviviruses is required for pathogenicity. *Cell Host Microbe*, **4,** 579-591.
59. Wallner, G., Mandl, C.W., Kunz, C. and Heinz, F.X. (1995) The flavivirus 3'-noncoding region: extensive size heterogeneity independent of evolutionary relationships among strains of tick-borne encephalitis virus. *Virology*, **213,** 169-178.
60. Mandl, C.W., Kunz, C. and Heinz, F.X. (1991) Presence of poly(A) in a flavivirus: significant differences between the 3' noncoding regions of the genomic RNAs of tick-borne encephalitis virus strains. *J Virol*, **65,** 4070-4077.
61. Mandl, C.W., Holzmann, H., Meixner, T., Rauscher, S., Stadler, P.F., Allison, S.L. and Heinz, F.X. (1998) Spontaneous and engineered deletions in the 3' noncoding region of tick-borne encephalitis virus: construction of highly attenuated mutants of a flavivirus. *J Virol*, **72,** 2132-2140.
62. Mandl, C.W., Holzmann, H., Kunz, C. and Heinz, F.X. (1993) Complete genomic sequence of Powassan virus: evaluation of genetic elements in tick-borne versus mosquito-borne flaviviruses. *Virology*, **194,** 173-184.
63. Gehrke, R., Heinz, F.X., Davis, N.L. and Mandl, C.W. (2005) Heterologous gene expression by infectious and replicon vectors derived from tick-borne encephalitis virus and direct comparison of this flavivirus system with an alphavirus replicon. *J Gen Virol*, **86,** 1045-1053.
64. Hayasaka, D., Yoshii, K., Ueki, T., Iwasaki, T. and Takashima, I. (2004) Sub-genomic replicons of Tick-borne encephalitis virus. *Arch Virol*, **149,** 1245-1256.

65. Orlinger, K.K., Hoenninger, V.M., Kofler, R.M. and Mandl, C.W. (2006) Construction and mutagenesis of an artificial bicistronic tick-borne encephalitis virus genome reveals an essential function of the second transmembrane region of protein e in flavivirus assembly. *J Virol*, **80,** 12197-12208.

66. Orlinger, K.K., Kofler, R.M., Heinz, F.X., Hoenninger, V.M. and Mandl, C.W. (2007) Selection and analysis of mutations in an encephalomyocarditis virus internal ribosome entry site that improve the efficiency of a bicistronic flavivirus construct. *J Virol*, **81,** 12619-12629.

67. Lee, R.C., Feinbaum, R.L. and Ambros, V. (1993) The C. elegans heterochronic gene lin-4 encodes small RNAs with antisense complementarity to lin-14. *Cell*, **75,** 843-854.

68. Wightman, B., Ha, I. and Ruvkun, G. (1993) Posttranscriptional regulation of the heterochronic gene lin-14 by lin-4 mediates temporal pattern formation in C. elegans. *Cell*, **75,** 855-862.

69. Kim, V.N., Han, J. and Siomi, M.C. (2009) Biogenesis of small RNAs in animals. *Nat Rev Mol Cell Biol*, **10,** 126-139.

70. Ghildiyal, M. and Zamore, P.D. (2009) Small silencing RNAs: an expanding universe. *Nat Rev Genet*, **10,** 94-108.

71. Aravin, A.A., Lagos-Quintana, M., Yalcin, A., Zavolan, M., Marks, D., Snyder, B., Gaasterland, T., Meyer, J. and Tuschl, T. (2003) The small RNA profile during Drosophila melanogaster development. *Dev Cell*, **5,** 337-350.

72. Vagin, V.V., Sigova, A., Li, C., Seitz, H., Gvozdev, V. and Zamore, P.D. (2006) A distinct small RNA pathway silences selfish genetic elements in the germline. *Science*, **313,** 320-324.

73. Grivna, S.T., Pyhtila, B. and Lin, H. (2006) MIWI associates with translational machinery and PIWI-interacting RNAs (piRNAs) in regulating spermatogenesis. *Proc Natl Acad Sci U S A*, **103,** 13415-13420.

74. Grimm, D. (2009), *Adv Drug Deliv Rev*, Vol. 61, pp. 672-703.

75. Meister, G. and Tuschl, T. (2004) Mechanisms of gene silencing by double-stranded RNA. *Nature*, **431,** 343-349.

76. Napoli, C., Lemieux, C. and Jorgensen, R. (1990) Introduction of a Chimeric Chalcone Synthase Gene into Petunia Results in Reversible Co-Suppression of Homologous Genes in trans. *Plant Cell*, **2,** 279-289.

77. Romano, N. and Macino, G. (1992) Quelling: transient inactivation of gene expression in Neurospora crassa by transformation with homologous sequences. *Mol Microbiol*, **6,** 3343-3353.

78. Baulcombe, D.C. (1996) Mechanisms of Pathogen-Derived Resistance to Viruses in Transgenic Plants. *Plant Cell*, **8,** 1833-1844.

79. Kumagai, M.H., Donson, J., della-Cioppa, G., Harvey, D., Hanley, K. and Grill, L.K. (1995) Cytoplasmic inhibition of carotenoid biosynthesis with virus-derived RNA. *Proc Natl Acad Sci U S A*, **92,** 1679-1683.

80. Fire, A., Xu, S., Montgomery, M.K., Kostas, S.A., Driver, S.E. and Mello, C.C. (1998) Potent and specific genetic interference by double-stranded RNA in Caenorhabditis elegans. *Nature*, **391,** 806-811.

81. Elbashir, S.M., Harborth, J., Lendeckel, W., Yalcin, A., Weber, K. and Tuschl, T. (2001) Duplexes of 21-nucleotide RNAs mediate RNA interference in cultured mammalian cells. *Nature*, **411,** 494-498.
82. Elbashir, S.M., Lendeckel, W. and Tuschl, T. (2001) RNA interference is mediated by 21- and 22-nucleotide RNAs. *Genes Dev*, **15,** 188-200.
83. Pei, Y. and Tuschl, T. (2006) On the art of identifying effective and specific siRNAs. *Nat Methods*, **3,** 670-676.
84. Baulcombe, D. (2004) RNA silencing in plants. *Nature*, **431,** 356-363.
85. Sanchez-Vargas, I., Travanty, E.A., Keene, K.M., Franz, A.W., Beaty, B.J., Blair, C.D. and Olson, K.E. (2004) RNA interference, arthropod-borne viruses, and mosquitoes. *Virus Res*, **102,** 65-74.
86. Voinnet, O. (2005) Induction and suppression of RNA silencing: insights from viral infections. *Nat Rev Genet*, **6,** 206-220.
87. Aliyari, R. and Ding, S.W. (2009) RNA-based viral immunity initiated by the Dicer family of host immune receptors. *Immunol Rev*, **227,** 176-188.
88. Hammond, S.M., Bernstein, E., Beach, D. and Hannon, G.J. (2000) An RNA-directed nuclease mediates post-transcriptional gene silencing in Drosophila cells. *Nature*, **404,** 293-296.
89. Li, H., Li, W.X. and Ding, S.W. (2002) Induction and suppression of RNA silencing by an animal virus. *Science*, **296,** 1319-1321.
90. Fenner, B.J., Goh, W. and Kwang, J. (2007) Dissection of double-stranded RNA binding protein B2 from betanodavirus. *J Virol*, **81,** 5449-5459.
91. Lingel, A., Simon, B., Izaurralde, E. and Sattler, M. (2005) The structure of the flock house virus B2 protein, a viral suppressor of RNA interference, shows a novel mode of double-stranded RNA recognition. *EMBO Rep*, **6,** 1149-1155.
92. Sullivan, C.S. and Ganem, D. (2005) A virus-encoded inhibitor that blocks RNA interference in mammalian cells. *J Virol*, **79,** 7371-7379.
93. Takeuchi, O. and Akira, S. (2009) Innate immunity to virus infection. *Immunol Rev*, **227,** 75-86.
94. Sadler, A.J. and Williams, B.R. (2008) Interferon-inducible antiviral effectors. *Nat Rev Immunol*, **8,** 559-568.
95. Der, S.D., Zhou, A., Williams, B.R. and Silverman, R.H. (1998) Identification of genes differentially regulated by interferon alpha, beta, or gamma using oligonucleotide arrays. *Proc Natl Acad Sci U S A*, **95,** 15623-15628.
96. Muller, U., Steinhoff, U., Reis, L.F., Hemmi, S., Pavlovic, J., Zinkernagel, R.M. and Aguet, M. (1994) Functional role of type I and type II interferons in antiviral defense. *Science*, **264,** 1918-1921.
97. Basler, C.F., Wang, X., Muhlberger, E., Volchkov, V., Paragas, J., Klenk, H.D., Garcia-Sastre, A. and Palese, P. (2000) The Ebola virus VP35 protein functions as a type I IFN antagonist. *Proc Natl Acad Sci U S A*, **97,** 12289-12294.

98. Garcia-Sastre, A., Egorov, A., Matassov, D., Brandt, S., Levy, D.E., Durbin, J.E., Palese, P. and Muster, T. (1998) Influenza A virus lacking the NS1 gene replicates in interferon-deficient systems. *Virology*, **252,** 324-330.

99. Cullen, B.R. (2006) Is RNA interference involved in intrinsic antiviral immunity in mammals? *Nat Immunol*, **7,** 563-567.

100. van Rij, R.P. and Andino, R. (2006) The silent treatment: RNAi as a defense against virus infection in mammals. *Trends Biotechnol*, **24,** 186-193.

101. Umbach, J.L. and Cullen, B.R. (2009) The role of RNAi and microRNAs in animal virus replication and antiviral immunity. *Genes Dev*, **23,** 1151-1164.

102. Haasnoot, J. and Berkhout, B. (2006) RNA interference: its use as antiviral therapy. *Handb Exp Pharmacol***,** 117-150.

103. Parameswaran, P., Sklan, E., Wilkins, C., Burgon, T., Samuel, M.A., Lu, R., Ansel, K.M., Heissmeyer, V., Einav, S., Jackson, W. *et al.* Six RNA viruses and forty-one hosts: viral small RNAs and modulation of small RNA repertoires in vertebrate and invertebrate systems. *PLoS Pathog*, **6,** e1000764.

104. Cai, X., Hagedorn, C.H. and Cullen, B.R. (2004) Human microRNAs are processed from capped, polyadenylated transcripts that can also function as mRNAs. *Rna*, **10,** 1957-1966.

105. Lee, Y., Jeon, K., Lee, J.T., Kim, S. and Kim, V.N. (2002) MicroRNA maturation: stepwise processing and subcellular localization. *Embo J*, **21,** 4663-4670.

106. Lee, Y., Kim, M., Han, J., Yeom, K.H., Lee, S., Baek, S.H. and Kim, V.N. (2004) MicroRNA genes are transcribed by RNA polymerase II. *Embo J*, **23,** 4051-4060.

107. Borchert, G.M., Lanier, W. and Davidson, B.L. (2006) RNA polymerase III transcribes human microRNAs. *Nat Struct Mol Biol*, **13,** 1097-1101.

108. Faller, M. and Guo, F. (2008) MicroRNA biogenesis: there's more than one way to skin a cat. *Biochim Biophys Acta*, **1779,** 663-667.

109. Bartel, D.P. (2004) MicroRNAs: genomics, biogenesis, mechanism, and function. *Cell*, **116,** 281-297.

110. Carthew, R.W. and Sontheimer, E.J. (2009) Origins and Mechanisms of miRNAs and siRNAs. *Cell*, **136,** 642-655.

111. Kim, V.N. (2005) MicroRNA biogenesis: coordinated cropping and dicing. *Nat Rev Mol Cell Biol*, **6,** 376-385.

112. Lee, Y., Ahn, C., Han, J., Choi, H., Kim, J., Yim, J., Lee, J., Provost, P., Radmark, O., Kim, S. *et al.* (2003) The nuclear RNase III Drosha initiates microRNA processing. *Nature*, **425,** 415-419.

113. Landthaler, M., Yalcin, A. and Tuschl, T. (2004) The human DiGeorge syndrome critical region gene 8 and Its D. melanogaster homolog are required for miRNA biogenesis. *Curr Biol*, **14,** 2162-2167.

114. Denli, A.M., Tops, B.B., Plasterk, R.H., Ketting, R.F. and Hannon, G.J. (2004) Processing of primary microRNAs by the Microprocessor complex. *Nature*, **432,** 231-235.

115. Gregory, R.I., Yan, K.P., Amuthan, G., Chendrimada, T., Doratotaj, B., Cooch, N. and Shiekhattar, R. (2004) The Microprocessor complex mediates the genesis of microRNAs. *Nature*, **432,** 235-240.

116. Han, J., Lee, Y., Yeom, K.H., Kim, Y.K., Jin, H. and Kim, V.N. (2004) The Drosha-DGCR8 complex in primary microRNA processing. *Genes Dev*, **18,** 3016-3027.

117. Yi, R., Qin, Y., Macara, I.G. and Cullen, B.R. (2003) Exportin-5 mediates the nuclear export of pre-microRNAs and short hairpin RNAs. *Genes Dev*, **17,** 3011-3016.

118. Bernstein, E., Caudy, A.A., Hammond, S.M. and Hannon, G.J. (2001) Role for a bidentate ribonuclease in the initiation step of RNA interference. *Nature*, **409,** 363-366.

119. Chendrimada, T.P., Gregory, R.I., Kumaraswamy, E., Norman, J., Cooch, N., Nishikura, K. and Shiekhattar, R. (2005) TRBP recruits the Dicer complex to Ago2 for microRNA processing and gene silencing. *Nature*, **436,** 740-744.

120. Hutvagner, G., McLachlan, J., Pasquinelli, A.E., Balint, E., Tuschl, T. and Zamore, P.D. (2001) A cellular function for the RNA-interference enzyme Dicer in the maturation of the let-7 small temporal RNA. *Science*, **293,** 834-838.

121. Khvorova, A., Reynolds, A. and Jayasena, S.D. (2003) Functional siRNAs and miRNAs exhibit strand bias. *Cell*, **115,** 209-216.

122. Schwarz, D.S., Hutvagner, G., Du, T., Xu, Z., Aronin, N. and Zamore, P.D. (2003) Asymmetry in the assembly of the RNAi enzyme complex. *Cell*, **115,** 199-208.

123. Berezikov, E., Chung, W.J., Willis, J., Cuppen, E. and Lai, E.C. (2007) Mammalian mirtron genes. *Mol Cell*, **28,** 328-336.

124. Okamura, K., Hagen, J.W., Duan, H., Tyler, D.M. and Lai, E.C. (2007) The mirtron pathway generates microRNA-class regulatory RNAs in Drosophila. *Cell*, **130,** 89-100.

125. Ruby, J.G., Jan, C.H. and Bartel, D.P. (2007) Intronic microRNA precursors that bypass Drosha processing. *Nature*, **448,** 83-86.

126. Griffiths-Jones, S., Saini, H.K., van Dongen, S. and Enright, A.J. (2008) miRBase: tools for microRNA genomics. *Nucleic Acids Res*, **36,** D154-158.

127. Friedman, J.M. and Jones, P.A. (2009) MicroRNAs: critical mediators of differentiation, development and disease. *Swiss Med Wkly*, **139,** 466-472.

128. Hebert, S.S., Horre, K., Nicolai, L., Papadopoulou, A.S., Mandemakers, W., Silahtaroglu, A.N., Kauppinen, S., Delacourte, A. and De Strooper, B. (2008) Loss of microRNA cluster miR-29a/b-1 in sporadic Alzheimer's disease correlates with increased BACE1/beta-secretase expression. *Proc Natl Acad Sci U S A*, **105,** 6415-6420.

129. Kim, J., Inoue, K., Ishii, J., Vanti, W.B., Voronov, S.V., Murchison, E., Hannon, G. and Abeliovich, A. (2007) A MicroRNA feedback circuit in midbrain dopamine neurons. *Science*, **317,** 1220-1224.

130. Thum, T., Gross, C., Fiedler, J., Fischer, T., Kissler, S., Bussen, M., Galuppo, P., Just, S., Rottbauer, W., Frantz, S. *et al.* (2008) MicroRNA-21 contributes to myocardial disease by stimulating MAP kinase signalling in fibroblasts. *Nature*, **456,** 980-984.

131. Gottwein, E. and Cullen, B.R. (2008) Viral and cellular microRNAs as determinants of viral pathogenesis and immunity. *Cell Host Microbe*, **3,** 375-387.

132. Pfeffer, S., Zavolan, M., Grasser, F.A., Chien, M., Russo, J.J., Ju, J., John, B., Enright, A.J., Marks, D., Sander, C. *et al.* (2004) Identification of virus-encoded microRNAs. *Science*, **304,** 734-736.

133. Klase, Z., Kale, P., Winograd, R., Gupta, M.V., Heydarian, M., Berro, R., McCaffrey, T. and Kashanchi, F. (2007) HIV-1 TAR element is processed by Dicer to yield a viral micro-RNA involved in chromatin remodeling of the viral LTR. *BMC Mol Biol*, **8,** 63.

134. Omoto, S., Ito, M., Tsutsumi, Y., Ichikawa, Y., Okuyama, H., Brisibe, E.A., Saksena, N.K. and Fujii, Y.R. (2004) HIV-1 nef suppression by virally encoded microRNA. *Retrovirology*, **1,** 44.

135. Ouellet, D.L., Plante, I., Landry, P., Barat, C., Janelle, M.E., Flamand, L., Tremblay, M.J. and Provost, P. (2008) Identification of functional microRNAs released through asymmetrical processing of HIV-1 TAR element. *Nucleic Acids Res*, **36,** 2353-2365.

136. Lin, J. and Cullen, B.R. (2007) Analysis of the interaction of primate retroviruses with the human RNA interference machinery. *J Virol*, **81,** 12218-12226.

137. Pfeffer, S., Sewer, A., Lagos-Quintana, M., Sheridan, R., Sander, C., Grasser, F.A., van Dyk, L.F., Ho, C.K., Shuman, S., Chien, M. *et al.* (2005) Identification of microRNAs of the herpesvirus family. *Nat Methods*, **2,** 269-276.

138. Cullen, B.R. (2009) Viral and cellular messenger RNA targets of viral microRNAs. *Nature*, **457,** 421-425.

139. Li, S.C., Shiau, C.K. and Lin, W.C. (2008) Vir-Mir db: prediction of viral microRNA candidate hairpins. *Nucleic Acids Res*, **36,** D184-189.

140. Chang, J., Nicolas, E., Marks, D., Sander, C., Lerro, A., Buendia, M.A., Xu, C., Mason, W.S., Moloshok, T., Bort, R. *et al.* (2004) miR-122, a mammalian liver-specific microRNA, is processed from hcr mRNA and may downregulate the high affinity cationic amino acid transporter CAT-1. *RNA Biol*, **1,** 106-113.

141. Esau, C., Davis, S., Murray, S.F., Yu, X.X., Pandey, S.K., Pear, M., Watts, L., Booten, S.L., Graham, M., McKay, R. *et al.* (2006) miR-122 regulation of lipid metabolism revealed by in vivo antisense targeting. *Cell Metab*, **3,** 87-98.

142. Jopling, C.L., Yi, M., Lancaster, A.M., Lemon, S.M. and Sarnow, P. (2005) Modulation of hepatitis C virus RNA abundance by a liver-specific MicroRNA. *Science*, **309,** 1577-1581.

143. Jopling, C.L. (2008) Regulation of hepatitis C virus by microRNA-122. *Biochem Soc Trans*, **36,** 1220-1223.

144. Barth, S., Pfuhl, T., Mamiani, A., Ehses, C., Roemer, K., Kremmer, E., Jaker, C., Hock, J., Meister, G. and Grasser, F.A. (2008) Epstein-Barr virus-encoded microRNA miR-BART2 down-regulates the viral DNA polymerase BALF5. *Nucleic Acids Res*, **36,** 666-675.

145. Cai, X., Schafer, A., Lu, S., Bilello, J.P., Desrosiers, R.C., Edwards, R., Raab-Traub, N. and Cullen, B.R. (2006) Epstein-Barr virus microRNAs are evolutionarily conserved and differentially expressed. *PLoS Pathog*, **2,** e23.

7 CURRICULUM VITAE

Personal Data

Name	Harald Rouha
Date of Birth	Dec 8th, 1981
Place of Birth	Linz, Upper Austria
Nationality	Austria
Business address	Medical University of Vienna Department of Virology Kinderspitalgasse 15 1095 Vienna, Austria harald.rouha@meduniwien.ac.at

---

Education

Mar 2007- present	**PhD thesis** Department of Virology, Medical University of Vienna Title: *"Molecular functions of endogenous and heterologous genetic RNA elements in the tick-borne encephalitis virus life cycle"* Jul 2009 – Dec 2009: Research stay at Novartis Vaccines and Diagnostics, Cambridge, Massachusetts, USA
Jan 2007	**Graduation**, Master of Science University of Vienna Faculty of Life Science
Oct 2005 – Jan 2007	**Master thesis** University of Vienna, Institute of Microbiology and Genetics performed at INTERCELL AG Title: *"Molecular cloning and characterization of EAEC and Shigella antigens for development of a vaccine against enteric pathogen caused Traveler's Diarrhea"*
Oct 2001 – Jan 2007	**Undergraduate Studies in Microbiology and Genetics** University of Vienna, Austria
Oct 2000 – Jun 2001	**Military Service**
Sep 1991 – May 2000	**Secondary school** Kollegium Aloisianum, Linz, Austria